TU-PM-SymII-1 NEW ENZYMES FROM OLD: ASPARTATE AMINOTRANSFERASE

D. Ringe, Massachusetts Institute of Technology, Cambridge, MA 02139
Jack F. Kirsch, University of California, Berkeley, CA 94720

Pyridoxal phosphate (vitamin B_6) is one of the most important cofactors in intermediary metabolism. It is found in the active sites of amino acid transaminases (ATases), decarboxylases and racemases. The ATase specific for L-aspartic acid AATase has been well characterized both mechanistically and kinetically. The enzyme from E. coli has now been cloned, sequenced and expressed at high levels in E. coli. Site-specific mutants have been prepared, designed to probe the mechanistic and specificity characteristics of the enzyme. The structures of the wild type and two mutant enzymes have been solved by X-ray crystallographic analysis, with the intent of understanding the structural basis for the very different observed kinetic and mechanistic properties of the mutant enzymes. In one of these mutants, K258A, the amino acid which forms the Schiff's base with pyridoxal phosphate has been replaced by alanine. The PLP form of the K258A mutant no longer functions as a transaminase. The PMP form of this mutant reacts with α-ketoglutarate to give the ketimine as a final stable product. The analogous reaction with oxalacetate forms the decarboxylated, transaminated aldimine of alanine as the final product. Part of the specificity pocket for the carboxylic acid side chain of the dicarboxylic amino acid substrates of the AATase is an arginine residue. In the second mutant, R292D, this arginine residue has been replaced by aspartic acid. The resulting enzyme is now a cationic amino acid transaminase, which preferentially catalyses the transamination of Arg or Lys over Asp or Glu.

TU-PM-SymII-2 GRAMICIDIN, A TRANSMEMBRANE CHANNEL. B. A. Wallace, Department of Chemistry and Center for Biophysics, Rensselaer Polytechnic Institute, Troy, New York 12180.

Gramicidin A is an linear polypeptide antibiotic that forms ion channels in phospholipid membranes. CD and NMR spectroscopic studies have shown that the molecules adopt different backbone conformations in membranes and in organic solvents, and that these forms, which appear to correspond to helical dimers and double helices respectively, interact in different manners with monovalent cations (Wallace, 1986). Comparisons of gramicidins A and C provide information on the organization of the Trp side chains in these structures (Callahan & Wallace, in preparation). Gramicidin crystallizes in a number of different forms in the presence and absence of lipid and/or cations. The structure of gramicidin/CsCl crystals ($P2_12_12_1$, a=32.1, b=52.1, c=31.2) (Kimball and Wallace, 1984) has been determined. Using single wavelength anomalous scattering from the cesium ions for phasing, we have calculated a 1.8 A resolution map (Wallace & Hendrickson in preparation), built a preliminary model, and are just completing refinement of the structure, including solvent molecules (Wallace & Ravikumar, unpublished results). The gramicidins in these crystals form a cylinder with a column of cesium and chloride ions complexing with the peptide backbone that lines the 4.4 A pore. The structure is a lefthanded anti-parallel intertwined double helix with beta-sheet-like hydrogen bonding and a superhelical twist of 6.3 residues per turn. A different crystal form ($P2_122$, a=32.8, b=27.5, c=26.8) has been prepared in the presence of lipid molecules and appears to contain a 4:1 lipid-to-gramicidin complex (Wallace, 1986), with the lipid molecules being highly ordered in the crystals (Short et al, 1986). The space group is compatible with a bilayer motif for the lipids. (Supported by NSF Grants DMB85-17866 and DMB87-96205 and a Dreyfus Teacher-Scholar Award).

TU-PM-SymII-3 CALCIUM CHANNELS INDUCE PARAMECIUM TO SWIM AND DANCE, BUT CAN THEY MAKE THEM SING? Barbara E. Ehrlich. Departments of Medicine and Physiology, University of Connecticut, Farmington, CT.

Paramecium are the lowest organism known to have calcium channels and their channels have characteristics that are similar to those found in invertebrates and vertebrates. I have studied calcium channels after they have been isolated from the rest of the cell. Specifically, native membrane vesicles that contain calcium channels were incorporated into planar lipid bilayers formed at the tip of patch-style pipettes. The behavior of the bilayer-incorporated channel was similar to that expected from in situ electrophysiological experiments. For example, the only pharmacological agent known to inhibit calcium currents in intact Paramecium also inhibits the bilayer-incorporated currents. Although this agent, W-7, is also used as a calmodulin antagonist, experiments suggest that it blocks the channel directly rather than acting through calmodulin. Other classes of calmodulin antagonists do not inhibit the calcium currents and the concentration of W-7 needed to inhibit the channel is 2.5 times less than that needed to inhibit calmodulin stimulation of phosphodiesterase. In the search for better channel blockers, analogs of W-7 were made. One compound, W(12)Br, was found to be 100 times more potent than W-7. In addition, the sensitivity to W-7 of calcium currents in representative organisms of the major animal phyla was tested. Only the lower invertebrates appear to be sensitive to the W compounds. BEE is a PEW Scholar in the Biomedical Sciences.

TU-PM-SymII-4 PERSPECTIVES ON PROTEIN-LIPID INTERACTIONS. Barbara A. Lewis, Department of Chemistry, University of Wisconsin-Madison, Madison, Wisconsin, 53706.

Most research in the area of protein-lipid interactions has focused either on the effects of proteins on lipid structure and dynamics or on the effects of lipids on the function of membrane proteins. A third issue of equal importance, the effects of the lipid environment on membrane protein structure, has been less studied, mainly for reasons of feasibility. An overview of this area will be given, along with current results of our studies of lipid effects on the transmembrane protein bacteriorhodopsin.

TU-PM-MinI-1 VIBRATIONAL SPECTROSCOPY OF BIOMOLECULES, Timothy J. O'Leary, Department of Cellular Pathology, Armed Forces Institute of Pathology, Washington, DC 20306.

Since Wright and Lee, and Edsall, first investigated the Raman spectra of ionized amino acids, infrared and Raman spectroscopy have taken on increasingly important roles in the elucidation of biological structures and structural alterations. The advances which have taken place in the fifty years since this work reflect improvements in both the instrumentation with which spectra can be obtained, and in the theoretical basis for spectral interpretation. The speakers in this minisymposium represent a distinguished subset of scientists working in biomolecular vibrational spectroscopy. Their interests include "ordinary" infrared and Raman spectroscopy of proteins, lipids and nucleic acids, as well as resonance Raman spectroscopy of excited states and vibrational circular dichroism. Together these speakers will present an overview of many new and useful biological applications of vibrational spectroscopic techniques.

TU-PM-MinI-2 MOLECULAR REORGANIZATIONS IN BIOLOGICAL MEMBRANES: IDENTIFICATION OF LIPID-LIPID AND LIPID PROTEIN INTERACTIONS BY RAMAN SPECTROSCOPY. Ira W. Levin, Laboratory of Chemical Physics, NIDDK, National Institutes of Health, Bethesda, MD 20892

For membrane bilayers vibrational Raman spectroscopy provides a sensitive technique for identifying and clarifying the structural reorganizations resulting from small intermolecular perturbations. These perturbations, manifest by changes in spectral band shapes, intensities and frequency shifts, are conveniently monitored as a function of temperature using both spontaneous and resonance Raman methodologies. In examining the destabilizing effects of an extrinsic protein on bilayer lipids, we utilized resonance Raman techniques to examine specifically alterations in the in-plane porphyrin vibrational modes of the heme group in ferricytochrome c during the protein's complexation to cardiolipin, a negatively charged lipid. Spontaneous Raman spectroscopy was used simultaneously to clarify the effects of the lipid-protein association upon the hydrophobic region of the bilayer lipids. This overall behavior was contrasted to the weak interactions of ferricytochrome c with bilayer dispersions of dipalmitoylphosphatidylcholine (DPPC), a zwitterionic lipid. With these models we attempt to emphasize the sequence of molecular details in which the membrane matrix is perturbed as the peripheral protein exhibits a capability of significantly altering the bilayer packing characteristics and the temperature dependent properties of the liposomal assemblies.

We will also briefly indicate the applications of Fourier-transform Raman spectroscopy, a new technique, to biological materials.

TU-PM-MinI-3 POLYPEPTIDE CHAIN CONFORMATION BY NORMAL MODE ANALYSIS OF INFRARED AND RAMAN SPECTRA. S. Krimm, Biophysics Research Division, University of Michigan, Ann Arbor, MI 48109

The use of a vibrational spectrum as a "fingerprint" for a polypeptide chain conformation can be useful in many applications, but this approach neither permits extracting the maximum amount of three-dimensional structural information in the spectrum nor does it aid in a more general understanding of the conformational basis for the spectrum. In addition, it relies on other techniques (x-ray, NMR, etc.) to provide the independent structural information on which the spectral correlations are based.

Strong inferences about conformation can be made if the normal modes of a given structure can be calculated and compared with observed infrared and Raman bands. We have refined a vibrational force field for the polypeptide chain that permits a reliable prediction of these frequencies, and have applied it to a number of systems (1). This force field, together with ab initio dipole derivatives of the peptide group (2), also permits a reliable reproduction of amide mode infrared intensities.

Examples will be discussed of how such normal mode analyses permit the testing of structural possibilities, help to discover spectral regularities, enable complete spectral interpretations for known structures, and allow spectral characterization of canonical conformations. This research has been supported by the National Science Foundation.

1. S. Krimm and J. Bandekar, Adv. Protein Chem. 38, 181 (1986).
2. T.C. Cheam and S. Krimm, J. Chem. Phys. 82, 1631 (1985).

TU-PM-MinI-4 RAMAN SPECTROSCOPY AS A PROBE OF DNA-PROTEIN INTERACTIONS IN VIRUSES
George J. Thomas, Jr., Division of Cell Biology and Biophysics, School of Basic Life Sciences, University of Missouri-Kansas City, Kansas City, MO 64145.

Using correlations established from Raman spectroscopy of DNA and RNA crystals of known structure,[1] we have determined conformational properties of nucleic acids packaged within protein coats of bacterial, plant and eukaryotic viruses. The Raman spectra are informative of the nucleic acid backbone geometry and of the nucleoside sugar ring puckers in the encapsidated viral genomes. Viruses investigated include the following: filamentous DNA bacteriophages (fd, If1, IKe, Pf1, Xf, Pf3), isometric DNA bacteriophages (ϕX174, P22, T7), isometric RNA plant viruses (TYMV, BDMV, CCMV, TBSV, CPMV), and a mammalian virus (adenovirus). The examination of specifically labeled isotopomers of several of the viruses has facilitated identification and assignment of the conformation-sensitive Raman bands of the viral DNA. Conventional DNA structures are absent from all of the ssDNA bacteriophages, indicating that DNA conformation in them is determined by specific protein-DNA interactions. In addition, the nucleoside conformations prevalent in different filamentous bacteriophages differ significantly from one another. Phosphodiester group geometries of dsDNA are also altered by packaging in the bacteriophages P22 and T7. (Supported by N.I.H.)

[1]Reviewed by Thomas, G.J., Jr. and Wang, A.H.-J. (1988), in Nucleic Acids and Molecular Biology, Vol. 2, Eckstein, F. and Lilley, D.M.J., Eds., Springer-Verlag, Berlin.

TU-PM-MinI-5 VIBRATIONAL CIRCULAR DICHROISM IN BIOMOLECULES by Laurence A. Nafie and Teresa B. Freedman, Department of Chemistry, Syracuse University, Syracuse, New York 13244-1200.

Vibrational circular dichroism (VCD) is the difference in the infrared vibrational absorption intensity of a chiral molecule for left versus right circularly polarized radiation. VCD spectra combine the structural specificity of ordinary vibrational spectroscopy with the stereochemical sensitivity of electronic optical activity. Although VCD spectra are three to four orders of magnitude smaller than the parent infrared absorption intensity, they contain detailed information related to the stereo-conformation of biomolecules in solution. Examples of molecules studied to date include, amino acids, transition metal complexes with amino acid ligands, sugars, steroids, polypeptides, proteins, nucleic acids, amino alcohols and diols.

VCD spectra can be interpreted on a number of levels. The most direct are the simple models and mechanisms. The coupled oscillator model can be applied to balanced bisignate VCD features arising from the coupling of two near-degenerate vibrational transitions and yields information on the stereo-orientation of the two transition moments. The ring current mechanism embodies several rules which relate biased, monosignate VCD intensity to the presence of an intramolecular ring closed by transition metal complexation, hydrogen bonding or covalent bonding. Other approaches to VCD spectral interpretation involve vibrational normal coordinate analysis followed by the application of either an approximate intensity model or exact ab initio molecular orbital calculations. Examples of VCD spectra and their interpretation, with particular emphasis on recent spectra of amino alcohols and diols, will be presented.

TU-PM-MinI-6 DETERMINATION OF RETINAL CHROMOPHORE STRUCTURE IN RHODOPSINS WITH RESONANCE RAMAN SPECTROSCOPY - THE MOVIE. Richard A. Mathies, Steven Lin, Stephen P. A. Fodor, Walter T. Pollard and Jim Ames, Chemistry Department, University of California, Berkeley, CA 94720; Ronald Gebhard, Ellen van den Berg, Chris Winkel and Johan Lugtenburg, Chemistry Department, Leiden University, 2300 RA Leiden, The Netherlands.

Resonance Raman vibrational spectroscopy provides a sensitive probe of retinal chromophore structure in rhodopsin, bacteriorhodopsin and their photointermediates. The structural information contained in these spectra can be elucidated through vibrational assignments with isotopic derivatives and normal coordinate calculations. The complete vibrational analysis of BR_{568} has recently been completed, and a computer animated motion picture will be used to present an overview of the normal modes. These assignments and the knowledge of the vibrational structure derived from them, permit the *in situ* determination of the structure of the retinal chromophore about all its single and double bonds. A summary of the basic effects of C=C and C-C isomerization on the vibrational modes in the 1100-1300 cm^{-1} fingerprint region will be presented. The "classical methods" for determining $C_{13}=C_{14}$, $C_{14}-C_{15}$ and $C_{15}=N$ configuration in bacteriorhodopsin will be reviewed. Finally, new methods for determining the $C_{15}=N$ configuration in unprotonated retinal Schiff bases and for determining $C_{14}-C_{15}$ conformation will be presented. The weak coupling of the C_{15}-D rock with the N-CH_2 stretch on the lysine indicates that the $C_{15}=N$ configuration in M_{412} is *anti*. The frequency of the symmetric deuterium rocking mode in 14,15-dideuterio derivatives of L_{550} (968 cm^{-1}) shows that the $C_{14}-C_{15}$ conformation in L_{550} is *s-trans*.

TU-PM-MinII-1 USE OF SITE-DIRECTED MUTAGENESIS TO STUDY A MEMBRANE TRANSPORT PROTEIN: PERMEASE ON PARADE. H. R. Kaback, Roche Institute of Molecular Biology, Nutley.

Lactose/H^+ symport in *E. coli* is catalyzed by the *lac* permease, a hydrophobic transmembrane protein encoded by the *lac Y* gene that has been purified to homogeneity and reconstituted into proteoliposomes in a completely functional state. Circular dichroic studies and hydropathy profiling of the amino-acid sequence of the permease suggest a secondary structure in which the polypeptide consists of 12 hydrophobic segments in α-helical conformation that traverse the membrane in zig-zag fashion connected by shorter, hydrophilic domains with most of the charged residues and most of the residues commonly found in β-turns. Preliminary support for certain general aspects of the model has been obtained from proteolysis experiments and from binding studies with monoclonal antibodies against purified permease and site-directed polyclonal antibodies against synthetic polypeptides corresponding to domains that are presumably exposed on the surfaces of the membrane. Oligonucleotide-directed, site-specific mutagenesis is currently being utilized to probe the structure and function of the permease. Recent application of the technique provides an indication that Arg-302 (helix IX), His-322 (helix X) and Glu-325 (helix X) may be sufficiently close to hydrogen bond and that they play a critical role in lactose-coupled H^+ translocation, possibly as components of a catalytic triad similar to that described in the serine proteases.

TU-PM-MinII-2 SLIP AND THE CONTROL OF PROTON PUMPING: BACTERIORHODOPSIN. S.Roy Caplan, Membrane Dept., The Weizmann Institute of Science, Rehovot, Israel.

It is generally assumed that ion pumps are completely coupled and that all uncoupling may be attributed to external leaks. However, several reports have recently appeared showing that a certain degree of intrinsic uncoupling is present in ion pumps and transport systems. Analysis of the six-state model of a redox proton pump studied by Pietrobon and Caplan (Biochemistry 24, 5764, 1985) shows the regulatory influence of the thermodynamic forces on the extent and relative contributions of redox slip and proton slip. Comparison between simulated behavior and experimental results leads to the conclusion that the typical relation between rate of electron transfer and $\Delta\hat{\mu}_H$ found in mitochondria at static head is a manifestation of intrinsic uncoupling in the redox pumps, which may well have physiological significance for the efficiency of oxidative phosphorylation (Pietrobon et al., Biochemistry 25, 767, 1986). In bacteriorhodopsin the photoreaction proceeds at an essentially fixed rate, and hence a $\Delta\hat{\mu}_H$-controlled slip regulation would provide a "safety valve" as suggested by the author some years ago. This has been observed by a number of workers (e.g. Westerhoff & Dancshazy, TIBS 9, 112, 1984). A detailed compartmental analysis of light-induced proton movement in bacteriorhodopsin vesicles has been given by Klausner et al. (Biochemistry 21, 3643, 1982). The fitting of a compartmental model to a large number of experimental data required the introduction of an arbitrary "control function". It is now shown by means of the Hill diagram method that this control function is a straight-forward consequence of intrinsic uncoupling. Reaction slip increases as the proton gradient increases. As Westerhoff & Dancshazy have pointed out, this property in pumps which constitute the first step in a free-energy transducing pathway permits those pumps to be at least partially controlled by the processes constituting the later steps.

TU-PM-MinII-3 MODELING OF ENERGY-COUPLED SECONDARY ION FLOWS IN H. halobium: TESTING THE LIMITS OF LINEARITY. S.L. Helgerson, Dept. of Chemistry, Montana State Univ., Bozeman, MT 59717

H. halobium provides a unique system for studying energy coupling mechanisms. The plasma membrane contains a specialized purple membrane structure with a single protein component, bacteriorhodopsin (bR). Bacteriorhodopsin acts as an electrogenic proton pump to create a transmembrane protonmotive force (pmf). The pmf drives transmembrane ion fluxes both by passive movements and by active transport via an Na^+/H^+ antiporter. The large sodium gradient which results drives the uptake of amino acids by Na^+-linked transport systems. Since bR is a light-driven proton pump, the pmf is strictly regulated by the illumination intensity (Figure). Thus, the movements of ions and metabolites are well-defined functions of the proton pumping rate. Irreversible thermodynamic models have been proposed for the energetics of bR in reconstituted proteoliposomes (1) and for the control of the bR photocycle by the pmf (2). The latter model for the energetics of H. halobium cell envelope vesicles (2) will be used to examine the range over which secondary ion fluxes can be fit by linear phenomenological coupling coefficients. The interaction of the linear ion flux coefficients with the pmf-controlled proton pumping and pmf-gated sodium transport rates determines the overall linearity of the system.

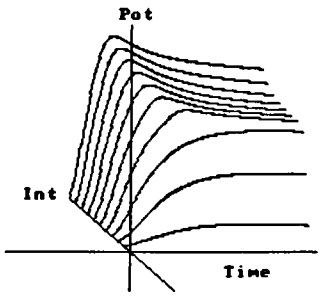

(1) H.V. Westerhoff, B.J. Scholte and K.J. Hellingwerf (1979) Biochim. Biophys. Acta 547:544; (2) S.L. Helgerson, M.K. Mathew, D.B. Bivin, P.K. Wolber, E. Heinz and W. Stoeckenius (1985) Biophys. J. 48:709.

TU-PM-MinII-4 REDOX COOPERATIVITY IN CYTOCHROME C OXIDASE. Richard W. Hendler, Laboratory of Cell Biology, NHLBI, and Hans V. Westerhoff, Section on Theoretical Biology, NIDDK, National Institutes of Health, Bethesda, MD 20892

We have recently described (Hendler et al., Biophys. J. 46: 717 (1987)) that the oxidation of cytochrome $\underline{a}_3$ accompanied the reduction of cytochrome $\underline{a}$ during a reductive titration in the voltage range 450-200 mV (vs S.H.E.). This phenomenon is reversed in an oxidative titration. This plus the direct demonstration of a low E_m titration of cytochrome $\underline{a}_3$ near 180 mV (ibid) and evidence for a high E_m near 770 mV (poster, this meeting) show that cytochrome $\underline{a}_3$ has (at least) two E_m's and that a high degree of redox cooperativity is present. In addition, we have observed two forms of cytochrome $\underline{a}$, one that titrates with an n value of 1 (uncoupled) and the other with an n value of 2 (coupled to Cu_A?). A cooperative model involving only the hemes (i.e. the "neoclassical model") can not account for these observations. In order to see if the presence of an additional controlling center [which may involve a free radical or extra Cu] and/or more complicated cooperativity can account for the experimental observations we have constructed and evaluated a variety of models. In this context, we have considered the effects of conformational changes and monomer/dimer equilibria on the redox affinities of the active sites. We shall illustrate a streamlined technique for evaluating models of this kind, and show how models with cooperative interactions involving all of the sites and either conformational or monomer-monomer cooperativity can account quantitatively for the experimental data. These observations plus related findings on electron-proton cooperativity offer new avenues of consideration for the control of electron flow and proton pumping.

TU-PM-MinII-5 HOW DO ENERGY-TRANSDUCING ORGANELLES REACH STEADY STATE?
Peter Nicholls and John M. Wrigglesworth Dept. of Biological Sciences, Brock Univ., St. Catharines, Ont. L2S 3A1, Canada, and Biochemistry Dept., King's College (KQC), London W8 7AH England.

Mitochondria, chloroplasts and reconstituted vesicles when metabolically functional, generate both pH gradients and membrane potentials. Each organelle produces a steady state $\Delta\mu H^+$ composed of $\Delta\Psi$ and ΔpH components, dependent upon the electrogenic pumps involved and upon the electrophoretic and electroneutral pathways that dissipate the gradients. In steady state the net fluxes of all ionic species must be zero; this is achieved if either the ion is at equilibrium or if it can cross the membrane using two pathways, one which allows for continuous entry and another for continuous exit during steady state. In cytochrome oxidase-containing proteoliposomes, addition of reductant and cytochrome c induces a rapid establishment of $\Delta\Psi$, followed by a slow monotonic creation of ΔpH (0.3 to 0.5 pH units). As ΔpH forms, $\Delta\Psi$ declines to a lower value, preserving an approximately constant $\Delta\mu H^+$. However, the small internal volume of most proteoliposomes implies that, if the geometric vesicle capacitance is between 0.4 and 0.7 $\mu F/cm^2$, sufficient charge must be moved electrically in the initial ($\Delta\Psi$only) phase to create an immediate internal pH change. Such fast pH changes are not normally observed, which prompts us to ask whether: (a) membrane capacitance is lower than geometry predicts (e.g., due to a double layer capacitance in series); or (b) initial buffering is higher than estimated (e.g., by the presence of dissociable phospholipids); or (c) the protons which move to establish the potentials are tightly bound at the membrane surface and non-exchangeable with bulk ions (but still mobile over the surface itself). Some experimental results bearing upon these questions will be presented. (Supported by Canadian NSERC grant A-0412 to PN and a UK SERC grant to JMW).

TU-PM-MinII-6 INTRAMEMBRANE PROTON TRANSFER IN OXIDATIVE PHOSPHORYLATION AND PHOTOPHOSPHORYLATION: EFFECTS OF PROTEIN AGGREGATION AND DECOUPLERS. Hagai Rottenberg, Pathology Department, Hahnamann University, Philadelphia, PA 19102.

Recent studies on the mechanism of oxidative phosphorylation in mitochondria and photophosphorylation in chloroplasts suggest the existence of a direct proton transfer pathway between the redox H^+ -pumps and the H^+-ATPase. We have studied the relationship between the magnitude of the proton electrochemical potential, $\Delta\tilde{\mu}_H$, and the efficiency of energy transfer employing various ionophores, protonphores, detergents and free fatty acids. Our results indicate that while uncoupling by ionophores is caused by the collapse of $\Delta\tilde{\mu}_H$, other reagents (decouplers) induce uncoupling without collapsing $\Delta\tilde{\mu}_H$, presumably by interferring with intramembranal proton transfer. Moreover protonophores, while collapsing $\Delta\tilde{\mu}_H$, also appear to interfer with intramembranal proton transfer. However, ATP synthesis driven by bulk $\Delta\tilde{\mu}_H$, generated artifically, is not inhibited by decouplers. Thus, two distinct, parallel, pathways of coupling appear to coexist. We have re-examined the relationships between $\Delta\tilde{\mu}_H$ and ΔGp in mitochondria and submitochondrial particles using ^{31}P-NMR and found that ΔGp is strictly correlated with $\Delta\tilde{\mu}_H$ only at low levels. Moreover, over a range of high values of $\Delta\tilde{\mu}_H$ when modulated by ionophores, ΔGp is almost independent of the value of $\Delta\tilde{\mu}_H$. These findings suggest that at high, physiological values of $\Delta\tilde{\mu}_H$, the intramembranal pathway dominates energy conversion. The contribution of protein aggregation to efficient, intramembranal proton transfer was demonstrated by the parallel effects of temperature on coupling efficiency and protein aggregation, as measured by fluorescence energy transfer, and by time-resolved phosphorescence anisotropy.

TU-PM-MinII-7 SUBSTRATE INDUCED PARADOXES IN CARDIAC BIOENERGETICS
William E. Jacobus and Jay L. Zweier, Dept. of Medicine, The Johns Hopkins Medical Institutions, Baltimore, MD 21205

TU-PM-MinII-8 A THERMOKINETIC MODEL FOR PANCREATIC FLUID SECRETION. *G.A.J.Kuijpers, ^J.J.H.H.M.De Pont and *H.V.Westerhoff, *NIDDK, NIH, Bethesda and ^University of Nijmegen, The Netherlands (Intr. by T.L.Hill).

The isolated rabbit pancreas secretes an isotonic fluid containing Na^+,K^+,HCO_3^- and Cl^-. We determined the effects of replacing Na^+ in the bathing medium by Li^+,K^+ or choline$^+$ on secretory rate and composition. In order to understand the results in qualitative and quantitative terms, we developed a theoretical model for pancreatic ion and water secretion based on thermodynamic and kinetic principles. The main features of the model are active, electrogenic, Na^+-dependent HCO_3^- transport and passive paracellular shunt permeation of all the secretory ions, with a component of the latter controlled by stimulants such as CCK-8. Assuming near-equilibrium, electroneutrality in bathing and secreted fluid and a zero osmotic gradient between the latter two, fluid secretion could be described by 4 rate equations in 4 unknown, J_v, $\Delta\psi$, $[Na^+]_s$ and $[HCO_3^-]_s$. The equations were solved numerically, and parameter values could be obtained so that the model adequately described all the data from the Na^+-replacement experiments. The model was also used to determine the control coefficients of the parameters (e.g. of the pump activity and the extracellular shunt permeabilities), which is a measure of their regulatory potential. In addition, we asked the model about the relative importance of the various secretion components, such as the electrical component and the passive anion flow. These theoretical experiments "pre"dicted results which have indeed been found experimentally. (Supported in part by the Netherlands Organization for the Advancement of Pure Research, Z.W.O.)

TU-PM-MinII-9 **Binding Capacity: Cooperativity and Buffering in Biopolymers** Enrico Di Cera, Stanley J Gill & Jeffries Wyman; Dept of Chem & Biochem, Univ of Colorado, Boulder, CO 80309.

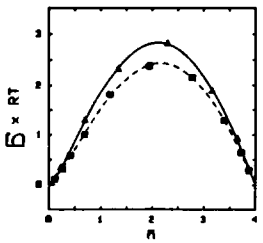

The group of linkage potentials [Wyman, (1975) PNAS 72, 1464] resulting from the energy of a physico-chemical system expressed per mole of macromolecule, leads to the concept of binding capacity [Di Cera et al (1988) PNAS, in press] $Ƃ = (\partial n/\partial \mu)$ as the change in the number of moles of ligand per mole of macromolecule which accompanies a change in the chemical potential of that ligand. This concept provides a means of exploring the consequences of thermodynamic stability on generalized binding phenomena in biopolymers. For the case of two ligands the fundamental inequality

$$Ƃ_{1,\mu_2} \geq Ƃ_{1,n_2}$$

shows that $Ƃ$ is always greater when the second ligand is held at constant μ than when it is held at constant n, i.e., when the system is open instead of closed to the second ligand. In the case of mass law binding $Ƃ$ can be measured directly by the differential thin-layer method [Gill et al (1987) Biochemistry 26, 3995]. An illustration of the inequality for O_2 binding to HbA_0 in buffered (triangles) and unbuffered (squares) solution conditions is shown in the Figure. In its canonical formulation the concept applies equally well to non-equilibrium thermodynamics where the inequality involves fluxes and forces and gives the effect of thermodynamic stability on energy transduction phenomena. [Supported by NIH HL22325 and NSF PCM772062 grants].

TU-PM-A1 CRAMBIN WATER STRUCTURE AT ATOMIC RESOLUTION FROM X-RAY AND NEUTRON DATA. Martha M. Teeter and Nam Ho Heo, Dept. of Chem., Boston College, Chestnut Hill, MA 02167.

Crystals of the hydrophobic protein crambin (4700 MW) diffract to better than 1.0 Å resolution and, at low temperature, have all of the solvent in the crystal ordered. This protein provides an excellent opportunity to study the distribution of water molecules at a protein surface in atomic detail that is not generally available for other protein crystal structures. Water is important not only in stabilizing a protein in its folded conformation but also can contribute to an enzyme's activity through binding at its active site. The function of the plant protein crambin is not yet known, however it is homologous to the membrane-active plant toxins purothionin (from wheat germ), which have been shown to bind calmodulin and appear to bind lipids.

Crambin's X-ray diffraction data to 0.945 Å at 300 K and to 0.83 Å at 140 K have been collected and the model of the structure has been refined. Neutron diffraction data to 1.1A at 300K has also been obtained and refined. Results of comparisons among these structures will be presented and compared. Neutron diffraction reveals the water deuterium positions as well as the exchange of the amide protons, which relate to the protein motion and disorder.

TU-PM-A2 THREE DIMENSIONAL STRUCTURAL ANALYSIS OF TETANUS TOXIN BY ELECTRON CRYSTALLOGRAPHY. M. F. Schmid, J. P. Robinson* and W. Chiu (Intr. by J. Schrag). Department of Biochemistry, University of Arizona, Tucson, AZ 85721 and *Department of Microbiology, Vanderbilt U. School of Med., Nashville, TN 37232.

Two dimensional crystalline arrays of native tetanus toxin have been formed at the interface between a solution of the toxin and a phospholipid monolayer containing the toxin's putative receptor molecule, ganglioside GT1. These arrays may mimic the first step in the intoxication process, that of binding to the cell surface prior to internalization. Electron crystallographic analysis has been used to study these periodic arrays. The arrays obey the symmetry of plane group $p12_1$ with a = 126 Å and b = 84 Å, and a thickness of 90 Å. The three dimensional structure of tetanus toxin in negative stain is reconstructed to a nominal resolution of 14 Å from multiple tilt images. The molecule presents an asymmetric three-lobed structure and could interact with the monolayer in two possible orientations.

TU-PM-A3 A NEW ALGORITHM FOR THE RAPID CALCULATION OF PROTEIN X-RAY SOLUTION SCATTERING PROFILES FROM ATOMIC COORDINATES Eaton Edward Lattman, Department of Biophysics, Johns Hopkins University School of Medicine, Baltimore, MD 21205 USA. BITNET address Lattman@JHUIGF.

If one expands the structure factor equation in spherical coordinates, the required rotational averaging of the molecule's Fourier transform is greatly simplified. It becomes a projection in the polar and azimuthal angular variables of the space. The profile is given by

$$I(R) = (1/2)\sum_{n=0}^{\infty}\sum_{m=0}^{n}\varepsilon_m N_{m,n}\left|G_{m,n}(R)\right|^2 \qquad \text{where} \qquad G_{m,n}(R) = \sum_j f_j(r)Y_{m,n}(\theta_j,\phi_j)j_n(2\pi r_j R).$$

The index j runs over all atoms; r, θ, φ are atomic coordinates and ε and N are constants; the $Y_{m,n}$ are complex spherical harmonics, and j_n are spherical Bessel functions; $R = 2\sin\theta/\lambda$. The effects of solvent have been modelled by subtracting from each protein atom a properly weighted water. Hydrogens have been included by using scattering curves f_j derived from the rotational averaging of protein atoms with their attached hydrogens. This approach may also be satisfactory for neutron scattering. Published scattering profiles (1) for lysozyme and BPTI have been accurately matched. Separate adjustable temperature factors for the protein, solvent and bound waters are used, and appear to be needed. Supported by GM-36358.

1. C.A. Pickover and D.M. Engelman, Biopolymers 21, 817, (1982).

TU-PM-A4 THE STRUCTURE OF RUBISCO FROM TOBACCO. Curmi, P.M.G., Chapman, M.S., Suh, S.W., Cascio, D., and Eisenberg, D. Introduced by Boyer, P.D. Molecular Biology Institute and the Department of Chemistry and Biochemistry, University of California, Los Angeles, CA 90024.

Ribulose 1,5-bisphosphate carboxylase-oxygenase (RuBisCO) converts carbon dioxide into sugar in the first step of photosynthesis. The structure of RuBisCO from tobacco (*Nicotiana tabacum*) has been determined by x-ray crystallography to a resolution of 2.8 A. The phases were determined by multiple isomorphous replacement and density modification. The protomer consists of one large and one small subunit that assemble in the form L_8S_8. The large subunit consists of three domains: (i) the N-terminal anti-parallel beta domain; (ii) an alpha/beta barrel; and (iii) a C-terminal anti-parallel alpha domain. The small subunit consists of a beta sheet with helices connecting the strands. The structural model has been refined at 2.8 A to give an R-factor of 30%. The structure will be discussed with reference to the functional properties of the enzyme.

TU-PM-A5 THE STRUCTURE OF DIPHTHERIA TOXIN AT 3.0 A RESOLUTION. Kantardjieff, K., Elkins, P., Fujii, G., Curmi, P.M.G., Collier, R.J. and Eisenberg, D. Molecular Biology Institute and Department of Chemistry and Biochemistry, University of California, Los Angeles, CA 90024.

Diphtheria toxin (M_r = 58,000) is a proenzyme that performs at least three functions: binding to an animal cell receptor, insertion and traversal of the endosomal membrane, and transfer of an ADP-ribose moiety to elongation factor 2, effectively shutting down protein synthesis and killing the cell. During internalization, diphtheria toxin is cleaved into two fragments, A and B, the former being responsible for enzymatic activity, the latter responsible for binding to receptors on the cell surface and for membrane insertion. From the amino acid sequence of the B fragment, it is possible to identify 4 putative transmembrane helices and one highly amphiphilic helix.

The electron density for a dimer of diphtheria toxin has been determined to 3.0 A resolution by single-crystal x-ray diffraction, using a combination of isomorphous replacement and density modification. Portions of the polypeptide sequence have been matched to the electron density, and the backbone of a monomer is being traced. There appear to be at least two domains, one predominantly helical, and another distinguishable by a four-stranded antiparallel beta sheet flanked by two alpha helices.

TU-PM-A6 **THE STRUCTURE OF HUMAN PANCREATIC THREAD PROTEIN.** A. Pande, C. Pande[+], R. Callender[+] and R. Ammann. Dept. of Medicine, University Hospital, Zuerich, Switzerland, [+]Physics Dept., City College of New York, U.S.A.

Partial amino acid sequence of pancreatic thread protein (PTP) from human pancreatic juice, apparent M.W. ca. 14000, was reported by Gross et al.,[1] in 1985. PTP may be related to a protein isolated from human pancreatic stones[2], but so far, neither the molecular structure, nor the physiological function is known, even though it is present in a large concentration in pancreatic secretions. We have, therefore, undertaken a structural/spectroscopic study to understand the role of PTP in pancreatic stone formation.

Of all the known protein sequences in the current Brookhaven Data Bank, PTP, more specifically the 45 residue long N-terminal end, shows a significant homology only with a segment of hepatic asialoglycoprotein receptor. Protein structure prediction methods show three strands of β-structure and two α-helical segments in this 45 residue chain. Infrared absorption spectrum of lyophilized PTP shows predominantly α-helical structure with amide I & II at 1653 and 1547 cm^{-1}, respectively. There are indications of β-structure, observed as shoulders around 1635 and 1690 cm^{-1}, in the infrared spectrum. Far U.V. circular dichroism (CD) of PTP solution, around pH 2, shows a distinct contribution from β-sheet structure. Strong contributions from aromatic amino acid residues, Trp, Tyr, and Phe, dominate the Raman spectrum as well as the near U.V. CD spectrum.

By monitoring the spectroscopic/structural features, it is now possible to observe the effect of different, physiologically significant, perturbations.

[1]Gross, J., et al., J. Clin. Invest.(1985) 76, 3115.
[2]Montalto, G., et al., Biochem. J. (1986) 238, 227.

TU-PM-A7 CARBAMYLATION OF GAMMA CRYSTALLIN AND ACTIN: EFFECTS ON ACTIN POLYMERIZATION. Charles Lee Kuckel, Beverly W. Lubit and Patricia N. Farnsworth (Intr. by Kenneth J. Friedman) Department of Physiology, UMD-New Jersey Medical School, Newark, NJ 07103-2757.

The cortical lens fiber cell matrix contains an actin cytoskeletal organization that is essential for lens fiber cell elongation and differentiation. Our previous in vitro studies have established that the gamma crystallins, a water-soluble 20KD lens protein family, modulate the rate, extent, and pattern of actin polymerization. Since uremia has been implicated in cataractogenesis due to cyanate derived from urea, the present study was designed to identify the effects of carbamylation on actin polymerization and the modulating properties of gamma crystallins. The lysines of both proteins and the N-terminal amino acid of the gamma crystallins were selectively carbamylated with methylisocyanate at pH 8.0 and 4°C. The carbamylation of lysine removes positive charges, which alters protein-protein/water interactions and disrupts protein surface ion-pair networks. The effects of carbamylation on the rate and extent of actin polymerization were measured by viscometry and fluorescence spectroscopy, and visualized by electron microscopy. The results of the experiments provide evidence that non-enzymatic carbamylation prevents the polymerization of actin. When added to polymerizing, nascent actin, carbamylated gamma crystallins continued to produce an increase in the rate of polymerization; however, there no longer was an increased extent of polyermization. The susceptibility of actin to alteration by carbamylation is related to the 19 lysines distributed along its length, while the mammalian gamma crystallins have an average of only one lysine near each amino- and carboxy-terminal end. (Supported by NIH grant EY05787, AHA grant #85-28 and Lions Eye Foundation of New Jersey.)

TU-PM-A8 MOLECULAR BASIS FOR α-GP BINDING TO BOVINE γ-CRYSTALLIN. Barbara Groth-Vasselli, Thomas Schleich* and Patricia N. Farnsworth. UMD-New Jersey Medical School, Newark, NJ 07103 and *U-C Santa Cruz, Santa Cruz, CA 95064

A mechanism for the control of lens metabolism may be the protein binding of a precursor or end product metabolite. In the red blood cell 2,3 DPG binds to hemoglobin and alters both glycolysis and hemoglobin O_2 affinity. We propose that α-glycerol phosphate which is present in the lens in substantial quantities is a candidate for a "control" metabolite. Our reasoning is supported by its concentration variations under stress conditions and its pivotal position in lens metabolism, i.e., the reversible transformation to dihydroxyacetone phosphate. Examination of the Blundell crystal structure of bovine γ_{II}-crystallin reveals that the charged residues Arg 79 and Arg 147 are in close proximity (~3A°) in the cleft between the two domains of the protein. In the absence of charge neutralization by ion-pair formation, this arrangement would provide a major source of electrostatic free energy destabilization. Computer graphics based docking experiments indicate that L-αGP fits in the cleft with the phosphomonoester group forming ion-pairs with these two Arg residues. Five hydrogen bonds may be formed between L-αGP and the protein, whereas for the unnatural D-isomer only 3 hydrogen bonds may be formed. These observations suggest the presence of an αGP binding site on γ-crystallin. Data from equilibrium binding studies based on the Paulus technique suggest the presence of one binding site per protein molecule. The binding of this metabolite to γ-crystallin may modify its interaction with other lens proteins and alter its function in the maintenance of lens transparency. Supported by NIH grant EY05787

TU-PM-A9 STRUCTURE AND EVOLUTION OF RELATED LYMPHOKINES, HEMOPOIETINS, GROWTH AND DIFFERENTIATION FACTORS

J. Fernando Bazan[1,2] and Fred E. Cohen[3], [1]Dept. of Biophysics, U. of Calif., Berkeley, CA 94720, and Depts. of [2]Biochemistry & Biophysics, [3]Medicine, and Pharmaceutical Chemistry, U. of Calif., San Francisco, CA 94143.

The sequences and genomic structures of a variety of proteins that regulate the growth, differentiation, and function of different cell types are known. These molecules include several lymphokines and hemopoietins such as interleukins -2, -3, -4, -5 and -6, erythropoietin, granulocyte-macrophage and granulocyte-specific colony stimulating factors. In addition, molecules with recognized sequence homology to growth hormone now form an extended family that includes prolactin and proliferin. All of these regulatory proteins exert their influence on a wide variety of biological processes by binding to cell-surface receptors that transmit and amplify the particular signal to other molecules within the cell. We propose a unifying structural and genetic basis for understanding the distinct and overlapping biological activities of these related regulatory molecules. A comprehensive secondary and tertiary structural study strongly predicts conformational homology among these proteins in spite of weak primary sequence similarities. A common tertiary structural motif, the four alpha-helix bundle, is predicted to be the evolutionarily conserved fold in these related proteins. Distinct helices and loops of the bundle structure are partitioned to homologous exons in growth factor genes. Conserved introns in these genes map to exposed loops connecting the 1st and 2nd, and 3rd and 4th helices of the bundle, regions that are predicted to be important in receptor binding. Furthermore, these introns are sites of size hypervariability. Genetic intrusion is then postulated to have driven the divergence of these numerous growth factors from an ancestral (four-helix bundle) progenitor molecule.

TU-PM-A10 THE EFFECTS ON ENZYME ACTIVATION OF GENETICALLY-ENGINEERED AMINO ACID DELETIONS IN THE CALMODULIN LONG HELIX. Anthony Persechini, Diane O. Hardy, Donald K. Blumenthal[1], Harry W. Jarrett[2], and Robert H. Kretsinger (Intr. by Brian R. Duling). Department of Biology, University of Virginia, Charlottesville, VA 22901. [1]Department of Biochemistry, UT Health Science Center at Tyler, Tyler, TX 75710. [2]Department of Biology, Purdue University School of Science, Indianapolis, IN 46233

As seen in the crystal $(Ca^{2+})_4$-calmodulin consists of two Ca^{2+} binding domains, each of which contains a pair of E-F hands. The two domains are joined together by a long helix, within which the following segment is exposed to solvent: R74-K-M-K-D-T-D-S-E-E-E84. Specific changes in the primary structure of this region were made by performing site-directed mutagenesis of a calmodulin-encoding template, followed by expression in *E. coli* JM101. We have evaluated in enzyme assays purified proteins expressed from unaltered template and a series of templates in which DNA encoding residues E82, E82-E83, and S81-E84 has been deleted. V_m values for activation by all bacterial calmodulins of skeletal muscle myosin light chain kinase and plant NAD kinase are, respectively, 10% less and 50% greater than for bovine calmodulin. Light chain kinase K_{act} values are not significantly different for bovine calmodulin and unaltered bacterial calmodulin, while corresponding NAD kinase values are 2-3 fold higher for the unaltered bacterial protein. NAD kinase and myosin light chain kinase K_{act} values for the altered calmodulins are all elevated 3-10 fold relative to values for the unaltered bacterial protein. Differences between bovine and unaltered bacterial calmodulins may be due to differences in post-translational processing. The bacterial protein does not contain trimethyllysine and its N-terminal alanine is not acetylated. These results indicate that the essential determinants for activation of myosin light chain kinase and plant NAD kinase are present in all the altered calmodulins. If the solvent-exposed region retains a helical structure, the deletions we have created would result in a relative movement of the Ca^{2+} binding domains by values of 1.5, 3.0, and 6.0 Å (translation); and 100, 200, and 400° (rotation). In order for altered proteins with these different conformations to form similar calmodulin-target complexes involving both Ca^{2+} binding domains, there must be a great potential for flexibility within the solvent-exposed region of the long helix. Alternatively, the calmodulin-target complex may involve only one domain or the other, so that their relative orientation is not critical. (supported in part by NSF grant DMB-8608878 and ACS grant JFRA-191)

TU-PM-A11 DYNAMIC LIGHT SCATTERING STUDIES OF PORCINE SUBMAXILLARY MUCINS AT LARGE SCATTERING ANGLES by B.K. Varma, A. Demers, A.M. Jamieson and J. Blackwell, Department of Macromolecular Science, Case Western Reserve University, Cleveland, Ohio 44106 U.S.A.

Dynamic light-scattering (DLS) studies of fractionated porcine submaxillary mucin glycoproteins (PSM) were carried out at large scattering vectors, where DLS behavior is strongly influenced by the internal configurational motions of the polymer chain. Our experiments were designed to explore the effects of solvation on PSM chain dynamics. The scattered intensity autocorrelation functions were measured as a function of scattering vector, PSM concentration, and molecular weight. Multi-exponential fitting methods were used to separate contributions of internal relaxation motions to the DLS data from the translational diffusion motion. The data were interpreted to determine values of the longest intramolecular relaxation time τ_1. The τ_1 values for PSM in 0.1 M NaCl and 6 M Gdn HCl are numerically similar when corrected for solvent viscosity and hydrodynamic volume, indicating similar hydrodynamic behavior for each solvent. These results are consistent with earlier studies which showed that the conformation of the heavily glycosylated PSM chain is not altered by denaturing solvents. Our studies are pertinent to understanding the relationship between mucin structure and the viscoelastic properties of mucin solutions and gels.

TU-PM-A12 SPECTROSCOPIC AND DSC STUDIES OF THE UNFOLDING AND REFOLDING OF SERUM RETINOL BINDING PROTEIN. D. Vincent Waterhous[1], Christie G. Brouillette[2] and Donald D. Muccio[1] Departments of [1] Chemistry and [2]Medicine. University of Alabama at Birmingham, 35294

Human serum retinol binding protein (sRBP) is a small molecular weight (21,000 D) globular protein expected to be a single domain from X-ray crystallography and is the vitamin A carrier protein in the blood. Thermal studies of sRBP were followed by circular dichroism (CD), absorbance (ABS) and differential scanning calorimetry (DSC). Changes in the far UV CD spectra with temperature at pH 7.4 have been analyzed in terms of a two state thermal unfolding-refolding and are found to be reversible. The midpoint temperature, Tm, is found at 77.8°C and the enthalpy change ($\Delta H°_{vH}$) is calculated to be 111 kcal/mol from a van't Hoff analysis of this data. The DSC results yield a nearly identical enthalpy and Tm to the aforementioned results. However, the temperature dependence of the near UV CD band centered at 320 nm and the ABS band centered at 330 nm due to the noncovalently bound retinol chromophore suggests a conformation change occurs prior to the unfolding of sRBP. Reversibility of this transition is dependent on the presence of retinol whereas no such dependence is found in the far UV CD. The data can be interpreted in terms of a three state model, $N \rightleftharpoons I \rightleftharpoons D$, where the first transition from the native protein, N, to an intermediate, I, (which goes undetected by DSC) has a much lower $\Delta H°_{vH}$ and Tm. The spectral results are consistent with tertiary structural changes localized near the retinol without changes in the secondary structure for the first transition. The second transition involves changes in the secondary structure of the protein. This work was supported in part by PO1 CA28103-08 from NCI.

TU-PM-B1 WATER DENSITY IN MONOLAYER AND BILAYER STATES. D. H. Wolfe and H. L. Brockman, Hormel Institute, University of Minnesota, Austin, Minnesota 55912

A water-based, quasi, two-dimensional equation of state has been developed and applied to surface pressure-area isotherms for lipids determined at the argon-buffer interface. The ratio of activity coefficients of water in surface and bulk phases, f_1, is > 1.0 for all lipids. Following the interpretation of such rationalized activity coefficients in bulk systems, f_1 can be considered as a linear scaler for the dimensions of water in the surface phase relative to bulk. If so, the density of interfacial water should be scaled by $1/f_1^3$. Applying this concept to the interpretation of X-ray spacing data for fully hydrated phospholipid bilayers yields lipid molecular areas equal to measured monolayer collapse areas. Assuming their equivalence, an equation of state relating surface force, surface pressure, area and lamellar spacing in bilayers was developed and successfully used to determine f_1 from published data for d-spacing of egg phosphatidylcholine as a function of osmotic pressure. Overall, the results show the importance of water activity in determining interfacial structure and indicate a thermodynamic equivalence of monolayer and bilayer states. (Supported by NIH grants HL 07311, HL 08214, HL 23003 and the Hormel Foundation.)

TU-PM-B2 *BEHAVIOR OF WATER IN HYDRATED LIPID BILAYERS.* Russell E. Jacobs & Stephen H. White, Dept. Physiology & Biophysics, UC Irvine, Irvine CA 92717.

The hydration properties of oriented and unoriented POPC lipid bilayers in $H_2O/^2H_2O$ mixtures have been investigated using ^2H NMR techniques. Oriented bilayer systems are typically employed for diffraction work, while unoriented dispersions are used in most magnetic resonance studies. In this work we examine the differences and similarities of these two bilayer systems. Quadrupolar splittings, T_1, $T_{2(Q\text{-echo})}$, and $T_{2(Q\text{-CPMG})}$ (Bloom & Sternin, Biochemistry 1987, 26, 2101) have been measured as a function of water content. Beginning with a dry sample, the lipid was hydrated via the vapor phase with the relative humidity (RH) maintained by the presence of a reservoir of saturated salt solution. Changing the RH from 34 to 93% caused a monotonic change in all the ^2H NMR parameters, splittings: 1.4->0.8 kHz, T_1: 14->60 msec, $T_{2(Q\text{-echo})}$: 8->30msec. Initial work indicates that $T_{2(Q\text{-echo})}=T_{2(Q\text{-CPMG})}$ in oriented samples, while $T_{2(Q\text{-echo})}>T_{2(Q\text{-CPMG})}$ in unoriented samples. In no case has signal attributable to isotropic water been observed. Since the dominant relaxation mechanism for deuterium is quadrupolar relaxation and the various relaxation times are sensitive to different time scales of motion, a quantitative interpretation of the relaxation times in terms of rate(s) of molecular motion is feasible. Models encompassing both average static and dynamic aspects of the interaction of water molecules with the lipid bilayer surface will be presented. This work supported by grants from the NIH and AHA. REJ is an Established Investigator of the American Heart Association.

TU-PM-B3 THE EFFECT OF UNSATURATION ON THE STRUCTURE AND THERMOTROPIC PROPERTIES OF CEREBROSIDES. R.A. Reed. Biophysics Institute, Boston University School of Medicine, Boston, MA 02118

Differential scanning calorimetry (DSC) and x-ray diffraction have been used to study hydrated N-stearoyl, -oleoyl, and -linoleoyl galactosyl sphingosine (NSGS, NOGS, and NLGS respectively). DSC of hydrated (70 wt.% H_2O) NSGS shows an endothermic transition at 85°C (ΔH=18.0 Kcal/mol NSGS), and a broad exothermic transition at 30-60°C dependent upon the previous cooling rate. X-ray diffraction patterns recorded at 21, 61, and 86°C provide evidence for interconversions between metastable and stable crystalline NSGS bilayer phases. The properties of the unsaturated cerebrosides were more complex. Hydrated NOGS gave a single endothermic transition at 44.8°C (ΔH=11.5 Kcal/mol NOGS). However, incubation of NOGS at 49°C for 24 hrs resulted in a second transition at 55.5°C. By cycling NOGS between 0 and 49°C complete conversion into this higher melting phase (ΔH=12.1 Kcal/mol NOGS) was achieved. X-ray diffraction at 21, 47, and 59°C confirmed a bilayer phase at all temperatures and delineated the interconversions between two crystalline phases at 21°C (d=55.3Å) and 47°C (d=69.5Å), and a liquid crystalline phase at 59°C (d = 52.0Å). The more unsaturated NLGS gave two transitions, a sharp transition at 28°C (ΔH=8.0 Kcal/mol NLGS) and a broad transition at 42°C (ΔH=0.4 Kcal/mol NLGS). Again, incubation between the two transitions led to a single transition at 44°C (ΔH=9.3 Kcal/mol NLGS). X-ray diffraction at 0, 34, and 55°C demonstrated conversions between crystalline bilayers at 0°C (d=57.0Å) and 34°C (d=69.0Å), and a liquid crystalline bilayer phase at 55°C (d=51.5Å). Thus, unsaturation in the amide-linked hydrocarbon chain has profound effects on the structural properties of cerebrosides.

TU-PM-B4 STRUCTURE AND DYNAMICS OF α-TOCOPHEROL IN MODEL MEMBRANES AND IN SOLUTION: A BROADLINE AND HIGH RESOLUTION NMR STUDY. I.H. Ekiel*, L. Hughes*, G.W. Burton*, P.A. Jovall**, K.U. Ingold* and I.C.P. Smith*. *Division of Biological Sciences, National Research Council of Canada, Ottawa, Ontario, Canada K1A 0R6. *Division of Chemistry, National Research Council of Canada, Ottawa, Ontario, Canada K1A 0R6. **Department of Biochemistry and Biophysics, Chalmers University of Technicology, S-41296 Gothenburg, Sweden.

Nuclear magnetic resonance has been applied to study the conformational dynamics of α-tocopherol (Vitamin E) in solution and in model membranes. In non-viscous solution, ^{1}H NMR showed that α-tocopherol is in rapid equilibrium between two or more puckered conformers of its heterocyclic ring. The most likely conformers to be so involved are the two half chair forms. Deuterium NMR spectra of specifically deuterated α-tocopherol in multilamellar dispersions of egg phosphatidylcholine, measured in the liquid crystalline state, were characteristic of axially symmetric motional averaging. The orientation of the rotational axis within the molecular framework was determined. Studies on oriented multilamellar membranes revealed that this axis is perpendicular to the surface of the membrane. The profile of quadrupolar splittings along the hydrophobic tail does not have a plateau, in contrast to that of the fatty acyl chains of the membrane lipids. Longitudinal relaxation times T_1 were short. The presence of a minimum in their temperature dependence shows that molecular motion with effective correlation time $\tau_{eff} \approx 3.10^{-9}$ s is responsible for relaxation. However, the temperatures and absolute values of the minima depend on the position of the deuterium in the molecule, demonstrating that τ_{eff} represents a complex blend of motions.

TU-PM-B5 The Elasticity of Bilayers of Anionic Phospholipids is Dominated by Ionic Strength. Is This due to Charge Density or to Ion Binding? Rutkowski, C., Li, W., Cummins, H. Z., Green, M. and Haines, T. H. Chem. and Phys. Depts. City College of CUNY, New York, NY 10031.

Using photon correlation spectroscopy (PCS) we have measured the modulus of preparations of uniform vesicles of anionic phospholipid bilayers swollen by osmotic pressure. The vesicles vary in their initial size from 200nm to 600nm. The vesicles swell linearly (following a modulus) to the bursting point. The data provide a modulus, the % surface expansion at bursting and the transbilayer pressure at bursting. DOPG or DOPA vesicles in 0.15 M KCl or NaCl are significantly less elastic than the same vesicles in non-electrolytes. Such data can be explained by ion concentration changes in the diffuse double layer using the Gouy-Chapman theory. Alternatively it can be explained by selective cation binding to the polyanionic surface. Studies on the surface charge density of DOPG bilayers suggest bilayers in K^+ and Na^+ solutions display lower charge density than is predicted by one charge per headgroup. In contrast the same bilayers in Cs^+ or tetramethyl ammonium have a higher charge density (approximating one charge per headgroup). Measurement of the modulus in a variety of cationic chloride solutions has allowed us to begin to sort out the contributions of the ionic binding and the charge density contributions to the modulus.

TU-PM-B6 THEORETICAL COMPARISON OF THE SELF DIFFUSION AND CONCENTRATION DIFFUSION OF INTERACTING MEMBRANE PROTEINS. Bethe A. Scalettar (1,3), James R. Abney (2,3), and John C. Owicki (2,3). (1) Division of Chemical Biodynamics and (2) Division of Biology and Medicine, Lawrence Berkeley Laboratory, University of California, and (3) Department of Biophysics and Medical Physics, University of California, Berkeley, CA 94720.

Membrane proteins can either be uniformly or inhomogeneously distributed in the plane of the bilayer. We show that this characteristic of protein arrangement can profoundly influence diffusional processes in the membrane.

If there are no lateral concentration gradients of protein in the bilayer, Brownian diffusive forces merely cause each particle to move randomly in two dimensions while leaving the macroscopic protein distribution unchanged. However, if the lateral density of the system varies with position, Brownian motion will lead to observable changes in protein arrangement. In a uniform system the particles are said to undergo self diffusion; in an inhomogeneous system the protein molecules exhibit concentration diffusion. If the particles do not interact, a single diffusion coefficient will describe both of these processes. However, membrane proteins do interact, and these interactions can produce markedly different density-dependent changes in the self- and concentration-diffusion coefficients.

We have cast into a two dimensional form the three dimensional diffusion theories of Ohtsuki and Okano (*J. Chem. Phys. 77:* 1443, 1982) and Felderhof (*J. Phys. A: Math. Gen. 11:* 929, 1978). The theories quantitatively pertain only to dilute systems; however, our qualitative conclusions should be valid for systems of all densities. Results were obtained for three analytical potentials: hard core repulsive, softly repulsive, and softly repulsive with weak attractions. Self diffusion is always inhibited by interactions. In contrast, concentration diffusion slows in the presence of attractions and is enhanced by repulsions. We note that both self and concentration diffusion are important physiologically and are monitored experimentally; therefore, the interaction-dependent differences in these phenomena should be noted.

This work was supported in part by National Institutes of Health grant AI-19605. Bethe Scalettar and James Abney are currently supported by appointments to the Alexander Hollaender Postdoctoral Fellowship Program sponsored by the Department of Energy.

TU-PM-B7 KINETICS OF FIRST ORDER AND FINITELY COOPERATIVE PHASE TRANSITION. APPLICATION TO DPPC MEMBRANE. Istvan P. Sugar Depts. of Biomath. Sci. and Phys./Biophys., The Mt. Sinai Med. Ctr. N.Y. 10029 and Inst. of Biophys., Semmelweis Med. Univ., Budapest

Phase transition kinetics have been calculated for systems which possess short-range order but do not show long-range order during the transition. The gel--liquid crystalline transitions of phospholipid membranes are considered as the prototypes of these phase transitions (I. Sugar, J.Phys Chem. (1987) 91:95).

The phase transition has been considered as a stochastic process, where the number of the gauche isomers is the stochastic variable. The transition probabilities of the elementary steps of the process have been determined by means of the cooperativity function and free energy function of the system. The cooperativity in the function of the fractional completion has been deduced from the equilibrium calorimetric data. The free energy function was taken from R. Priest's membrane model (Mol. Cryst. Liq. Cryst. (1980) 60:167). The stochastic equation of the transition process has been solved numerically when the transition is excited by: i/ linear heating/cooling, ii/ T up/down jump, iii/sinusoidal temperature change. The time evolutions of the probability distribution and different thermodinamic averages (order parameter, order parameter fluctuation, enthalpy, free energy) have been determined. (Supported by Dr. T.E. Thompson's USPHS grant GM-14628)

TU-PM-B8 EFFECTS OF LIPID COMPOSITION ON THE BINDING OF LASALOCID A TO SMALL UNILAMELLAR PHOSPHOLIPID VESICLES. Ron Grunwald†, Ned Porter*, and George Painter†, †Wellcome Research Laboratories, Research Triangle Park, NC 27709 and *Dept of Chemistry, Duke University, Durham, NC 27706. (intro. B.C. Pressman)

The binding of the carboxylic ionophore Lasalocid A (X537A) to small unilamellar phospholipid vesicles has been examined by steady state fluorescence spectroscopy. The ionophore fluorescence emission is sensitive to the protonation state of the ionophore and to the polarity of the the fluorophore environment. The increase in fluorescence intensity observed upon interaction with phospholipid (PL) vesicles is used to calculate an apparent binding constant (K_{app}) for the anionic ionophore with DMPC vesicles (pH 9.4, 31°C) of 2.2 x 10^4 M^{-1}. The protonated species has a greater affinity for DMPC vesicles (K_{app} = 5.3 x 10^4 M^{-1}, pH 4.5). The lipid phase state of the DMPC vesicle has no effect on K_{app} at pH 9.4. In contrast, the K_{app} for the protonated ionophore (pH 4.5) decreases sharply below the phase transition temperature. Above the phase transition temperature, the binding of both the anionic and protonated ionophore appears to be driven by hydrophobic interactions. Below the phase transition temperature the binding of the protonated species is driven by a large negative ΔH. K_{app} decreases with mixed PL/PC vesicles in the order PC>PE>PG≥PA, while incorporation of cholesterol or unsaturated acyl chains has little effect on binding at pH 9.4. The decrease in binding affinity with negatively charged lipids can be attributed to charge repulsion and is accompanied by a change in binding mechanism. These results are interpreted in terms of the location the protonated and unprotonated ionophore. It is concluded that the unprotonated ionophore is bound at the membrane surface and the primary determinates of binding are surface packing density of the polar head groups and membrane surface potential. In contrast, the protonated ionophore distributes within the bilayer and is effected by the phase state of the acyl chain region. We find no evidence for specific interactions of Lasalocid A with PE.

TU-PM-B9 LIPID STABILIZED AMPHOTERICIN B COMPLEXES: A MOLECULAR RATIONALE FOR THE ATTENUATION OF TOXICITY. A.S. JANOFF[1], L. T. Boni[1], M.C. Popescu[1], P.R. Cullis[2], T.D. Madden[2], T. Taraschi[3], S.M. Gruner[4], E. Shyamsunder[4], M.W. Tate[4], R. Mendelsohn[5] and D.P. Bonner[6]. [1]The Liposome Company, Inc., Princeton, NJ, [2]Department of Biochemistry, University of British Columbia, [3]Department of Pathology, Thomas Jefferson University, [4]Department of Physics, Princeton University, [5]Department of Chemistry, Rutgers University, [6]The Squibb Institute for Medical Research, Princeton, NJ

Previously undescribed ribbon-like structures result when Amphotericin B interacts with lipid in an aqueous environment. At high Amphotericin to lipid ratios these structures, which are lipid stabilized Amphotericin aggregates, become prevalent resulting in a dramatic attenuation of Amphotericin mediated mammalian cell but not fungal cell toxicity. Studies utilizing freeze-etch electron microscopy, differential scanning calorimetry, phosphorous NMR, x-ray diffraction and optical spectroscopy revealed that this toxicity attenuation is related to the macromolecular structure of the ribbons in a definable fashion. It is likely that Amphotericin in this unique form will have a much improved therapeutic utility.

TU-PM-B10 PARTITION OF HEADGROUP-LABELED FLUORESCENT LIPIDS BETWEEN COEXISTING GEL AND LIQUID-CRYSTAL PHASES IN MULTILAMELLAR PHOSPHOLIPID VESICLES. K. Florine-Casteel* and G.W. Feigenson, Section of Biochemistry, Molecular and Cell Biology, Clark Hall, Cornell University, Ithaca, NY 14853.

The partition behavior of the headgroup-labeled fluorescent lipid probes NBD-eggPE, NBD-dipalmitoyl-PE (NBD-DPPE), rhodamine B-PE (Rho-PE), and octadecyl rhodamine B (R18) between coexisting thermotropic or Ca^{2+}-induced lipid gel phase and fluid liquid-crystal phase in multilamellar phospholipid vesicles has been investigated using contact quenching of probe fluorescence by the spin-labeled phosphatidylcholine (7,6)PC in binary lipid mixtures of well-characterized phase behavior. In DPPC/(7,6)PC vesicles, all probes partition into the fluid phase with K_p = 2-3, except for NBD-DPPE for which K_p = 1. In dioleoylphosphatidylserine (DOPS)/(7,6)PC in the presence of excess Ca^{2+}, the NBD probes partition even more strongly into the fluid phase, with K_p = 6-7, while Rho-PE and R18 appear to strongly favor the interfacial regions between $Ca(PS)_2$ gel and PS/PC fluid liquid domains.

*Present address: Laboratories for Cell Biology, Department of Cell Biology and Anatomy, School of Medicine, University of North Carolina at Chapel Hill, Chapel Hill, NC 27599.

TU-PM-B11 PARTITION STUDIES OF FLUORESCENT LYSOLIPIDS IN SMALL UNILAMELLAR VESICLES OF PHOSPHATIDYLCHOLINES: AN APPROACH TO pH-SENSITIVE LIPOSOMES. Inga-Mai Tegmo-Larsson and Lisa N. Gentile, Department of Chemistry, Colgate University, Hamilton, NY 13346

A series of single chain lipids with amino acid head groups have been synthesized and incorporated into the walls of DPPC & DHPC SUVs for the purpose of investigating the potential use of these vesicles as drug carriers in cancer therapy. Release studies of the entrapped water soluable dye, calcein, by fluorescence spectroscopy gave us an estimate of the relative permeability and fluidity of the vesicles. However, these liposomes showed limited pH-effect in the range 6.0-8.5 and low stability. With the aim of assessing the distribution and location of the lysolipids in the bilayer we decided to undertake a study of the intrinsic photophysical properties of tryptophan and tyrosine as head groups. The fluorescence characteristics of N-Palmitoyltryp and N-PTyr were determined in homogeneous media of different polarity and in liposomes. They revealed a red shift of maximum emission with increasing polarity and a shift to longer wavelength was also observed when the liposomes were lysed into the aqueous medium. Quenching studies by adding acrylamide as well as Cs^+ & I^- ions to preformed liposomes led to significant decrease of Tryp and Tyr fluorescence with acrylamide but insignificant effects were seen with Cs^+ & I^-. All three quenchers were however effective in homogeneous media. Fluorescence polarization decreased with increasing temperature in the liposomes. From these data we postulate that the Tryp & Tyr lysolipids are located within or close to the hydrophobic lipid bilayer. pH-sensitive lysolipid headgroups might therefore be mainly uneffected by changes in pH of the external environment. Efficient energy transfer from N-PTyr to N-PTryp in vesicles suggests a uniform distribution within the bilayer.

TU-PM-B12 CHOLESTEROL EXCHANGE BETWEEN VESICLES. EFFECTS OF SUBSTITUTING ESTER LINKAGES IN PHOSPHATIDYLCHOLINE BY ETHER OR AMIDO LINKAGES. Robert Bittman, Chu-cheng Kan, Department of Chemistry, Queens College of CUNY, Flushing, NY 11367, and S.K. Bhatia, Joseph Hajdu, Department of Chemistry, California State University, Northridge, CA 91330.

As part of our program to understand the factors influencing cholesterol movement between membranes, we have synthesized a series of PC analogs and incorporated them into SUVs with [C-14]cholesterol. Donor SUVs contained 6 mol% cholesterol, 79 mol% phospholipid, 15 mol% dicetyl phosphate; acceptors (10-fold excess) contained 6 mol% cholesterol, 94 mol% dipalmitoyl-PC, and [9,10-H-3]triolein. The incubation medium contained 2% (w/v) albumin. PC's with N-palmitoyl-aminodeoxy (RCONH-) at the sn-2 position are: A, 1-O-hexadecyl and B, 1-thiohexadecyl. The half-times for [C-14]cholesterol exchange at 50°C were: A, 296 and B, 245 min; the difference in rates indicates the influence of hydrogen bonding of oxygen vs. sulfur atoms at the sn-1 position to nearest neighbors. A faster exchange rate (207 min) was observed in SUVs prepared with the carbamate analog (ROCONH-) of B. Much tighter packing was found in bilayers containing 79 mol% N-palmitoylsphingomyelin; complete exchange of cholesterol took place with a half-time of 1409 min. Thus, the amido group appears to contribute such less to the decrease in cholesterol exchange kinetics than the RCH=CH(OH)- group of the sphingomyelin molecule. However, the amido group induces tighter packing than the corresponding ester group. The half-times for cholesterol exchange from DPPC (192 min) and 1-palmitoyl-2-thiopalmitoyl-PC SUVs (119 min) also indicate weaker packing of thio- vs. oxygen-containing groups. (Supported by NIH HL 16660)

TU-PM-B13 KINETICS OF MOVEMENT OF SYNTHETIC [C-14]CHOLESTEROL ANALOGS BETWEEN MEMBRANES.

Robert Bittman, Chu-cheng Kan, and Jiasheng Yan, Department of Chemistry, Queens College of CUNY, Flushing, NY 11367.

The following cholesterol analogs were synthesized with C-14 at the 4 position: epicholesterol, 3α-triethoxycholesterol, dihydrocholesterol, and 3α- and 3β-cholesteryl amine. These sterols were incorporated at 24 mol% into SUVs prepared with 61 mol% dipalmitoylphosphatidylcholine (DPPC) and 15 mol% dicetyl phosphate. Acceptor SUVs contained 24 mol% of the sterol undergoing exchange and 76 mol% DPPC. The half-times for [C-14]sterol exchange at 50°C in the presence of 2% albumin were: dihydrocholesterol, 477 min; cholesterol, 362 min; 3α-triethoxycholesterol, 42 min; epicholesterol, 38 min. In this system, [C-14]β-sitosterol (24α-ethylcholesterol) underwent faster exchange ($t_{\frac{1}{2}}$ = 302 min) than cholesterol; however, when donor SUVs contained egg PC instead of DPPC exchange of sitosterol was much slower than that of cholesterol ($t_{\frac{1}{2}}$ = 173 min for sitosterol, 44 min for cholesterol). The results are discussed in terms of the molecular packing of sterol and PC in the donor SUVs vs. the aqueous solubility of the sterol. (Supported by NIH Grant HL 16660)

TU-PM-C1 DEVELOPMENT OF A TRANSIENT OUTWARD CURRENT IN *XENOPUS* SPINAL NEURONS DIFFERENTIATING IN CULTURE. Angeles B. Ribera and Nicholas C. Spitzer, Department of Biology, B-022, University of California, San Diego, La Jolla, CA 92093

During the first day in culture, embryonic amphibian spinal neurons undergo marked changes in the ionic dependence and duration of their action potential. Increases in density and accelerated kinetics of sodium and delayed rectifer and calcium-dependent potassium currents during the same period contribute to this maturation of the action potential, with potassium current showing the most substantial changes. During the second day in culture, the duration of the action potential continues to decrease significantly but to a smaller extent (from 1.6 to 1.3 msec). We have investigated whether there are changes in outward current during this period that may underlie this change. The delayed rectifier current, which increases three fold in density and activates twice as rapidly after the first day in culture, shows no further increase in its density or rate of activation during the second day in culture. However, inspection of the recordings from 2 day old neurons reveals that there is consistently a small inactivating component of the total outward current. Further investigation of this current necessitated isolating it from the much larger delayed rectifier current. The inactivating component is relatively insensitive to 2.5 mM tetraethylammonium and relatively sensitive to 1-2 mM 4-aminopyridine, although even at these concentrations 4-aminopyridine affects the delayed rectifier current as well. A cleaner separation of these two currents is achieved by isolating the current inactivated at a depolarized holding potential of -40 mV. An inactivating A-like current component is isolated in 100 % of the 2 day old neurons (n= 19) by subtracting the outward currents recorded in response to depolarizing voltage steps from a holding potential of -40 mV from those recorded at a holding potential of -80 mV. The same subtraction protocol applied to 1 day old neurons indicates that only 45 % of the neurons (n=11) possess a detectable A current. Thus, the maturation of this A current extends to times later than those involved in the development of the delayed rectifier current. The maturation of both the A current and the delayed rectifier current is blocked by chronic inhibition of RNA synthesis.

TU-PM-C2 RECONSTRUCTION OF ACTION POTENTIALS OF EMBRYONIC SPINAL NEURONS FROM WHOLE CELL VOLTAGE CLAMPED CURRENTS. Nicholas C. Spitzer (Intr. by P.A.G. Fortes), Department of Biology, B-022, University of California, San Diego, La Jolla, CA 92093

The long duration calcium-dependent action potential of embryonic *Xenopus* spinal neurons shortens by roughly two orders of magnitude during the first day in culture and becomes principally sodium-dependent. Whole cell voltage clamp recordings identify changes in voltage-activated calcium and sodium currents and both voltage-activated and calcium-dependent potassium currents (O'Dowd et al., in press). Reconstruction of the impulse was undertaken to understand the specific contributions of the separate currents to its maturation and to assess the extent to which together they fully account for its differentiation (see also Barish, 1986). The membrane action potential was simulated with a modification of a program for the cardiac action potential (Beeler and Reuter, 1977). Currents were described by Hodgkin-Huxley type equations that were adjusted to reproduce the four currents recorded from young and from mature neurons under voltage clamp. Currents characteristic of mature neurons yield action potentials ~1 msec in duration that depend principally on inward sodium current. Currents characteristic of young neurons produce action potentials ~ 100 msec in duration for which inward current is primarily carried by calcium. Calcium current shows no developmental change in peak amplitude. The normal doubling of sodium current density and appearance of an inactivating calcium-dependent potassium current exert opposing effects on the initial overshoot, but do not affect the duration of the action potential. The normal increase in voltage-activated potassium current in combination with the sustained calcium-dependent potassium current causes a large decrease in duration of the action potential, while the increase in rate of activation of the delayed-rectifier current has less effect. The changes in recorded currents can account for changes in recorded action potentials.

TU-PM-C3 CHARYBDOTOXIN INHIBITS THE 250 pS Ca^{2+}-ACTIVATED K^+ CHANNEL IN AORTA AND CONTRACTS AORTA SMOOTH MUSCLE. Jane A. Talvenheimo, Grant Lam, and Craig Gelband (Intr. by Birgit Rose) Dept. of Pharmacology (R-189), Univ. of Miami, P.O. Box 016189, Miami, FL. 33101

Charybdotoxin (CTX), a peptide toxin isolated from scorpion venom (Smith et al., J. Biol. Chem. 261: 14607, 1986), inhibits large conductance Ca^{2+}-activated K^+ channels from skeletal muscle (Miller et al., Nature 313: 316, 1985). We tested the effect of CTX on vascular smooth muscle by applying 1-5 nM CTX to rabbit aorta rings. CTX caused slow reversible contraction, which was not blocked by the α-adrenergic antagonist phentolamine, but was reversed by the vasorelaxant BRL 34915. Vascular smooth muscle contains at least two types of voltage-dependent Ca^{2+}-activated K^+ channel: a 92 pS channel and a 270 pS channel (Inoue et al., Pflug. Arch. 405: 173, 1985). We incorporated large conductance Ca^{2+}-activated K^+ channels from bovine aorta plasma membranes into planar lipid bilayers. The channel had a conductance γ_S = 254 pS in symmetric 150 mM KCl, was selective for K^+ (P_K/P_{Na} = 7), was voltage-sensitive, and was activated by Ca^{2+} on only one side (designated the "intracellular" side) of the bilayer. CTX reversibly inhibited the 254 pS channel when added to the "extracellular" side, reducing P(open) without affecting γ_S. At V_m = +20 mV (cell convention) in symmetric 150 mM KCl, 50 μM Ca^{2+}, CTX reduced P(open) with a K_i of 1.1 nM. CTX inhibition of the channel was not antagonised by BRL 34915. These results suggest that CTX contracts aorta by depolarization resulting from inhibition of the 254 pS Ca^{2+}-activated K^+ channel. (Supported by grants from the MDA and NIH RO1 HL36029.)

TU-PM-C4 ATP-SENSITIVE K^+-CHANNELS IN H^+-ATPase MUTANT OF THE YEAST SACCAROMYCES CEREVISIAE.

J.A. Ramirez, V. Vacata, W.G. Owen & H. Lecar, Department of Biophysics and Lawrence Berkeley Laboratory, University of California, Berkeley, CA 94720.

Patch-clamp studies of pmal-105 mutant of the yeast S. cerevisiae, a mutant of the gene which codes for the plasma-membrane H^+-ATPase, reveal K^+ channels activated by intracellular ATP. Excised patches of membrane exposed to micromolar concentrations of ATP show increased channel activity at both positive and negative voltages. The effect is reversible, and the channels are not activated by ADP or the ATP analog ATP-γ-S. The proton-pump inhibitor, DCCD, blocks the channels completely. The parent strain containing the wild-type gene has similar voltage-gated K channels, but does not exhibit ATP sensitivity. The unit conductance with 150 mM K^+ inside and outside the patch pipette is 17 pS. The probability of channel opening as a function of membrane potential was measured in both the mutant and the parent strain. The probability curve shows two sigmoid regions, with opening probability increasing at both positive and negative potentials. In the parent strain, probability of opening is independent of ATP concentration, but in the mutant the addition of micromolar concentrations of ATP shifts both the positive and negative gating regions towards zero mV. Since the mutation specifically alters the association of ATP with the ATPase binding site, the strong shifts in the K^+ channel gating suggest that there is close contact between the K^+ channel and the multimeric ATPase complex.

TU-PM-C5 A MAXIMUM IN CONDUCTANCE OCCURS FOR THE LARGE Ca-ACTIVATED K CHANNEL AT HIGH Rb CONCENTRATION. **A. Villarroel, O. Alvarez and G. Eisenman. Physiol. Dept. UCLA Med. School and Biol. Dept. Univ. of Chile.** **Supp. by USPHS GM24749, NSF BNS8411033 and FONDECYT 483-1987.**

Although a maximum in conductance with increasing ion concentration is expected for a multi-ion channel, no maximum has been reported to date for the large Ca-activated K channel channel (K(Ca)channel). We show here that a maximum is indeed found for the K(Ca) channel when its I-V behavior is studied for Rb over a broad range of concentration by voltage ramps of single rat t-tubule channels in neutral bilayers (see I-V's in the figure, noting that I at 2000 mM > I at 3000 mM). We also show that I-V shape for K is undistorted by fast block from contaminant (sub-μM) levels of Ca. The Rb data can be described by the same 2-ion barrier model used before for K, with the same (species independent) values of surface charge, locations of barriers and wells, and repulsions. Indeed, only the energy levels are species specific. The maximum in conductance with increasing concentration is shown in the figure by the I^{80} data points and the theoretical curves for log I^{80} vs. log C_{Rb}. Compared to K, the inner well for Rb is deeper and the outer well is less deep. Because Rb binding to the inner site is stronger than K the channel reaches the 2-ion state at a measurable concentration for Rb (see calculated occupancies for the outer|inner sites: empty (0|0), 1-ion (0|Rb, Rb|0), and 2-ion (Rb|Rb). Errata: Interchange "outer" and "inner".

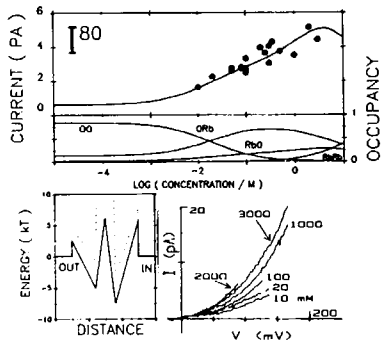

TU-PM-C6 EXTERNAL PERMEANT CATIONS LOCK Ba^{++} IONS INTO THE LARGE Ca^{++}-ACTIVATED K^+ CHANNEL.

Jacques Neyton and Christopher Miller, Graduate Dept. of Biochemistry, Brandeis Univ., Waltham, MA 02254

Internal Ba^{++}at micromolar concentrations induces long-lived blocking events in the high-conductance Ca^{++}-activated K^+ channel from rat muscle inserted into planar lipid bilayers. These experiments study the effects of external K^+ and other ions on the kinetics of internal Ba^{++} block. In the presence of 150 mM internal KCl, the off-rate for Ba^{++} is high ($\sim$4 s^{-1} at 50 mV) in the rigorous absence of external K^+ (with 150 mM external NaCl). The Ba^{++} off-rate decreases profoundly when external K^+ is added over the range 50μM-1mM. Concomitantly, the voltage dependence of the off-rate changes sign as external K^+ is increased; at zero external K^+, Ba^{++} off-rate increases with depolarization, while above 10 mM K^+, the off-rate decreases with depolarization. The efficacy of external ions to lower the off-rate for Ba^{++} decreases in the order $Rb^+ \sim Tl^+ > K^+ > Cs^+ > NH4^+$. The results conform to a picture in which Ba^{++}, entering the channel's conduction pathway from the internal solution, can leave either to the external or internal solution. Occupancy of a site near the external solution by K^+, however, prevents Ba^{++} from leaving to that side, and forces dissociation to the inside only, a process which is slower than dissociation to the outside. Thus, external K^+ "locks" Ba^{++} into the channel.

TU-PM-C7 TRIMETHYLOXONIUM MODIFICATION OF THE HIGH CONDUCTANCE Ca^{2+}-ACTIVATED K^+ CHANNEL.
Roderick MacKinnon and Christopher Miller, Dept. of Biochemistry, Brandeis University, Waltham, MA 02254

Single Ca^{2+}-activated K^+ channels from rat skeletal muscle were studied in neutral phospholipid bilayers. Following insertion, channels were modified by adding 50mM trimethyloxonium (TMO) to the external solution. Modification decreases the single-channel conductance and the relative decrease is greater at low ionic strength. In symmetric K^+, the zero-voltage conductance of a modified channel is reduced by 50 percent when $[K^+]$=5mM, but the effect is less prominent as we raise ionic strength by increasing the K^+ concentration. (See figure.) Modification also increases the apparent K_d for external TEA block, but the difference is masked by raising the ionic strength. At 2mM external K^+ the K_d is 40μM in control channels and 80μM in modified channels. At 150mM external Na^+ the K_d is 200μM for both. Charybdotoxin (CTX) affinity for the channel is vastly decreased by TMO modification. Bound CTX protects the channel from TMO modification and TEA does not. We conclude that at least one carboxyl group resides close to the external mouth of the channel. TMO modification alters conductance by changing the local electrostatic potential. The carboxyl group is external to the TEA blocking site and participates in CTX binding, a result consistent with the proposal that CTX blocks by capping the pore.

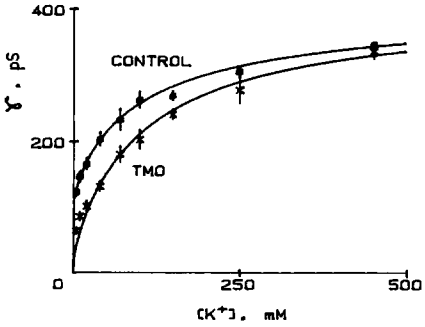

TU-PM-C8 CHARYBDOTOXIN BLOCKS VOLTAGE-GATED K^+ CHANNELS IN T LYMPHOCYTES. Steven B. Sands, Richard S. Lewis, and Michael D. Cahalan, Dept. of Physiology & Biophysics, UC Irvine, CA 92717.

A variety of scorpion venoms, including charybdotoxin, a peptide purified from *Leiurus quinquestriatus* venom, were tested for effects on voltage-gated potassium channels in human T lymphocytes, in a related cell line, Jurkat E6-1, and in mouse thymocytes, using the whole-cell patch clamp method. Nanomolar amounts of purified charybdotoxin blocked "type *n*" voltage-gated K^+ channels in human or murine T-lymphoid cells. These channels have a conductance of 18 pS, exhibit complex inactivation kinetics, and, by a variety of criteria, are not activated by intracellular calcium. A dose-response curve for block of K^+ channels by charybdotoxin in Jurkat cells was fitted with a K_i of 200 pM. Two additional populations of K^+ channels are found in $CD8^+$ (cytotoxic/suppressor) thymocytes from mice. One type, distinguishable from type *n* on the basis of inactivation kinetics and resistance to block by tetraethylammonium (TEA), was also blocked by charybdotoxin; we call this channel type *n'* to suggest a possible structural similarity to type *n* channels. A third channel type - *l*, named for its larger single channel conductance (27 pS)- is unaffected by 20 nM charybdotoxin. Type *n* K^+ channels were also blocked by several types of crude scorpion venom. Rates of recovery from block upon washout were slow and in some cases incomplete. We conclude that purified scorpion toxins will provide useful probes of voltage-gated K^+ channels in T lymphocytes, and that charybdotoxin is not selective for calcium-activated K^+ channels. We would like to thank Dr. Chris Miller for providing a highly purified form of charybdotoxin. Supported by NIH grants NS14609 and AI21808 and NIH postdoctoral fellowship NS08021 (RSL).

TU-PM-C9 Ba^{2+} AND Ca^{2+} TRAPPED INSIDE THE K^+ CHANNELS OF HUMAN T LYMPHOCYTES. Stephan Grissmer and Michael Cahalan (introduced by J. Hall), Dept. of Physiology & Biophysics, UC Irvine, CA 92717.

In the human T-cell line Jurkat E6-1 we investigated the effects of Ca^{2+}, Ba^{2+} and Rb^+ on the K^+ channel kinetics using the whole-cell voltage clamp technique. Depolarizing test pulses from -80 to +40 mV elicit rapidly activating K^+ currents which inactivate almost completely during 2-s pulses. On changing the bath solution from normal Ringer (2 mM Ca^{2+}), Ringer + 10 mM Ba^{2+} or 107 mM Ca^{2+} to 160 mM Rb^+ an additional slowly activating "hump" in the time course of K^+ current appeared during the initial test pulse to +40 mV given after the solution change. This slowly activating part of the K^+ current is not present during subsequent pulses. We assume that the "hump" represents removal of divalent ions from the K^+ channel. The difference between the first and second current traces in high $[Rb^+]_o$ would then represent the unblocking time course. The level of block of I_K by Ba^{2+} correlates with the initial amplitude of the difference current between the first and second trace after changing to high $[Rb^+]_o$, suggesting that the amplitude of the difference current reflects the percentage of K^+ channels blocked by divalent cations. From this correlation we conclude that 20% of the K^+ channels in normal Ringer are occupied by Ca^{2+}. The time course of the difference current is independent of the species of the blocking ion. A simple explanation for this is that Rb^+ binds to a site where it prevents the removal of Ca^{2+} or Ba^{2+} block. In this case the time course of the difference current would be limited by the time course for Rb^+ leaving its site. Raising $[Ca^{2+}]_i$ to 10^{-5} M resulted in an increase in the percentage of channels blocked by Ca^{2+} to 50%. We conclude that divalent cations can be trapped inside the channel in its closed state. Supported by a DFG fellowship Gr 848/2-2 (S.G.) and by NIH grants NS14609 and AI21808.

TU-PM-C10 MODULATION OF THE K-CURRENT BY PHOTORELEASED Ca IN SQUID GIANT AXONS. E. Perozo, J. Vergara and F. Bezanilla. Dept. of Physiology UCLA, Los Angeles CA 90024.

We have previously demonstrated that the K conductance in ATP depleted squid axons can be increased by up to 30% by intracellular calcium concentrations in the micromolar range (Perozo & Bezanilla, Biophys. J. 51:547a 1987). To study the kinetic properties of this calcium regulation we used the Ca-photoreleasable chelator nitr-5 in internally dialyzed voltage clamped axons. The axons were predialyzed for about an hour with a solution free of Ca and ATP. Nitr-5 was internally dialyzed at a concentration of 8 mM and 50 % saturated with Ca. The preparation was illuminated with a Xenon flash lamp, and a UV filter was used to select for short wavelengts. Flash effective duration was less than a millisecond and in the average, the energy content per flash was actinometrically determined at about 0.2 uEinstein/cm^2 in a bandwidth of 100 nm centered at 340 nm. Nitr-5 transformation was verified by spectral analysis of the dialysate before and after ligth flashes. The flash was triggered when the K current reached its steady value, and an additional outward current was elicited by the "Ca step". Such current did not appear in the absence of nitr-5 or when short wavelengths were blocked by a high bandpass yellow filter. The Ca induced current comprises 20% of the total outward current, shows an exponential time course and a steep voltage dependence. The change in free Ca concentration produced per flash was calculated to be between 2 and 5 uM, based on the steady state data. This value is consistent with the expected free Ca increase produced by the nitr-5 transformation. Ca relaxations lasted for at least during the voltage pulse (20 msec), but it was not maintained for long periods of time, probably reflecting the Ca buffering capacity of the axoplasm. Considering the time course of the effective flash, fast relaxations at high potentials are most likely limited by the Ca release process. The kinetics of K current activation was made slower by nitr-5 alone, independent of any light induced transformation. Thanks to R.Y. Tsien for the gift of nitr-5. Supported by MDA and USPHS grant GM 30376.

TU-PM-C11 ^{32}P LABELING OF MEMBRANE PROTEINS DURING ATP STIMULATION OF K-CURRENTS IN SQUID GIANT AXONS. E. Perozo, W.S. Agnew and F. Bezanilla. Dept. of Physiology UCLA, Los Angeles CA 90024 and Dept. of Physiology Yale University, New Haven CT.

K currents in squid axons can be modulated by an ATP-dependent phosphorylation process, with an increase in conductance and a slow-down of its turn-on kinetics (Biophys. J. 47:222a 1985 and 49:215a 1986). In order to study the molecular entities involved in such effect, internally dialyzed and voltage-clamped axons were exposed to γ ^{32}P ATP and subsequently the axon itself subjected to electrophoretic analysis. Three different types of experiments were performed: direct labeling with ^{32}P ATP, protection of phosphorylation sites with non-radioactive ATPγ-S and then labeling, or labeling and revertion of the effect by washing out the isotope. The internal solution contained (in mM) 310 K, 30 PO_4, 110 Glycine, 4 Mg, 1 EGTA, 0 Na, 0 Ca. The external medium was artificial sea water plus 300 nM TTX and 1 mM NaCN. 2 mCi of labeled ATP (3000 Ci/mmol) were diluted to a final concentration of 7 uM plus 50 uM carrier ATP. Axons were initially dialyzed with a 0 ATP internal solution for 1-2 h before addition of ^{32}P ATP, and the amplitude of the K-current was measured throughout the experiment by pulsing to 0 mV from a holding potential of -50 mV. Segments of axons from the voltage controlled zone of the chamber were extruded of axoplasm, placed in denaturing sample buffer (containing SDS and 2-mercaptoethanol) and sonicated for 1 min at 90° C. SDS-PAGE was used on gels with a linear acrylamide gradient of 4.5-15 %. The gels were stained with Comassie Brilliant blue and dried for autoradiogram exposure of 3 to 11 days. Electrophysiological correlates of I_K stimulation were compared with densitograms from gel autoradiograms. A group of bands labeled independently of the presence of ATPγ-S or the wash out, reflecting the isotope availability. These bands were used as the normalizing intensity per experiment. At high MW, three bands with MW 190, 265 and 290 Kd were labeled according to the amount of current stimulation by ^{32}P ATP, those peptides are highly marked by direct ^{32}P ATP incubation, but are faint if ATPγ-S is previously dialyzed or the isotope is washed out. Supported by MDA and USPHS grant GM30376.

TU-PM-C12 *CHEMICAL MODIFICATION OF K CHANNELS: MACROSCOPIC IONIC, GATING, AND SINGLE CHANNEL CURRENTS.* Sherrill Spires, Ruth Anne Eatock, Tara Nealey, and Ted Begenisich. Department of Physiology, University of Rochester, Rochester, NY 14642.

Treatment of the external surface of squid axons with the amino reagent trinitrobenzene sulfonic acid (TNBS) slowed the kinetics of the activation of potassium channel ionic current (by as much as 4-5 times) with a smaller (ca. two-fold) effect on the deactivation time course. In addition TNBS increased the magnitude of steady-state current (by 1.3 - 1.5 times). This latter effect is a function of membrane voltage: there is little effect near zero but an increasingly large effect at more depolarized potentials. The rate of reaction of TNBS was much faster at a pH of 9 compared to 7.5, consistent with its known reaction with the neutral form of amino groups. The specificity for amino groups is supported by the action of many other compounds with known reactivity toward these groups. All amino group-specific reagents investigated either produced the same qualitative effects as TNBS or were without effect. Methyl acetimidate produced results quantitatively as large as those produced by TNBS. 4-acetoamido-4'-isothiocyano-stilbene-2,2'-disulfonic acid (SITS) and succinic anhydride produced similar but smaller effects. Acetic anhydride and tetrahydrophthalic anhydride were without effect. Therefore, the functional modification of the channel proteins is independent of whether the reaction product preserves, neutralizes, or reverses the positive charge of the amino group. Potassium channel gating currents were also affected by treatment with TNBS. The kinetics of the charge movement were slowed but to a smaller extent than were the ionic currents. There was, however, a large reduction in the charge moved. In an effort to investigate the mechanism for the enhancement of macroscopic ionic current produced by TNBS, we examined the action of this reagent on single K channels in squid giant fiber lobe cells. (TNBS also increased the macroscopic ionic current in these cells). We found no significant effect of TNBS on the magnitude of single channel currents.

TU-PM-C13 A NEW INTERPRETATION OF THE EFFECTS OF MONOVALENT CATIONS ON POTASSIUM CHANNEL GATING IN SQUID AXONS. John R. Clay, Lab. of Biophysics, NINCDS, NIH, Bethesda, MD 20892.

K channel closing in squid axons is slowed by various monovalent metallic cations, most notably K^+ itself, as well as Rb^+ and Cs^+ (Swenson, R.P. and Armstrong, C.M. Nature 291:427-429,1981; Matteson, D.R. and Swenson, R.P. J. gen. Physiol. 87:795-816,1986; Clay, J.R. Biophys. J. 50:197-200, 1986). These results suggest that K channel gating and ion permeation may be coupled. Alternatively, the effect could be mediated by a direct action of cations on gating. In support of the latter view, I have recently observed a lack of effect of K^+ on K channel closing in some preparations, which provides a counterexample to the idea that gating and permeation are coupled. This result together with the lack of voltage dependence of the effect in preparations in which it does occur suggests that it is mediated at a site external to the electric field of the channel which, for unknown reasons, is accessible to K ions in some axons but not in others. Cs^+ and Rb^+ also slow K channel closing in all preparations thus far observed. However, the voltage dependence of these effects argues against a correlation between occupancy of the channel by these ions and channel gating. In particular 200 mM Cs^+ reduces the closing rate five-fold at -60 mV, whereas the effect is only two-fold at -120 mV. Blockade of inward current by external Cs^+ demonstrates that occupancy increases with hyperpolarization from -60 to -120 mV, which is opposite to the effects of Cs^+ on gating. This result and similar negative correlations between the effects of Rb^+ on gating and the IV relation suggest that these ions also modify channel kinetics by acting directly on the gating process.

TU-PM-C14 INWARD AND OUTWARD IONIC CURRENTS OF ISOLATED DOG CORONARY SMOOTH MUSCLE CELLS AND EFFECTS OF ACh AND MINOXIDIL SULFATE. **DIXON W. WILDE AND KAI S. LEE, CARDIOVASCULAR DISEASES RESEARCH,THE UPJOHN CO.,KALAMAZOO,MI.**

Membrane ionic currents were examined using freshly dispersed, single,coronary smooth muscle cells from the beagle. Microelectrode recordings of relaxed cells averaging 97 x 7 μm showed a mean resting membrane potential of -47 mV (n=55). Voltage-clamp analyses utilized the suction-pipette with intracellular dialysis. Depolarizing steps produced a robust, fast activating, time dependent outward current appearing at -45 mV and increasing with further depolarization to a maximum of 20 nA at +50 mV. The outward current was blocked by 20mM TEA,10mM Ba and by internal perfusion with Cs, establishing it as a K-current. The reversal potential shifted with the external K concentration indicating a K-selective channel. Removal of Ca_o reduced the outward current by 85%. A slowly decaying inward tail current was observed on repolarization from a depolarizing step. The tail current was abolished by Ca removal and potentiated by BAY k 8644. Replacement of K_i by Cs revealed a very slowly developing net inward current. This current had a -70 mV threshold and developed to nearly 1 nA at -30 mV. Time to peak was in excess of 600 msec. ACh increased the inward tail and elicited contraction. Minoxidil sulfate increased the K-current 1-2 times and reduced the slow inward tail current by >90% after long exposure. Canine coronary smooth muscle posesses at least two opposing ionic currents which may be essential for the regulation of coronary cell membrane potential and tone.

TU-PM-D1 MODIFICATION OF COLICIN E1 CHANNEL FUNCTION BY MUTATIONS IN THE COOH-TERMINAL DOMAIN. K. Shirabe[2], A.A. Peterson[1], J.W. Shiver[1], F.S. Cohen[3], A. Nakazawa[2] and W.A. Cramer[1] Dept. of Biol. Sci.[1], Purdue Univ., W. Lafayette, IN, 47907; Dept. of Biochemistry[2], Yamaguchi Univ. School of Medicine, Ube, Yamaguchi 755, Japan; Dept. of Physiol.[3], Rush Med. Coll., Chicago, IL, 60612.

Point mutants of the 522 amino acid channel-forming colicin E1, located in the COOH-terminal domain, were compared to the wild type protein with respect to: (i) cytotoxicity, (ii) pH and membrane potential dependence of channel activity in artificial membrane vesicles, (iii) binding to these vesicles, and (iv) activity and ion selectivity in planar membranes. (1) A G-502→E mutation, six residues from the end of the 35 residue hydrophobic segment had reduced [(5-10)-fold] cytotoxicity and *in vitro* activity in vesicles. The mutant was able to associate with vesicles, but was labeled to a smaller extent than wild type by a phospholipid photolabel probe. (2) A G-439→R mutation also resulted in a (5-10)-fold decrease in cytotoxicity. The mutant showed a decrease in *in vitro* channel activity assayed on membrane vesicles, but binding/insertion comparable to wild type. The dependence of channel activity on pH and membrane potential and the anion selectivity in planar membranes were similar to wild type. (3) A P-462→S mutation changed the only proline residue in the COOH-terminal domain, a residue conserved in five channel-forming colicins, and caused a decrease in the voltage dependence of channel activity in vesicles, but little change in cytotoxicity, ion selectivity, or pH dependence. It appears that Gly-502 resides in a hydrophobic membrane anchor region, and Pro-462 is involved in or affected by voltage gating of the channel. Gly-439 may be in an amphipathic membrane-spanning channel peptide. [Supported by a U.S.-Japan Cooperative Program through the NSF and JSPS, and NIH grants GM-18457 and GM-27367.]

TU-PM-D2 SITE-DIRECTED MUTAGENESIS OF THE CHARGED RESIDUES AT THE CARBOXY-TERMINUS OF THE COLICIN E1 CHANNEL. J.W. Shiver, W.A. Cramer, and F.S. Cohen[1], Dept. of Biol. Sci., Purdue Univ., W. Lafayette, IN, 47907, and Dept. of Physiol.[1], Rush Med. Coll., Chicago, IL, 60612 [Intr. by M. G. Rossmann].

The colicin E1 residues, D-509 and K-512, were changed to *amber* and *ochre* stop codons by site-directed mutagenesis. These charged residues immediately follow the 35 residue hydrophobic sequence which is thought to function as a membrane anchor for the colicin ion channel. D-509 is one of six conserved acidic residues in the carboxy-terminal, channel-forming portion of colicins A, B, E1, Ia, and Ib, and is the first charged residue following the hydrophobic segment. The basic residue K-512 may be important for binding to the membrane. Proteins truncated prior to these residues were obtained from a non-suppressing cell strain harboring a mutant plasmid, while full length colicin molecules with single residue changes to L-, S-, and Q- at 509 and Y- at 512 were obtained using appropriate suppressor strains. The truncated proteins, missing the last 14 or 11 residues and purified by immunoaffinity chromatography, displayed a similar low cytotoxicity, ~1% of intact colicin. The mutations with a single substituted residue showed a range of cytotoxicities, 40%, 20%, and 4% for S-509, Q-509, and L-509, respectively, and 57% for Y-512. Each of the latter proteins had *in vitro* channel activities, using membrane vesicles, comparable to that of wild type colicin at pH 4, although planar bilayer measurements indicated some loss of activity for S-509. *am*-509 was lytic with planar bilayers and each truncated protein was nearly ten-fold less active than wild type with membrane vesicles. It appears that the residues following N-511 are important for *in vitro* and *in vivo* activity, and the particular residue at position 509 for cytotoxicity. [Supported by NIH grants GM-18457 and GM-27367.]

TU-PM-D3 **Patch Clamping Astrocytes in Primary Cell Culture.** Charles L. Bowman, 105 Parker Hall, The Channel Group, Department of Biophysical Sciences, State University of New York at Buffalo, Buffalo, New York 14214.

I am studying the membrane channel properties of rat astrocytes in primary cell culture using the patch clamp technique, under conditions of continuous perfusion. In the cell-attached configuration, there is generally little, if any, channel activity near the resting membrane potential of these cells (-60 to -70 mV). Upon excision of the patch, single channel activity becomes noticeable, even in patches that were originally quiescent in the cell-attached configuration. The gating of this channel in symmetrical HEPES buffered Ringer's solution appears to be very sensitive to pipette potentials over a range of 10 to 20 mV. The conductance of this channel is at least 60 pS. Some of the excised patches may be vesicles containing single channels, as I sometimes observe activity at 0 mV pipette potential. At 33°C, the single channel appears to have one open state (approximately 0.2 milliseconds) and two closed states (approximately 0.3 and 4.0 milliseconds). The probability of being open is strongly voltage dependent (0.34 at +10 mV and 0.07 at 0 mV). The lifetime of both closed states seem to be voltage dependent. In some cases, the channel appears to have multiple conducting states for negative pipette potentials.

Supported by NIH grants R23 NS24891 (to CLB) and DK37792 to Frederick Sachs.

TU-PM-D4 MECHANISM OF PLASMA MEMBRANE TRANSPORT IN GUARD CELLS AS A MODEL FOR ION TRANSPORT ACROSS HIGHER PLANT MEMBRANES. Julian I. Schroeder
Max-Planck-Institut f. biophysk. Chemie, D-3400 Göttingen, F.R.G.

Molecular mechanisms of ion transport across higher plant membranes can be studied by applying patch-clamp techniques to protoplasts. These techniques were employed to identify mechanisms of ion uptake and release during guard cell movements, which regulate the gas exchange of plants. Inwardly and outwardly rectifying K^+-channels were characterized (Schroeder, Raschke & Neher, 1987, PNAS 84, 4108-4112). Accumulation and release of K^+ by guard cells can be accounted for by passive transport through K^+-channels. Ions which are known to inhibit K^+ uptake in guard cells also blocked inwardly rectifying K^+-channels. This finding supports the hypothesis that K^+ accumulation is mediated via these K^+-channels. The voltage dependence of K^+-channels implies that depolarisation and hyperpolarisation are required for activation of K^+ transport. The following ionic currents were found, which provide the capability of inducing shifts in the membrane potential upon physiological stimulation: a) stretching of the membrane leads to activation of channels which can depolarize the membrane and therefore may function as turgor sensors and regulators. b) blue light induces hyperpolarisation by stimulation of electrogenic pumps. From slow-whole-cell recordings it was concluded that electrogenic pumps require cytoplasmic substrates for full activation. A basic model for fundamental mechanisms of ion transport and osmoregulation in plant cells can be constructed from these findings.

TU-PM-D5 EVIDENCE FOR A NOVEL VOLTAGE ACTIVATED CHANNEL IN THE OUTER MITOCHONDRIAL MEMBRANE. K.W. Kinnally, H. Tedeschi, Department of Biological Sciences and the Neurobiology Research Center, State University of New York at Albany and C.A. Mannella, Wadsworth Center for Laboratories and Research, N.Y. State Department of Health, Albany, N.Y.

Voltage pulses (1-50 mv) positive in relation to the exterior induce an increase in conductance in outer membrane patches of giant mitochondria. This increase in conductance is biphasic. A rapid increase in conductance is followed by a slowly developing increase (see diagram, companion abstract). The data suggest that this second increase results from the assembly of channels from subunits. (a) The conductance increases with time after a long delay, whereas recovery is extremely rapid. (b) During the latency period following onset of voltage, smaller voltage pulses delivered at later times are progressively more effective in increasing the conductance. (c) Decreasing the time interval (less than two seconds) between two equal voltage pulses elicits a progressively larger response from the second pulse. (d) Concanavalin A enhances the conductance change induced by voltage, presumably by favoring aggregation. (e) The rate of the conductance changes increases with temperature from 5° to approximately 30°C, then decreases abruptly above this temperature. This temperature dependence resembles that observed with the oligomeric channels of the antibiotic alamethicin incorporated into bilayers.

Supported by ONR grant N0001485-K-0681 and NSF grant DMP-8613702.

TU-PM-D6 KINETIC STUDIES OF THE VOLTAGE ACTIVATED CHANNELS OF THE OUTER MITOCHONDRIAL MEMBRANE. K.W. Kinnally, H. Tedeschi, Department of Biological Sciences and the Neurobiology Research Center, State University of New York at Albany and C.A. Mannella, Wadsworth Center for Laboratories and Research, N.Y. State Department of Health, Albany, N.Y.

The increase in conductance induced by voltage pulses positive relative to the exterior of outer membrane patches of giant mitochondria is biphasic. A fast increase in conductance is followed by a second slowly developing increase of much greater magnitude (see diagram).

The magnitude of the initial conductance change is voltage dependent but the rate at which it is reached is not. This finding suggests that the voltage determines the number of channels capable of opening. The kinetic relationship between the two phases of the conductance changes suggests a model in which channels activated during the first phase serve as precursors for higher conductance channels formed during the second phase. By this model the kinetics of the conductance changes permit approximate estimates of the number of subunits forming the higher conductance channels.

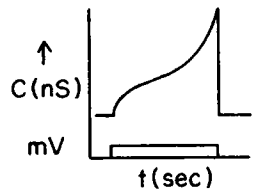

Supported by ONR grant N0001485-K-0681 and NSF grant DMP 8613702.

TU-PM-D7 SINGLE CHANNEL-LIKE ELECTRONIC ARTIFACT RECORDED FROM PATCH CLAMP AMPLIFIERS

Larry S. Liebovitch, Dept. of Ophthalmology, Columbia Univ., College of Phys. & Surgeons, NY 10032
Henk P. Buisman, Dept. Physiology and Physiological Physics, Univ. Leiden, The Netherlands

Single channel recordings from cell membrane ion channels have the form known in electrical engineering as a random telegraph signal. Such a signal can be produced by any spontaneously fluctuating gate where the energy difference between the closed and open states $\Delta E \approx kT$ where k is the Boltzmann constant and T the absolute temperature. Such signals can therefore be produced by mechanical, electronic, molecular, and atomic systems. We observed such a signal from defective operational amplifiers in two out of three patch clamp amplifiers tested. The kinetics of this signal were well fit by a two state Markov process. These artifacts were very small, only 0.1 mV, and in circuit locations that do not interfere with typical single-channel recordings.

Supported in part by NIH grants EY1080, EY6178, and EY6234.

TU-PM-D8 BRADYKININ AND THROMBIN-ACTIVATED CATION CHANNELS IN CULTURED ENDOTHELIAL CELLS FROM BOVINE PULMONARY ARTERY.

N.J. Lodge, U.S. Ryan*, C. van Breemen and D.J. Adams.
Departments of Pharmacology and Medicine*, University of Miami School of Medicine, Miami, FL 33101.

Bradykinin and thrombin release endothelium-derived relaxing factor (EDRF) and prostacyclin from endothelial cells via a mechanism requiring extracellular calcium (Johns et al. Fed. Proc. **46**: 360a 1987; Hallam & Needam, J. Physiol. **384**: 587P 1987). Calcium influx into the cell is mediated by receptor-operated non-selective cation channels (Johns et al. Tissue & Cell **19**, 1987). The aim of the present study was to further examine receptor-operated ion channels in isolated endothelial cells using the patch clamp recording technique. Local application of bradykinin (10^{-6}M) or thrombin (2U/ml) evoked inward whole-cell currents (at the resting membrane potential, -60mV) whose amplitude was sensitive to the extracellular Na^+ and Ca^{2+} concentrations. In cell-attached patches with either 140mM CsCl or 100mM $BaCl_2$ in the patch pipette to block inward rectifier K^+ channels (Johns et al. Tissue & Cell **19**, 1987), bradykinin (10^{-7}M) or thrombin (0.1 U/ml) induced channel openings dependent on agonist concentration. Agonist-activated channels were observed in ~15% of patches suggesting a low receptor-channel density. The reversal (zero-current) potential for both bradykinin and thrombin-activated currents was ~0mV and the ion selectivity for both agonist activated channels was similar; 35-40 pS with 140mM CsCl and 15-20 pS with 100mM $BaCl_2$ in the patch pipette. Single channel currents carried by Cs^+ were not blocked by 1.5mM $CaCl_2$ unlike voltage-dependent calcium channels in cardiac muscle cells (Hess & Tsien, Nature **309**: 453, 1984). Agonist-activated channels remained active in excised membrane patches and did not depend on intracellular Ca^{2+}. We propose that the distinct bradykinin and thrombin receptors may be coupled to the same ion channels through a mechanism which does not require the continued presence of a cytosolic second messenger.

TU-PM-D9 EVIDENCE OF A Mg-ACTIVATED CHANNEL WHICH APPEARS ONLY IN INTACT SQUID AXONS BUT NOT IN INTERNALLY PERFUSED AXONS,

D.C. Chang and J.R. Hunt, Department of Physiology & Molecular Biophysics, Baylor College of Medicine, Houston, Tx. 77030.

In the course of studying the resting conductance of intact squid axons, we observed a component of inward current which was time-dependent and activated at potentials more negative than-100 mV. I_X is peculiar because it appears only in the intact axon. Several axons were first studied in the intact state and then internally perfused with standard perfusion solution. The anomalous current disappeared completely following internal perfusion. Furthermore, we found that Mg ions were required to activate I_X. When Mg was replaced by Ca, I_X was greatly reduced or absent. Monovalent ions including Na, K, Rb, or choline failed to activate I_X. Although activation of I_X is strongly dependent on the external concentration of Mg, this anomalous conductance appears to have very poor ion selectivity. In the presence of external Mg, I_X is not very sensitive to the principal external cations, among which Na, K, NH_4, Rb, Cs, Li, Ca, Mg, and choline have been tested. I_X showed inward rectification and is apparently separate from the commonly observed linear leakage current. Adding Mg to the internal perfusion solution or reducing internal Ca could not restore I_X in the perfused axon. It is suspected that activation of I_X may involve the action of cytoplasmic enzymes that require the presence of external Mg.

TU-PM-D10 STRETCH-ACTIVATED ION CHANNELS IN VENTRICULAR MYOCYTES. V.Chen; W.Craelius and N.El-Sherif, Department of Biophysical Sciences,SUNY HealthSciences,Buffalo, NY 14214;Department of Cardiology, VAMC SUNY Health Sciences, Brooklyn, NY 11209

Patch clamp recording from ventricular myocytes of neonatal rats identified ionic channels that open in response to membrane stretch caused by applied suction 1-30mm Hg in the electrode. The stretch-activated (SA)channels were frequently observed 14/37 trials in cell attached patch with isotonic (Ca++free)KCl in electrode, were not seen when the electrode was filled with $BaCl_2$or $CaCl_2$. In isotonic KCl the SA channels had ohmic conductances within the range of 60mV above and below the resting potential (100pS, n=9). The unitary currents were inward at potentials more negative than resting potential+24mV(n=9) and outward at more positive potentials. Sodium pereability of SA channels tested in isolated patch was small relative to potassium. The channel openning rate was dependent on the degree of applied stretch and did not adapt during long(1min.) stretch applications. The data suggest that these channels are gated by physiological levels of tension, conducting primarily K currents that are not dependent on voltage changes or external Ca++for activation. The channel represents a cellular reflex whereby stretch regulates resting membrane conductance. Fundamental role of the stretch activated channels could be in pacemaking, trophic regulation or in the cardic impulse.

TU-PM-D11 **A CELLULAR PROTEIN MODULATES THE BEHAVIOR OF THE MITOCHONDRIAL OUTER MEMBRANE CHANNEL, VDAC.** M.J. Holden & M. Colombini, Dept. of Zoology, University of Maryland, College Park, MD 20742

The large voltage-dependent channel, VDAC, provides the primary permeability pathway for molecular traffic between the cytoplasm and the mitochondrial inner membrane and matrix space. VDAC exists in different permeability states dependent on the transmembrane potential. The probability of assuming a closed (or less conductive) state increases with increasing potential (+ or -). We have discovered a soluble protein in the mitochondrial fraction (of N. crassa) which greatly enhances the response of N. crassa VDAC to transmembrane potential. The effect of the modulator was studied on VDAC reconstituted into planar bilayer membranes (voltage clamp). Modulator added to one side of multichannel membranes increased the rate of closure (relaxation time reduced as much as 15 fold) and decreased the voltage at which the channels close at negative potentials. Symmetrical addition resulted in increased closure at + or - potentials. As little as 0.9 ug prot/ml (final conc. in the aqueous phase) of a partially purified modulator preparation significantly altered VDAC behavior. Studies of single VDAC channels revealed that VDAC can assume a number of reduced conductance states. Assumption of one state may be followed in time by a shift into a yet lower conductance state (10% or less of open channel conductance). Modulator shortened the time required for channel closure at any given voltage and increased the probability that the channel would remain closed and would achieve the lower conductance states. Modulator-treated channels tended to remain closed when the potential was returned to 0 mV (unlike control channels). This modulator may play a role in regulating the channel conductance and ultimately mitochondrial function and cellular energy transduction. (Supported by NSF grant # DCB-85-10335)

TU-PM-D12 NON-EQUILIBRIUM GATING UNDER STEADY STATE CONDITIONS OF THE TORPEDO ELECTROPLAX CHLORIDE CHANNEL. E.A. Richard and C. Miller, Graduate Dept. of Biochemistry, Brandeis University, Waltham, MA 02178

The chloride channel of Torpedo electroplax is a dimer of independent voltage-dependent protochannels in series with a voltage-dependent inactivation gate that controls both protochannels simultaneously. Since the protochannels open and close much more rapidly than the inactivating gate, current records show distinct bursts with three levels (U = up, M = middle, D = down). Entry and exit from bursts to the inactivated state can be observed from both the U state (both protochannels open) and from the M state (one protochannel open). The D state (both protochannels closed) is non-conducting.

Large bore electrodes treated with dimethyldichlorosilane were sealed to planar lipid bilayers fused with light vesicles from Torpedo electroplax. Single chloride channel records so obtained show transitions from the I to U state exceeding those from U to I at constant negative membrane potentials in symmetrical 250 mM KCl. This leads to net cyclic gating of the channel in the direction U-M-I-U. As the membrane potential is decreased from -60 to -20 mV, the cyclic behavior disappears. An asymmetrical chloride gradient (250 mM KCl versus 250 mM K acetate) restores cyclic behavior at small negative potentials. The gating of this voltage-dependent channel is altered by the electrochemical gradient for chloride. (Supported by NIH GM31768).

TU-PM-D13 MEMBRANE PROPERTIES OF HUMAN THYROTROPIN-SECRETING PITUITARY TUMOUR CELLS.

Alison M. Gurney, Dept. of Pharmacology, United Medical and Dental Schools, St. Thomas's Campus, London, UK.

The anterior pituitary contains heterogeneous cell types, which secrete different hormones. Electrophysiological studies of identified cells have relied mainly on clonal lines, derived from pituitary tumours of a particular cell type, such as the GH_3 line, which secretes prolactin on exposure to thyrotropin releasing hormone (TRH). Relatively little is known about thyrotrophs, which respond to TRH by secreting thyrotropin (TSH), as there is no comparable TSH-secreting line. Although TSH-secreting tumours are rare in humans, one was recently identified, and dissociated cell cultures were prepared from surgically removed fragments. The membrane currents in these thyrotrophs, and their modulation by TRH, were the subject of this patch-clamp study. In the whole-cell configuration, with isotonic KCl in the pipette, cells had resting membrane potentials of -37 ± 8 mV (SD; n=44) and input impedances of 2.1 ± 0.8 gigohms (SD; n=32). At least 2 outward currents were apparent; a rapidly activating, transient one and a slower activating, sustained current. The relative contribution of each to the total outward current varied with the holding potential, and from cell to cell. Outward currents were blocked when the pipette contained CsCl, revealing a transient inward current that was abolished by tetrodotoxin (10^{-6}M), but unaffected by Cd^{2+} (10^{-4}M). Application of TRH (up to 10^{-6}M) did not affect inward current, but altered outward currents. The hormone appeared to suppress the transient component while potentiating the delayed current. The characteristics of currents in the TSH-secreting cells, as well as their modulation by TRH, were similar to those previously reported in GH_3 cells. TRH may induce secretion from these two cell types by similar mechanisms.

TU-PM-E1 KINETIC BEHAVIOR AND N-TERMINAL AMINO ACID SEQUENCE OF AURACYANIN.
James D. McManus, Jeffrey T. Trost and Robert E. Blankenship, Department of Chemistry, Arizona State University, Tempe, AZ 85287-1604 USA.

Auracyanin is a small Type I blue copper protein isolated from the thermophilic green photosynthetic bacterium Chloroflexus aurantiacus (Trost et. al. (1987) Biophys. J. 51, 309a). Chloroflexus is unusual in that it contains a quinone type reaction center similar to that found in purple photosynthetic bacteria, yet apparently lacks soluble c-type cytochromes. It contains a membrane-bound cytochrome, c-554, that rereduces the oxidized reaction center. We report here that added auracyanin reduces photooxidized c-554, suggesting that auracyanin may be functionally equivalent to cyt c_2 found in purple bacteria, and in some respects similar to plastocyanin. Plastocyanin is a copper protein that functions between the photosystems in oxygen-evolving photosynthetic organisms. Auracyanin was purified from isolated membranes of Chloroflexus aurantiacus by incubating the membranes with 200 mM NaCl, 20 mM $MgCl_2$, followed by ultracentrifugation, ammonium sulfate precipitation, gel filtration and ion exchange chromatography. Membranes were illuminated with 5 sec flashes of >720 nm light, and absorbance changes monitored from 540 nm to 615 nm. An absorbance increase due to the oxidized form of auracyanin was observed and the reduction of c-554 was accelerated in samples to which 8.3 μM auracyanin had been added. The amino acid sequence of the N-terminal 39 residues of auracyanin was determined by M. Miyao and N. Murata (National Institute for Basic Biology, Okazaki, Japan). The conserved sequences of both plastocyanin and azurin are not found in the N-terminal region of auracyanin. By starting the comparison at residue 3 of stellacyanin, 6 matches are found. three of which are found between residues 33 and 37 of auracyanin, with the two intermediate residues being replacements of alanine for valine. Supported by a grant from the CRGO-USDA.

TU-PM-E2 PURIFICATION AND PROPERTIES OF A PHOTOSYSTEM I REACTION CENTER LACKING THE LOW MOLECULAR WEIGHT POLYPEPTIDES AND THE TERMINAL ELECTRON ACCEPTORS FA AND FB.
John H. Golbeck, Tetemke Mehari, Kevin Parrett and Karen Jones. (Intro. by Arnold D. Pickar), Department of Chemistry, Portland State University, Portland, OR 97207.

We reported earlier [Golbeck et al, BBA 893 (1987) 149-160] that in the presence of 1% lithium dodecyl sulfate (LDS), iron-sulfur centers FA and FB are partially removed from the photosystem I reaction center, which results in efficient charge separation between P700 and iron-sulfur center FX. This observation contributed to a model for photosystem I in which FX was depicted as a [2Fe-2S] cluster located on the P700-containing polypeptides, PSI-A1 and PSI-A2. We now report that a photosystem I reaction center treated with 8 M urea shows loss of the 30-ms optical kinetic phase due to the P700+ FA/FB- backreaction concomitant with appearance of the 1.2-ms kinetic phase due to the P700+ FX- backreaction. Unlike treatment with 1% LDS which effects only a partial loss of FA/FB, 8 M urea causes total loss of FA/FB from the photosystem I reaction center. Ultracentrifugation of the 8 M urea-treated reaction center in a 0.1 to 1 M sucrose gradient results in two protein-containing bands: the upper band contains all of the low molecular weight polypeptides and the lower band contains only the high molecular weight polypeptides. The lower band is photochemically active and shows the optical transient due to the P700+ FX- backreaction. This finding is in agreement with our ealier suggestion that FX is located solely on the high molecular-weight polypeptides. The preparation also represents the first isolation of an intact photosystem I reaction center core protein showing electron flow from P700 to iron-sulfur center FX.
Funded by a grant from the United States Department of Agriculture, Competitive Grants Research Office (87-CRCR-1-2382).

TU-PM-E3 OBSERVATION OF THE CYCLICAL S STATES OF OXYGEN FORMATION IN INTACT LEAVES BY PULSED PHOTOACOUSTICS. D. Mauzerall, O. Canaani and S. Malkin, Rockefeller University, New York, NY and The Weizmann Institute, Rehovot, Israel.

Oxygen production following single turnover flashes to intact leaf discs can be measured with a photoacoustic cell designed for modulated light (1) by control of the noise input. The O_2 signal is seen as a pulse delayed by 1-2 ms after the photothermal signal. This signal is shown to be caused by O_2 in five ways: 1) The cycle of S states with maximum O_2 yield at 3 and 7 flashes to dark adapted leaves is seen. 2) The O_2 signal on the third flash saturates with increasing flash energy, whereas the photothermal signal increases linearly. The saturation curve shows the expected cubic dependence on the saturation function. This signal is inhibited by 3) DCMU; 4) heating the leaf to 80° and 5) by infiltration with water. The last criteria shows that the signal is a gas phase, not a thermal, acoustic effect (1). The lag, caused by diffusion of O_2 to the air space, is in agreement with this view. The decay of the S states is fast, with a half life of about 30 secs. The damping of the S states is also rapid. The ratio of the third flash yield to that of the steady state is nearly 3. Thus it is possible for the first time to directly compare O_2 production from isolated chloroplasts measured on an O_2 electrode with that from in vivo chloroplasts. (1) Bults, Horwitz, Malkin and Cahen. Biochim. Biophys. Acta 679 452 (1982).
This work was supported by the NIH, GM25693 and by the Weizmann-Rockefeller Fund.

TU-PM-E4 CYTOCHROME b_{559} MAY FUNCTION TO PROTECT PHOTOSYSTEM II FROM PHOTOINHIBITION

Lynmarie K. Thompson and Gary W. Brudvig, Dept. of Chemistry, Yale University, New Haven, CT 06511

Photosystem II (PSII) is the most susceptible of the photosynthetic systems to photoinhibition. Photoinhibition of PSII occurs at high light intensities or when the normal electron donation pathways are blocked, and damages the reaction center itself, rather than the water oxidizing complex. The initial charge separation which occurs in the PSII reaction center generates $P680^+$, with a midpoint potential greater than one volt. This is a much more highly oxidizing molecule than the primary electron donors of photosystem I or of the bacterial reaction centers. Thus, it seems likely that when the normal electron donor pathways are insufficient or blocked, an alternate donor could be oxidized by this powerful oxidant and lead to inactivation of the PSII reaction center. This explains the particular susceptibility of PSII to photoinhibition. Since cytochrome b_{559} (also unique to PSII) is known to be oxidized by PSII when the normal electron donor pathways are inhibited and to be reduced by hydroplastoquinone, we propose that this cyclic electron transfer pathway exists to protect PSII against photoinhibition. We present preliminary evidence correlating the rate of photoinhibition with the reduction potential of the medium. At high potentials, when cyt. b_{559} is oxidized, photoinhibition occurs more rapidly than at low potentials. We further suggest that the alternate electron donor which is oxidized during photoinhibition and reduced by cyt. b_{559} is a chlorophyll molecule. EPR studies have shown that a chlorophyll is photo-oxidized in PSII when electron donation from all other donors, including cyt. b_{559}, is blocked, consistent with a pathway for oxidation of cyt. b_{559} via oxidation of the chlorophyll. This chlorophyll is probably the closest one to P680 and may serve to couple the chlorophyll antenna to P680. Such proximity would be required for efficient energy transfer but would also make this chlorophyll especially susceptible to oxidation by P680. By incorporating cyt. b_{559} as an electron donor to reduce photo-oxidized antenna chlorophyll, PSII may be able to protect against this unique photoinhibition problem.

This work was supported by NIH (GM32715) and an AAUW American Fellowship to LKT.

TU-PM-E5 FLUORESCENCE QUANTUM YIELD CHANGES IN PHOTOSYSTEM II.

Hermann Keuper and Kenneth Sauer, Dept. of Chemistry and Laboratory of Chemical Biodynamics, Lawrence Berkeley Laboratory, University of California, Berkeley, CA 94720

The fluorescence quantum yield of Photosystem II (PSII) increases when reaction centers are closed by actinic light. Using a single photon timing technique, we measured the fluorescence decay as a function of the degree of reaction center closure which was varied by changing the preillumination intensity. The sample, triton-extracted PSII-particles from spinach in a highly dispersed, aqueous suspension, was flowed at high speed and entered the fluorescence cuvette 2ms after preillumination. We have evidence, based on fluorescence induction curves, that the reaction centers are not connected (i.e. each antenna complex is coupled to only one reaction center). To improve the reliability of our data analysis, decays were measured under the same conditions at different emission wavelengths and analyzed with a global analysis procedure which constrains the lifetimes to be wavelength-independent. Only three exponential components are needed to fit the data.

The increase in quantum yield upon reaction center closure is brought about predominantly by an increase in the amplitude of the middle component (lifetime τ: 400-500ps) from less than 35% to more than 65%, whilst the fast component amplitude (τ: 180-250ps) decreases simultaneously. The lifetimes and the sum of the amplitudes of the three components are not significantly altered under our experimental conditions. The amplitude of the slow component (τ: 1.0-1.5ns) is approximately constant at less than 1% of the total and probably represents non-functional chlorophyll. We assign the fast component to open and the middle component to closed reaction centers.

TU-PM-E6 OBSERVATION OF INACTIVE PHOTOSYSTEM II REACTION CENTERS in vivo.

Roger A. Chylla and John Whitmarsh, Department of Plant Biology, University of Illinois, USDA/ARS, Urbana, IL 61801

We investigated the turnover time of photosystem II in attached leaves of higher plants. We developed two techniques to determine the reoxidation time of Q_A^-, the reduced primary acceptor of photosystem II in leaves. In the first technique we probed electron transfer in photosystem II by measuring the electrochromic shift at 518 nm induced by a single turnover flash. Using two short actinic flashes separated by a variable time interval, we determined the time required after the first flash for the electrochromic shift to recover to its full extent on the second flash. In the second technique, we used fluorescence induction to monitor the redox state of Q_A at variable times after a saturating flash. Previous experiments performed upon thylakoid membranes (Chylla, Garab, and Whitmarsh (1987) Biochim. Biophys. Acta In press) revealed that about one-third of photosystem II reaction centers recover slowly (2-3 s) compared to normal recovery rates (2-4 ms). The oxidation of Q_A^- appears to be the rate-limiting step in the recovery. Present experiments upon spinach leaves in vivo indicate that about 20% of the total number of reaction centers (photosystem I and/or photosystem II) have a turnover half-time approximately 1 s. The fluorescence induction technique indicates that a significant fraction of the slowly-recovering centers are photosystem II. Similar data obtained using detached leaves of maize, sorghum, soybean, blackeyed peas, and sunflower suggest that slowly recovering centers may be a universal feature of higher plants.

TU-PM-E7 STARK EFFECT IN PSII RCS FROM SPINACH*; M. Lösche, K. Satoh+, G. Feher and M.Y. Okamura, +Okayama U., U.C.S.D., La Jolla, CA.

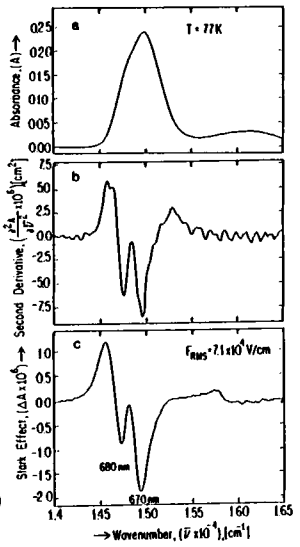

The effect of an applied electric field on the optical absorption spectrum (Stark effect) of PSII RCs (1) in polyvinyl alcohol films (T=77K) was measured. The Stark spectrum (Fig. c) showed two bands with minima at 680 and 670 nm and had a shape similar to the second derivative (Fig. b) of the absorption spectrum (Fig. a). The band at 680 nm has contributions from the primary donor P680 and the pheophytin intermediate acceptor (1) which were not resolved. The change in the dipole moment, $\Delta\mu$, between the ground and excited states obtained from the ratio of the Stark and second derivative spectra were 0.8 and 1.5 Debye for the 680 and 670 (accessory chlorophyll) nm peaks, respectively. The angles between respective $\Delta\mu$s and transition moments were 40° and 20°. These results differ significantly from the situation in bacterial RCs where the primary donor, a bacteriochlorophyll dimer, has a much larger $\Delta\mu$ than its monomeric accessory bacteriochlorophylls (2). This suggests that P680 is a monomeric chlorophyll species although a symmetric dimer cannot be excluded.

(1) O. Nanba and K. Satoh, Proc. Natl. Acad. Sci. 84 (1987) 109-112.
(2) D. deLeeuw, M. Malley, G. Butterman, M.Y. Okamura and G. Feher, Biophys. J. 37 (1982) 111a; D. Lockhardt and S. Boxer, Biochemistry 26 (1987) 2664-2668; M. Lösche, G. Feher and M.Y. Okamura, Proc. Natl. Acad. Sci. 84 (1987) 7537-7541. *Work supported by the NSF and DFG.

TU-PM-E8 SITE-DIRECTED MUTAGENESIS IDENTIFIES THE SPECIFIC TYROSINE RESIDUES SHOWN TO BE REDOX COMPONENTS OF PHOTOSYSTEM II

R.J. Debus*, B.A. Barry*#, G.T. Babcock#, and L. McIntosh*+, MSU-DOE Plant Research Laboratory*, Departments of Chemistry# and Biochemistry+, Michigan State University, East Lansing, MI 48824

Photosystem II contains the organic components Z and D. Z mediates electron transfer from the Mn cluster at the site of water oxidation to the oxidized reaction center primary donor, $P680^{+}$. The function of D is uncertain, but D^{+} gives rise to the dark-stable EPR spectrum known as Signal II. D^{+} has recently been shown to be a tyrosine radical (1). Z is likely to be a second tyrosine located in a similar environment. The reaction center core of Photosystem II, where light-induced charge-separation takes place, is a heterodimer of two homologous polypeptides called D1 and D2 (2,3). By site-directed mutagenesis of a psbD gene in the unicellular cyanobacterium Synechocystis 6803, we have recently shown that D is tyr-160 of the D2 polypeptide (4). We are now extending these studies to include the identification of Z by site-directed mutagenesis of a psbA gene encoding the D1 polypeptide.

Work supported by the DOE, NIH, NSF, USDA, and the McKnight Foundation.

(1) B.A. Barry & G.T. Babcock (1987) Proc. Natl. Acad. Sci. USA 84, in press.
(2) O. Nanba & Ki. Satoh (1987) Proc. Natl. Acad. Sci. USA 84, 109-112.
(3) M.Y. Okamura, Ki. Satoh, R.A. Isaacson & G. Feher (1987) in Progress in Photosynthesis Research (J. Biggins, ed.) Martinus Nijhoff, Dordrecht, Vol. 1, pp. 379-381.
(4) R.J. Debus, B.A. Barry, G.T. Babcock & L. McIntosh, Proc. Natl. Acad. Sci. USA, in press.

TU-PM-E9 DEPENDENCE OF THE RECOMBINATION RATE $D^{+}Q_A^{-} \rightarrow DQ_A$ ON THE ELECTRIC FIELD APPLIED TO REACTION CENTERS FROM RB. SPHAEROIDES R-26 INCORPORATED INTO A PLANAR LIPID BILAYER*, T. Arno, A. Gopher, M.Y. Okamura and G. Feher, U.C.S.D., La Jolla, CA 92093

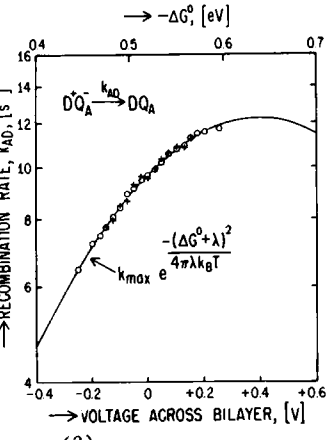

The rate of electron transfer given by the classical Marcus theory(1) depends on the difference in free energy between product and reactant, ΔG° and the reorganization energy λ; $k=k_{max}\exp\left[-(\Delta G^{\circ}+\lambda)^2/(4\pi\lambda k_B T)\right]$. We have measured the change in the charge recombination rate, k_{AD}, in RCs that were functionally oriented in a planar lipid bilayer across which an electric field was applied(2). The experimental results on two membranes (dots and crosses) are shown in the figure. The solid line represents the theoretical fit with $\lambda = 0.64$ eV and the energy scale of $-\Delta G^{\circ}$ as indicated at the top. The value of $-\Delta G^{\circ}$ at zero electric field (i.e. difference in redox energies) was taken to be 0.52 eV. The ratio between ΔG° and the applied voltage is ~ 0.3 suggesting that only $\sim 30\%$ of the applied voltage appeared across $D^{+}Q_A^{-}$. This value varied from membrane to membrane, indicating that the topology of the RCs in the membrane is not constant. This may explain the failure to observe a voltage dependence of k_{AD} in previous work(2).

(1) R.A. Marcus; J. Chem. Phys. 24, 966 (1956).
(2) A. Gopher, Y. Blatt, M. Schonfeld, M.Y. Okamura, G. Feher and M. Montal; Biophys. J. 48, 311 (1985). *Work supported by the NSF and NIH.

TU-PM-E10 pH-DEPENDENCE OF THE CHARGE RECOMBINATION RATE $D^+Q_A^- \rightarrow DQ_A$ IN REACTION CENTERS FROM RB. SPHAEROIDES R-26*; P.H. McPherson, T. Arno, M.Y. Okamura and G. Feher, U.C.S.D., La Jolla.

In the preceding abstract (1) we discussed the change in the recombination rate, k_{AD}, caused by an *applied* electric field. Here we report on the change in k_{AD} caused by an *internal* electric field, created by charges associated with titratable amino acid residues of the RC (Fig. A). The decrease in k_{AD} with decreasing pH is caused by the field associated with the increase in the number of bound protons. These protons interact more strongly with Q_A^- than with D^+, thereby stabilizing $D^+Q_A^-$ (i.e., lowering the free energy.) This stabilization is also shown by a net uptake of protons in the reaction $DQ_A \rightarrow D^+Q_A^-$ (2,3). The proton uptake determined in (3) was integrated to obtain the free energy ΔG^o_{obs} (Fig. B.) For small changes (< 50 meV), $-\Delta G^o_{obs}$ is expected to be proportional to k_{AD} (1). The shapes of the curves of k_{AD} and $-\Delta G^o_{obs}$ as a function of pH are in good qualitative agreement. A change in k_{AD} from 8 to 12 s^{-1} is brought about by a change in $-\Delta G^o_{obs}$ of 50 meV. This result agrees within a factor of 2 with that for an *applied* field (1), for which the same change in k_{AD} is brought about by a change in free energy of 100 meV.

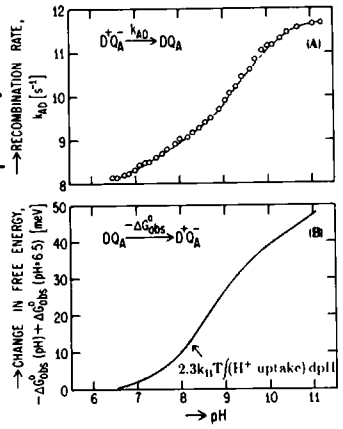

(1) T. Arno, A. Gopher, M.Y. Okamura and G. Feher; preceding abstract.
(2) P. Maroti and C.A. Wraight; Biophys. J. 47, 5a (1985).
(3) P.H. McPherson, M.Y. Okamura, G. Feher and M. Schonfeld; Biophys. J. 51, 125a (1987).

*Work supported by the NSF.

TU-PM-E11 CHARGE SEPARATION IN UBIQUINOL CYT C_2 OXIDOREDUCTASE. D.E. Robertson and P.L. Dutton Dept. of Biochemistry and Biophysics, Univ. of Pennsylvania, Phila, Pa. 19104

Two separate redox reactions result in fractional transdielectric charge separation by the ubiquinol cyt c_2 oxidoreductase. Accounting for light saturation, RC unconnected to cyt c_2, the active fraction of cyt bc_1 and the spectral contribution of other components to flash kinetics traces permits detailed quantitation of; a)the red carotenoid bandshift accompanying electron transfer from the ubiquinol oxidation site (Q_z) to cyt b_H, b)the blue bandshift associated with cyt b_H reduction via site Q_c (a reversal of the physiological reaction at Q_c) and c) the effect of $\Delta\psi$ on the Q_c-cyt b_H redox equilibrium. The dielectric distance of charge movement for each reaction was calculated. To account for the nature (electron or proton) of the charge moved across the dielectric, studies were performed at pH values above and below the redox-linked pK values of the redox centers involved in each reaction. The results may be summarized: 1) the redox reactions between cyt b_L and cyt b_H and between cyt b_H and Q_c constitute the full electrogenic span; 2) electron transfer is the predominant if not the sole contributor to charge separation; 3) the dielectric distance between cyt b_L and cyt b_H is 59 +/- 8% of the full membrane dielectric profile; 4) the distance between cyt b_H and Q_c is 49+/-5% of the full dielectric distance calculated from the blue bandshift or the $\Delta\psi$—dependent equilibrium shift; 5) there is no pH dependence of the Q_z-cyt b_H or Q_c-cyt b_H charge separation reactions; 6) Q_z and Q_c are on opposite sides of the membrane dielectric. Supported by GM 27309.

TU-PM-E12 MIMICRY OF PHOTOSYNTHETIC CHARGE SEPARATION IN A CAROTENOID-PORPHYRIN-DIQUINONE MOLECULAR TETRAD. Devens Gust, Thomas A. Moore, Ana L. Moore, Donna Barrett, Larry O. Harding, Lewis R. Makings, and Paul A. Liddell, Department of Chemistry, Arizona State University, Tempe, Arizona 85287-1604.

Photosynthetic organisms achieve long-lived photoinitiated charge separation with high quantum yield by employing a series of short-range, efficient electron transfer reactions. A molecular tetrad which mimics this strategy has been synthesized. The tetrad consists of a porphyrin (P) covalently linked to a carotenoid polyene (C) and a diquinone moiety (Q_A-Q_B). Excitation of the porphyrin yields C-^{1}P-Q_A-Q_B which undergoes electron transfer to generate C-$P^{+\cdot}$-$Q_A^{-\cdot}$-Q_B. This state can in turn give two more intermediate states, C-$P^{+\cdot}$-Q_A-$Q_B^{-\cdot}$ and $C^{+\cdot}$-P-$Q_A^{-\cdot}$-Q_B, both of which can go on to produce the final $C^{+\cdot}$-P-Q_A-$Q_B^{-\cdot}$ charge separated state. This final state has a lifetime of 460 ns in dichloromethane (4 µs in acetonitrile) and is produced with a quantum yield of 0.23 at ambient temperatures and 0.50 at 240 K. Since the quantum yield is calculated by a comparative method using literature values of the extinction coefficient for the carotenoid radical cation, which are uncertain, the yield at 240 K may well be near the theoretical maximum. Comparison of the results for this tetrad with those for related C-P-Q triad molecules reveals an enhanced quantum yield which may be attributed to the multiple electron transfer steps.

T-Pos1 THE INTERACTION OF ZINC PROTOPORPHYRIN WITH INTACT HEMOGLOBIN. Rhoda Elison Hirsch*, Margaret J. Lin*, and Constance M. Park*+,*Albert Einstein College of Medicine, Bronx, N.Y. 10461 and +Columbia University College of Physicians & Surgeons, New York City, 10032

In erythropoietic porphyria and lead poisoning, free protoporphyrin (EPP) and zinc protoporphyrin (ZPP), respectively, accumulate in erythrocytes. That EPP and ZPP bind to human hemoglobin A (Hb_4) is established, but the site of binding is still a matter of controversy. We pursued this problem by studying ZPP in the presence of intact, tetrameric oxy Hb_4, using batch microcalorimetry, front-face fluorometry, absorption difference spectroscopy, oxygen-equilibrium studies, and isoelectric focusing (IEF). In the presence of Hb_4 (pH7.4, 0.05M phosphate), the fluorescence emission maximum (excitation 420nm) of ZPP immediately shifts from 587nm (ZPP alone) to 594nm, as expected when binding to protein. The fluorescence intensity increases with time and is correlated with the mole ratio of ZPP:Hb_4. This slow, time-dependent reaction is also observed with microcalorimetry: the rate of heat of reaction exhibits both a fast and slow component. The heats of reaction range from -2.1 to -14.8 mcals depending upon the ratio of ZPP:Hb_4 4:1 to 40:1, respectively; and are typical of weak electrostatic protein-ligand interactions. The optical difference spectra are correlated to the mole ratio and also exhibit a slow increase in intensity over time. No time dependent changes are observed with ZPP nor with Hb_4 alone. The oxygen affinity of Hb_4 in the presence of ZPP decreases with increasing mole ratio. During IEF, all ZPP separates from Hb_4 consistent with a weak, non-covalent interaction at a non-heme pocket site. Because stoichiometry is never defined, we conclude that ZPP binds to Hb_4 at non-heme pocket sites in a non-specific, weak, electrostatic interaction.

T-Pos2 THE KINETICS OF HUMAN OXYHEMOGLOBIN RECONSTITUTION. Melisenda J. McDonald, Susan M. Turci and Linda A. Michalski, Biochemistry Program, Department of Chemistry, University of Lowell, Lowell, Massachusetts 01854

Solution studies of hemoglobin reconstitution in vitro have been complicated by the oligomeric property of the beta subunits. Indeed, in 0.1 M potassium phosphate buffer, pH 7, the rate limiting step in hemoglobin assembly is the beta tetramer first order dissociation reaction. In our continuing effort to study the effect of physiological relevant modifiers on this chain dissociation reaction, we have monitored spectrophotometrically the effect of pH on the rate of dissociation of two oxyhemoglobin beta chain variants, N-Baltimore beta chains (95 Lys to Gly) and Sickle beta chains (6 Glu to Val) and have compared these findings to those of normal beta chains. Equivalent concentrations (on a heme basis) of oxygenated alpha and beta subunits, in 0.1 M potassium phosphate buffer (pH 7 or 8), and 20 degrees were mixed and the change in absorbance at 583nm was monitored as a function of time in a Cary 2200 recording spectrophotometer, or alternatively in a Kinetics Instruments stopped flow device. A 6.5 fold increase in the rate of beta tetramer dissociation was observed over a pH range of 7 to 8 for normal beta chains. Furthermore, the first order dissociation rates increased 8.5 and 3.5 fold, respectively for Sickle beta chains and N-Baltimore beta chains and presumably reflect intrinsic differences in surface charge and hence stability of the subunits.

This work was supported by NIH Grant #HL38456.

T-Pos3 RESOLVABILITY OF THE QUATERNARY ENHANCEMENT EFFECT IN HUMAN HEMOGLOBIN A$_o$. Martin Straume and Michael L. Johnson, Department of Pharmacology, University of Virginia School of Medicine, Charlottesville, VA 22908

A controversy currently exists regarding the magnitude of the quaternary enhancement effect in human hemoglobin. A Monte-Carlo study was therefore undertaken to address the resolvability of this phenomenon as evaluated from oxygen binding curves ($\bar{Y}$ vs. [O_2] at a series of hemoglobin concentrations [Hb]) based on previously published thermodynamic studies of stripped human hemoglobin A$_o$ at 21.5°C and pH 7.4 (Mills, F.C., Johnson, M.L., and Ackers, G.K. (1976) Biochemistry 15, 5350-5362; Chu, A.H., Turner, B.W., and Ackers, G.K. (1984) Biochemistry 23, 604-617). Data was simulated for the same distributions of [O_2] and [Hb] as employed in these experiments and for the derived free energies of O_2 binding and dimer to tetramer subunit assembly. Five hundred different sets of Gaussian distributed random noise, consistent with the approximate uncertainties present in the experimentally observed data, were then superimposed on the simulated data. Five hundred nonlinear least-squares parameter estimations were performed and all parameter values were recorded for each estimation. The resulting distributions of the various free energy changes provide a direct measure of the resolvability of these parameters. The most probable quaternary enhancement free energy changes and approximate 67% confidence limits were -0.297 (-0.567, -0.146) kcal/mol for the Mills et al. data and -0.595 (-0.769, -0.500) kcal/mol for the Chu et al. data. These results indicate that ($\Delta g'_{44} - \Delta g'_{22}$) is significantly negative under these conditions and that currently available experimental accuracy and precision permit resolution of sufficient quality to allow confidence in this conclusion.

T-Pos4 A PROTON NMR STUDY OF THE INTERACTION OF Cu^{2+} and Zn^{2+} WITH HUMAN CARBOXYHEMOGLOBIN*
P. Mohanakrishnan, Gray Freshwater Biol. Institute, P.O. Box 100, Navarre, MN. 55392
and D.L. Rabenstein, Chem. Dept., Univ. of California, Riverside, CA. 92521-0403.

The interaction of Cu^{2+} and Zn^{2+} with bovine, chicken and human carboxyhemoglobins was studied using spin-echo proton NMR. It was found that histidines were involved in metal ion binding. The histidines involved in binding Cu^{2+} and Zn^{2+} appeared to be the same for chicken and human carboxyhemoglobins, but different for bovine carboxyhemoglobin. For the human protein, the interaction was also studied at different pH's. Near physiological pH, our finding is that two histidines are involved in binding for human hemoglobin. From our NMR pH-titration and pK_a-estimates by Ohe and Kajita (Biochemistry 19, 4443 (1980)), the two histidines were identified as β-2 and β-143. There appears to be a third histidine involved in the binding of Cu^{2+} and Zn^{2+} to human carboxyhemoglobin at basic and acidic pH values. But we do not have convincing evidence for its participation in the metal ion binding near physiological pH. On the basis of our pK_a assignments and Baldwin's coordinates (J. Mol. Biol. 136, 103 (1980)), we propose that the binding site involves N-terminal amino acid residues (β-1 Val and β-2 His) of one beta chain and β-143 His (and maybe β-146 His) of the second beta chain. Thus, the Zn^{2+}-sites of the human carboxyhemoglobin are the same as the primary copper-sites and there are two sites per tetramer. The proposed model agrees with that proposed for the primary Cu^{2+} sites of human deoxy- and oxyhemoglobins by Tabak and Louro (J. Magn. Reson. 62, 370 (1985)).
*This study was performed at Chemistry Dept., Univ. of Alberta, Edmonton, Alberta, CANADA.

T-Pos5 EFFECTS OF HEME PERIPHERAL SUBSTITUTION ON THE SPECTROSCOPIC AND BIOLOGICAL PROPERTIES OF MYOGLOBIN.
Michael Atamian and David F. Bocian, Department of Chemistry, Carnegie Mellon University, Pittsburgh, PA 15213

Resonance Raman (RR) spectra have been acquired for the deoxy, oxy, and metcyano species of sperm whale myoglobin (mb) reconstituted with deuteroheme, 2-acetyldeuteroheme, 4-acetyldeuteroheme, and 2,4-diacetyldeuteroheme. The functional inequivalence of the 2- and 4-positions of the heme moiety is manifested in the vibrational frequencies of the carbonyl and certain heme skeletal modes. The RR data indicate that the protein influences the porphyrin π-system primarily through the 2-substituent. In the deoxy Mbs, the 2-acetyl group is more conjugated into the chromophore than the 4-acetyl group. In the ligated Mbs however, the extent of conjugation of the 2-group is less than in the deoxy forms. This result indicates that ligand binding differentially alters the π-electronic structure for 2- vs. 4-substituted systems. RR spectra recorded immediately after heme reconstitution indicate the presence of two inequivalent forms of the protein. ^1H NMR spectroscopy indicates that these two forms are the normal and reversed heme orientational isomers previously described by La Mar and coworkers(La Mar et al, *Proc. Natl. Acad. Sci. USA* 75,5755-5759). The RR spectra demonstrate that in the deoxy species the 2-acetyl group of the normal form is conjugated into the macrocycle to approximately the same extent as the 4-acetyl group of the reversed form and vice-versa.

T-Pos6 CALCULATIONS OF THE ANISOTROPIC OPTICAL DIELECTRIC TENSOR FOR SOLUTIONS OF SICKLE HEMOGLOBIN POLYMERS AND MONOMERS.
Marilyn F. Bishop, Department of Physics, Virginia Commonwealth University, 1020 West Main Street, Richmond, Virginia 23284-2000.

We have calculated the optical dielectric tensor for a solution of polymerizing sickle hemoglobin using Bruggeman's Symmetrical Effective Medium Approximation. In this theory, we assume that all polymers and monomers are embedded in an effective medium, and that the solution surrounding them is represented by spherical water "particles" embedded in the same medium. The polymers are represented by infinitely long rigid cylindrical particles and the monomers by spherical particles, where the dielectric constant inside a monomer or polymer is the same. We require that the sum of the dipole moments of the monomers, of the polymers, and of the solution "particles" adds to zero, which yields the dielectric tensor of the effective medium. Because the polarizability per unit volume of a cylindrical particle is different from that of a spherical particle, the dielectric tensor for randomly oriented particles increases as the fraction of polymers increases. If the polymers are aligned, the resultant dielectric tensor of the entire solution is anisotropic even if the absorption is neglected, arising from the geometrical shape of the particles, giving rise to what is known as form birefringence. These anisotropic effects of the medium can have important consequences for light scattering.

This work is supported by NIH Grant Number HL38614.

T-Pos7 **The Orientation of CO in Sperm Whale Myoglobin: An Infrared Photoselection Study.**

Pál Ormos, David Braunstein, Mi Kyung Hong, Shuo-Liang Lin, Todd B. Sauke, Joseph Vittitow, Departments of Biophyics and Physics,University of Illinois, Urbana, IL 61801.

FTIR spectroscopy of the ν(C-O) bands in MbCO reveals three major CO configurations in the liganded state, represented by the A_0,A_1,and A_3 bands. To learn more about the nature of these bands, and to assign them to the different states observed by X-ray crystallography[1] and other techniques , we carried out photoselection experiments to determine the orientation of CO in the A_i(bound) and B_i(photolyzed) substates. Small fractions of CO were photolyzed with polarized light in the β visible absorption band at 10K. By measuring the resulting linear dichroism in the A and B infrared bands, the angle between the heme plane and CO was determined. The average angles are $\theta(A_0)=75^o\pm4^o$, $\theta(A_1)=62^o\pm2^o$ and $\theta(A_3)=57^o\pm4^o$. The A bands are inhomogeneously broadened[2] ; the angle between the CO axis and the heme plane shows a wavenumber dependence within the A bands. This observation is interpreted as a distribution of orientation within the individually inhomogeneous A substates, thus providing a well defined geometrical parameter to characterize the distribution of the protein conformational substates. The B-states exhibit no induced linear dichroism; in the B_1 and B_2 states the ligand is randomly oriented with respect to the heme plane.

[1] J.Kuriyan, et al.,*J. Mol. Bio.* (1986) **192**, 133-154.

[2]See accompanying poster on *Inhomogeneous Broadening of the Soret and ν(CO) bands of MbCO.*

T-Pos8 **Kinetic Hole-Burning and Conformational Relaxation in Myoglobin**

Anjum Ansari, Benjamin R. Cowen, Hans Frauenfelder, Pál Ormos, Todd B. Sauke, Alfons Schulte, and Robert D. Young, Departments of Physics and Biophysics, University of Illinois, Urbana, Il 61801.

The charge transfer band near 760nm (band III) in myoglobin (Mb) is sensitive to local heme conformation. In photodissociated MbCO at 5K, the band is red shifted with respect to the deoxy wavelength; the protein structure differs from the equilibrium deoxy structure. After photodissociation the area of band III decreases with time as the ligands rebind and the peak frequency shifts toward the deoxy value[1]. The peak shift can be due to two different mechanisms: kinetic hole-burning or conformational relaxation. Kinetic hole-burning results from different parts of an inhomogeneously broadened spectrum rebinding with different rates. Conformational relaxation is a change in the protein structure toward the deoxy structure. An experiment by Friedman and co-workers[2] distinguishes between the two mechanisms. Our data taken with a similar technique show that when the protein is photodissociated with a single short flash, the entire peak shift below 80K is a result of kinetic hole-burning. In sperm whale Mb the band width decreases by less than 2% and the peak shift is about 10% of the total width after 50% of all ligands have rebound. The data are consistent with a small inhomogeneous broadening. The underlying homogeneous width is approximately 90% of the total width. We have measured the rebinding from 5K to 80K and mapped different parts of the spectrum to the distribution of rebinding enthalpies.

Relaxation does occur when MbCO is exposed to intense white light for a time geater than about 10 s, and is interpreted as local conformational relaxation of the heme and the residues around the heme pocket. Relaxation was measured from 10K to 120K for varying illumination times and intensities.

[1]Ansari, A., Berendzen, J., Bowne, S. F., Frauenfelder, H., Iben, I. E. T., Sauke, T. B., Shyamsunder, E., and Young, R. D., *Proc. Natl. Acad. Sci. USA*, **82**:5000, 1985.

[2]Campbell, B., Chance, M., Friedman, J. M., *Science*, in press, 1987.

T-Pos9 **FTIR Studies of Genetically Engineered Sperm Whale Carbonmonoxymyoglobins.**

Stephen Sligar, Barry Springer ,Karen Egeberg, David Braunstein, Hans Frauenfelder, Mi Kyung Hong, Pál Ormos, Departments of Physics and Biochemistry, University of Illinois, Urbana, IL 61801.

We have measured the ν(CO) bands (1900 cm^{-1}-2300 cm^{-1}) of sperm whale carbonmonoxymyoglobin (MbCO). The protein was obtained by the expression of a totally synthetic gene using the expression vector pUC19[1]. FTIR spectra were collected in a 75% glycerol-water solution over the temperature range 10 to 300K. Three IR lines, denoted A_0 to A_3, are observed. The observed peak positions at 10K, are A_0 at 1966 cm^{-1}, A_1 at 1945 cm^{-1}, and A_3 at 1927 cm^{-1} are identical to those of native sperm whale MbCO. Also, recombination kinetics following flash photolysis at 40K were measured. The observed rates are consistent with those previously measured. In addition, following photoselective flash photolysis, the linear dichroism of the samples were measured and the calculated angles of the ligand to the heme plane agree with those of earlier studies. Additionally, a number of site-directed distal histidine (His E7) exchanged mutants were measured by the methods mentioned above.

[1] B. Springer and S. Sligar, *High Level Expression of Sperm Whale Myoglobin in Escherichia Coli*, PNAS, in press, 1987.

[2] See accompanying poster on *Orientation of CO in Sperm Whale Myoglobin.*

T-Pos10 **CO Rebinding to Protoheme**

Dana D. Dlott, Mathew J. Cote, Jeffrey R. Hill, John F. Kauffman, J. Douglas McDonald, Jeffrey Miers, Jay Postlewaite,* School of Chemical Sciences, University of Illinois, Urbana, IL 61801.
Hans Frauenfelder, Peter J. Steinbach, Physics Department, University of Illinois, Urbana, IL 61801.

CO rebinding to protoheme (Fe-Protoporphyrin IX) in a 75% glycerol/water solvent studied from picoseconds to seconds with flash photolysis exhibits three distinct recombination processes in the temperature range 30 to 300K. The slow exponential process S is seen at temperatures above 230K as some CO ligands rebind via the solvent. The geminate process I is nonexponential in protoheme-CO over the entire temperature range. Also observed in protoheme-CO at temperatures below about 200K is the ultrafast exponential geminate process I*. At 100K its rate k* is about 3.5×10^{10} s^{-1} [1]. We explain process I with a distributed Arrhenius rate in which the peak enthalpy is about 2.5 kJ/mole, and the rate's preexponential factor of about 2×10^{11} s^{-1} at 100K is two orders of magnitude larger than that of MbCO and other protein-ligand systems. These smaller preexponentials can be attributed to the entropy lost in going from the pocket to the transition state [2]. Recent experiments have monitored rebinding from 400 to 438 nm and reveal wavelength dependent kinetics of the two geminate processes.

[1] Hill, J.R., et al. *Ultrafast Phenomena V* (1986) pp 433-435.
[2] Frauenfelder H., Wolynes, P.G., *Science*, 229, (1985), pp 337
*Work supported by grant NSF DMR 84-15070

T-Pos11 **Protein States and Motions Probed by Pressure-Temperature Studies of CO Ligands in the Myoglobin Pocket**

Icko E.T. Iben, David Braunstein, Hans Frauenfelder, Mi Kyung Hong, J. Bruce Johnson, Stan Luck, Pál Ormos, Alfons Schulte, Robert D. Young,* Departments of Physics and Biophysics, University of Illinois,Urbana, IL 61801.

The temperature (140 K to 320 K) and pressure (0.1 MPa to 100 MPa) dependence of the CO stretching bands in sperm whale myoglobin have been studied with FTIR spectroscopy. Solvents used are glycerol-water, ethylene glycol-water and water all buffered to pH 7 with potassium phosphate. The spectra can be resolved into three lines A_0, A_1 and A_3 with peaks at 1966, 1946 and 1933 cm^{-1}. A plot of the logarithm of the intensity ratios as a function of the inverse temperature reveals two striking features : i) below a transition temperature (about 180 K) which weakly increases with pressure the protein-solvent system is frozen into a glassy state [1] and the spectral properties depend on the pressure-temperature pathway: ii) at higher temperatures the A substates interconvert but the logarithm of the intensity ratio A_0/A_1 passes through a minimum around 260 K. This indicates that MbCO may have two states with similar spectroscopic but different thermodynamic (energy, entropy, volume) properties. Further evidence for the glass transition around 180 K comes from heat capacity measurements using differential scanning calorimetry.

[1] A. Ansari et al., Biophys. Chemistry **26**:337, 1987. * Permanent address: Physics Dept., Illinois State Univ., Normal IL 61761

T-Pos12 **Pressure-Induced Protein Relaxations Probed by Heme-Carbonyl Substates in Myoglobin**

Icko E.T. Iben, David Braunstein, Hans Frauenfelder, J. Bruce Johnson, Pál Ormos, Alfons Schulte, Peter J. Steinbach, Robert D. Young, Physics Department, University of Illinois,Urbana, IL 61801.

FTIR spectroscopy on the three A substates of MbCO below about 220 K shows that the protein-ligand solvent system is not in equilibrium, but acts like a glass. We study the dynamic response of the three A substates after a fast pressure release (100 MPa to 7 MPa) by monitoring their spectral properties from 10 s to 10^4 s in the temperature range from 170 K to 210 K. Between 170 K and 195 K for the absorption band of A_0 the width narrows and the peak frequency shifts toward the low pressure values indicating internal redistribution of A_0. Slow interconversion of A_1 with A_3 also occurs in this temperature range. Above 200 K the three A substates each show fast internal redistribution while A_1 and A_3 interconvert rapidly with one another. Between 195 K and 210 K slow interconversion of A_0 with A_1 and A_3 is observed.

These results show similarities with the dynamics of glasses: i) the observed relaxations are non-exponential in time indicating a distribution of relaxation rates. Each A substate thus can consist of many sub-substates; ii) The relaxations "freeze" out within a narrow temperature range of 20 K with the rates having Vogel-Fulcher like behavior.

T-Pos13 **Inhomogeneous Broadening in the Soret and ν(CO) IR Bands of MbCO: The Connection of the Spectral and Functional Heterogeniety of Sperm Whale Myoglobin.**

*Pál Ormos, Anjum Ansari, David Braunstein, Benjamin R. Cowen, Hans Frauenfelder, Mi Kyung Hong, Icko E.T. Iben, Todd B. Sauke, Peter J. Steinbach, Robert D. Young**, Departments of Biophysics and Physics , University of Illinois, Urbana, IL 61801.

The rebinding kinetics of CO to myoglobin after flash photolysis is nonexponential below 180K; the kinetics is governed by a distribution of activation enthalpies. This distribution results from an inhomogeneity in the protein conformation. We have done hole-burning experiments on the Soret and IR CO-stretching bands to test the assumption that an inhomogeneous distribution of protein conformations should result in an inhomogeneously broadened spectrum. CO was slowly photolyzed at different wavelengths in the Soret at 10K. Both the Soret and the A_1 bands shift during photolysis demonstrating that different wavelengths excite different parts of the distributed population. We have also done kinetic hole-burning experiments and measured peak shifts in the Soret and A_1 bands as the CO molecules rebind[1,2], indicating that there is some correlation between the spectral and enthalpic distributions. In the IR the spectral and enthalpic distributions are highly correlated while in the Soret this correlation is weak. From the peak shifts in the spectral and kinetic hole-burning experiments the inhomogeneous broadening in the Soret is estimated to be approx. 18% of the total width and that in A_1 is about 57%.

[1]See accompanying poster on *Kinetic Hole-Burning and Conformational Relaxation in Myoglobin.*

[2] B.F.Campbell et al.,*Science*, in press, 1987.

* Permanent address: Physics Dept. , Illinois State. University, Normal IL 61761.

T-Pos14 **AN ALCOHOL-INDUCED ALTERATION OF THE RESONANCE RAMAN SPECTRUM OF HUMAN FERRIHEMOGLOBIN.** Barry B. Muhoberac, Cecilia Wells, Mark Chavez, Mark R. Ondrias and John A. Shelnutt. Departments of Chemistry, Indiana University-Purdue University at Indianapolis, Indianapolis, IN 46223 and University of New Mexico, Albuquerque, NM 87131; and Solid State Materials Division, Sandia National Laboratories, Albuquerque, NM 87185.

Methanol and ethanol binding are known to induce modest changes in the optical absorption and EPR spectra of ferrihemoglobin consistent with the conservative replacement of water by alcohol at the iron or with alcohol binding in a hydrophobic crevice. Resonance Raman spectroscopy has previously uncovered iron-ligand stretches as well as other specific vibrations and has the potential to distinguish different modes of alcohol interaction with ferrihemoglobin. This study shows that after binding either methanol or ethanol, the low frequency resonance Raman spectra of human ferrihemoglobin are essentially identical to that of the unperturbed spectrum except for a shift in the 310 cm^{-1} band to higher frequency by as much as 8 cm^{-1}. The ethanol-induced shift is greater than that of methanol even though complex formation was less for ethanol (80%) than methanol (98%). This change in only one resonance Raman band implies a site-specific interaction of these alcohols with the protein in contrast to the more general interaction that would be expected for multiple alcohol binding sites, multiple orientations of alcohol at a single binding site, or an alcohol-induced protein conformational change. The similarity of the spectral changes produced by both alcohols along with their common structure features argues for the same or similar sites and mechanisms of interaction of both alcohols. The spectral changes are also consistent with differential steric constraints on alcohol binding. In addition, ethanol alters the spin-state marker bands in the high frequency resonance Raman spectrum of ferrihemoglobin minimally. These alcohol perturbations will be discussed in terms of the following four possible assignments of the 310 cm^{-1} band: (1) a vinyl out-of-phase bending mode, (2) the iron-nitrogen (histidine) stretch, (3) an iron-oxygen (water) stretch and (4) a methine out-of-plane deformation. (This work was supported by Grant AA06935.)

T-Pos15 **FAILURE OF HALDANE'S LAWS FOR THE PARTITIONING OF OXYGEN AND CARBON MONOXIDE TO HUMAN HEMOGLOBIN.** M.L. Doyle, P.R. Connelly, E. Di Cera, & S.J. Gill; Department of Chemistry & Biochemistry, University of Colorado, Boulder, CO 80309-0215.

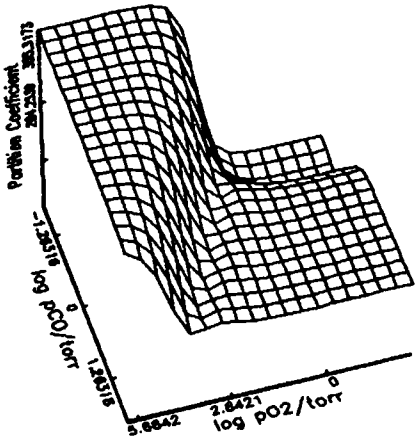

A differential thin-layer optical technique has enabled high precision measurements of carbon monoxide and oxygen binding to human hemoglobin A in particular solution conditions, i.e., 600 μM heme, 10 mM inositol hexaphosphate, pH 6.94, 25 °C. We find the binding curves of O_2 and CO are not parallel, with CO exhibiting higher cooperativity [Di Cera, E., Doyle, M.L., Connelly, P.R. & Gill, S.J. (1987) Biochemistry, in press]. This result demonstrates that the partition coefficient changes as a function of the degree of ligation (the Figure displays a surface representing the partition coefficient), and invalidates Haldane's laws. Moreover, it reveals that, although subtle differences are observed in the functional chemistry of these two ligands at low degrees of saturation, the overall cooperative mechanism of ligation is essentially the same for both ligands, and is consistent with a quaternary transition between two major structural states. [Supported by NIH HL22325 grant.]

T-Pos16 **USING MUTANT AND CHEMICALLY-MODIFIED HEMOGLOBINS TO PROBE THE MOLECULAR MECHANISM OF COOPERATIVITY.** George J. Turner and Gary K. Ackers, Department of Biology, The Johns Hopkins University, Baltimore, MD 21218

The strategy of mapping by structure-function pertubation has been employed to determine the structural location of cooperative free energy in human hemoglobin: Gibbs free energies of cooperativity (ΔG_C) were determined for a series of hemoglobins possessing single-site amino acid substitutions or chemical modifications. The perturbations in ΔG_C brought about by the local-site modifications are mapped against the corresponding structural locations (1). This analysis (2) has now been extended to include 55 human hemoglobins, yielding the conclusion that the $\alpha^1\beta^2$ intersubunit contact is the structural location of ligand-linked interactions that generate the cooperative free energy ΔG_C. Many of the hemoglobins studied may be grouped in clusters of sites previously implicated as critical to cooperative oxygenation and the Bohr Effect. It is now possible to selectively assess the energetic consequences of altering non-covalent bonding interactions in these clusters. Cooperative enthalpies and entropies have been determined at several proton activities for a series of hemoglobins where putatively critical proton-linked salt-bridge partners are perturbed. Hemoglobins investigated include Cowtown (β146 His-Leu), Bunbury (β94 Asp-Asn), and Kariya (α40 Lys-Glu). The temperature dependence of these mutant hemoglobins at pH7.4 (standard buffer conditions of .1M NaCl, .1M Tris-base, 1mM EDTA) suggest that the non-covalent bonding interactions responsible for their cooperative mechanisms are identical to those of hemoglobin Ao. 1. Ackers, G.K. and Smith, F.R., (1985) Ann. Rev. Biochem. 54. 597. 2. Pettigrew et al., (1982) PNAS 79. 1849.

T-Pos17 ^{1}H NMR STUDIES OF THE EFFECT OF IONIC STRENGTH, pH AND THE BINDING OF CYTOCHROME C PEROXIDASE ON THE PHE-82 RESIDUE OF THREE SPECIES OF CYTOCHROME C. Susan J. Moench, Ting-Mei Shih, James E. Erman* and James D. Satterlee, Departments of Chemistry, University of New Mexico, Albuquerque, NM 87131 and *Northern Illinois University, DeKalb, IL 60115.

Phe-82 is an invariant amino acid residue of cytochromes c which is located in very close proximity to the 3-CH_3 group of the heme. It is involved in the formation of the heme environment and has been postulated to be directly involved in the electron transfer reactions mediated by cytochromes c. In this study we have monitored the chemical shift position of two protons of phe-82 in three species of cytochromes c (Fe^{+3}) (yeast iso-2, horse and tuna) with changes in ionic strength, pH and in the presence of cytochrome c peroxidase (CCP). Irradiation of the heme 3-CH_3 results in a distinct NOE to the phe-82 resonances along with NOE's to other protons in the vicinity of the heme 3-CH_3. When the ionic srength of the cyt c samples is increased from 10 mM to 500 mM, the heme 3-CH_3 of all three cytochromes c shifts downfield (+0.2-(+0.45)ppm) with an accompanying downfield shift of the phe-82 resonance (+0.04-(+0.08)ppm). Yeast cyt c differs from horse and tuna in that it exhibits shifts which are about twice as large as those observed for the other two. In addition, chemical shift and linewidth changes of the 3-CH_3 resonance with changes in pH indicate that movement of phe-82 is less constrained in the yeast protein. Finally, ^{1}H NMR spectra of the 1:1 complexes of these cytochromes with CCP reveal that while the complexes with horse and tuna cyt c exhibit similar 3-CH_3 (~+0.7ppm) and phe-82 (~+0.1ppm) shifts, the 1:1 complex of yeast cyt c with CCP exhibits a 3-CH_3 shift of ~+1.6ppm and a phe-82 shift of ~+0.26ppm.

T-Pos18 STRUCTURAL AND REDOX MODELS OF F430, THE NICKEL TETRAPYRROLE COMPLEX FROM METHANOGENIC BACTERIA. M.W. Renner, A. Forman, J. Fajer, D. Simpson, K.M. Smith and K. M. Barkigia. Brookhaven National Laboratory, Upton, New York 11973.

F430 is a nickel tetrapyrrole found in the methyl reductase that catalyzes the final steps in the generation of methane from carbon dioxide in methanogenic bacteria. F430 is believed to function as a methyl or electron transfer agent, and can be reduced to Ni(I) in vivo and in vitro. Porphyrin, chlorin, isobacteriochlorin (iBC, see structure), hexahydro and octahydro derivatives that incorporate the six-membered exocyclic ring of F430 have been synthesized in order to assess the effects of progressively saturating the porphyrin macrocycle on redox properties and sites of reduction. The iBC derivative exhibits clear EPR evidence of reduction to Ni(I), as observed for F430, whereas the other compounds are reduced to free radicals with some metal character. Cyclic voltammetry shows that the compound that yields Ni(I) also reacts catalytically with halogenated methanes. A single crystal structure of the Ni(II) iBC compound shows the macrocycle to be severely distorted. Possible roles of the macrocycle in stabilizing metal versus ring reductions will be considered in terms of structural flexibility and molecular energy levels.

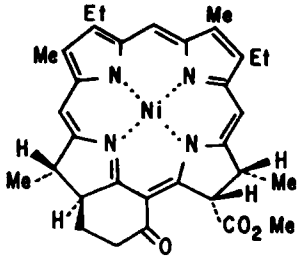

(This work was supported by the Division of Chemical Sciences, U.S. Department of Energy, Washington, D.C., under contract No. DE-AC02-76CH00016.)

T-Pos19 KINETIC RESOLUTION OF THE AFFINITY FOR BINDING THE LAST OXYGEN TO THE ALPHA OR BETA SUBUNITS WITHIN HEMOGLOBIN TETRAMERS AND DIMERS. John S. Philo and Jeffrey W. Lary, Molecular & Cell Biology U-125, The University of Connecticut, Storrs, CT 06268

Recently there has been some dispute over the correct value of the affinity for binding the 4th O_2 to human Hb,[1] and evidence that neither the 3rd and 4th Adair constants nor the R state affinity in allosteric models can be uniquely determined by fitting equilibrium binding data.[2,3] We feel that kinetic data can, and should, be used to independently determine parameters in equilibrium models and to address questions of alpha/beta heterogeneity. Therefore, we have obtained kinetic data which resolve both association and dissociation rates for the 4th O_2 for both alpha and beta subunits (the first time an alpha/beta difference in association rates has been determined), and can thus compute the O_2 affinity for each chain. These kinetically-determined affinities are significantly lower than those determined from fits to equilibrium isotherms under identical solution conditions by Ackers and coworkers,[4] and are an order of magnitude smaller than the R state value from the recent α_2-cooperon allosteric model.[3]

We have also done experiments at low protein concentrations to look for differences in affinity and/or kinetics between tetramers and dimers. These data do not show that the affinity of triply ligated tetramers is significantly enhanced over that of dimers, as has been reported.[4]

It appears that there is a discrepancy between equilibrium and kinetic data, and the origin and significance of this discrepancy needs to be addressed. (Supported by NIH HL-24644)

[1]Q. Gibson & S. Edelstein (1987) J.Biol.Chem. 262:516. [2]S. Gill et al. (1987) Biochemistry 26:3995. [3]E. Di Cera et al. (1987) Biochemistry 26:4003. [4]A. Chu et al. (1984) Biochemistry 23:604.

T-Pos20 POWER DEPENDENT BEHAVIOR OF MYOGLOBIN RAMAN MODES IN THE PICOSECOND TIME REGIME. Eric W. Findsen[1,2], Joel M. Friedman[2], and Mark R. Ondrias[1]. [1]Department of Chemistry, University of New Mexico, Albuquerque, NM 87131 and [2]AT&T Bell Laboratories, Murray Hill, NJ 07974.

We present the results of a study of the power dependent behavior of the transient Raman spectra of deoxy and carboxy myoglobin using ~30 ps long blue (436 nm) laser pulses. The width of the Raman mode sensitive to porphyrin π-electron density, ν_4, widens significantly, and shifts to lower frequency as the incident photon density is increased. The mode width varies approximately linearly with incident photon density. Also, the coresize density marker, ν_2, undergoes broadening, and an apparent shift to lower frequency at high photon densities. These effects are totally reversible. The implications of these results upon recent picosecond transient Raman studies is discussed. Possible explanations include, heating of the heme by photon absorption, formation of a heme excited state, and a non-linear excitation process. This work partially supported by the NSF (DMB8604435).

T-Pos21 BASIS SPECTRA FOR KINETIC OBSERVATIONS OF THE ALLOSTERIC TRANSITION IN HEMOGLOBIN. Alison J. Graf, Anthony J. Martino, and Frank A. Ferrone, Department of Physics and Atmospheric Science, Drexel University, Philadelphia, PA 19104.

Modulated kinetic spectroscopic studies of the allosteric transition in hemoglobin depend on the existence of reliable basis spectra. (Biophys. J., 1985, **48**, 269-282) Typical approaches to meet this need employ mutant hemoglobins or model compounds (i.e. modified hemoglobins) to generate such spectra. We describe an alternative approach in which we generate a ligand binding curve by variation of steady-state laser photolysis. At each level of photolysis, a difference spectrum is obtained. Small excitation levels are measured by phase-sensitive detection, while large excitations are measured as direct difference spectra. This allows us to cover photolysis levels spanning 3 decades. The resultant spectra are analyzed by the method of singular-value-decomposition (see Hofrichter *et al.*, PNAS, 1983, **80**, 2235-2239.) This new approach provides a sensitive means of determining the principal spectral components present as the molecule titrates from R to T. We will describe the technique and its use in Soret and near UV spectra. The results of the analysis can then be used to determine kinetic rates. Finally, we discuss the properties of the binding curves generated as a biproduct of the analysis.

T-Pos22 THE RATE OF CONFORMATIONAL CHANGE IN 3-LIGANDED HbA MEASURED BY FLUORESCENCE QUENCHING OF PTS Anthony J. Martino and Frank A. Ferrone, Department of Physics and Atmospheric Science, Drexel University, Philadelphia, PA 19104.

An analog of DPG, 8-hydroxy-1,3,6 pyrene trisulfonic acid (PTS) permits the allosteric state of HbA to be monitored by quenching of its fluorescence when the probe is bound to the T state. We have used this probe, coupled with the method of modulated excitation (Biophys. J., 1985, **48**, 269-282) to follow the allosteric kinetics of HbA with three ligands bound. An argon laser pumps a dye laser, which in turn provides the modulated photolysis (at 570 nm) to drive the system. Excitation of the dye is by the 476 nm line of the argon ion laser; dye emission is monitored at 515 nm . Stability and improved sinusoidal compliance are provided by an optical feedback system couped to the modulator. The binding constant for the PTS-Hb complex is determined in a novel way by using DC photolysis to adjust the concentration of deoxy-HB. The kinetics of the PTS-bound species are followed by the amplitude and phase of the modulated fluorescence signal. The fluorescence signal is tuned with respect to the ligand rebinding signal, so that the kinetics of rebinding need not be separated in the resulting analysis. The allosteric kinetics determined by the PTS quenching are compared with kinetics determined by observation of the Soret difference spectra known for R and T states. The kinetic parameters determined by the two methods are in good agreement. This validates the technique, and allows the PTS quenching method to be used in cases where the allosteric spectra may be altered (e.g. mutations).

T-Pos23 Resonance Raman Studies of the Equilibrium Structures and Dynamics of the Heme Sites of Heat Treated and pHMB Modified Cytochrome Oxidase

R.W. Larsen[1], P.M. Li[2], R.A. Copeland[2], S.I. Chan[2], and M.R. Ondrias[1]
[1]Department of Chemistry, University of New Mexico and [2]Arthur Amos Noyes Laboratory of Chemical Physics, California Institute of Technology

Modification of the Cu_A site in mammalian cytochrome oxidase has been used to help elucidate the functional role of this site in the catalytic cycle of the enzyme. Both heat treatment and chemical modification by p-(hydroxymercuri)benzoate convert the CuA site to a lower potential type II copper and effectively remove the site from the electron transfer pathway. Resonance raman spectroscopy was employed to probe the equilibrium structure of the heme active sites of the heat treated and pHMB modified enzymes. Our studies indicate that the formyl groups of both heme a and heme a_3 are in slightly different environments for the heat treated and pHMB modified enzyme. The Fe-his vibrational mode for the heme a_3 is also diminished in intensity for both forms of modification. We are currently investigating the transient CO ligand binding dynamics of the modified enzymes. Our results will be discussed in relation to the reduced activity of the modified enzymes.

Supported by the NIH (GM22432 and GM33330).

T-Pos24 Resonance Raman Characterization of the Equilibrium and Photolytic Transient Species of Cytochrome C' from C. vinosum.

J.D. Hobbs[1], R.W. Larsen[1], T.E. Meyer[2], M.A. Cusanovich[2], and M.R. Ondrias[1]
[1]Department of Chemistry, University of New Mexico, Albuquerque, NM 87131 and [2]Department of Biochemistry, University of Arizona, Tucson, AZ.

Resonance Raman spectra of Chromatium vinosum cytochrome c' have been obtained of the five unique states previously characterized in the absorption spectra for the oxidized: types I(pH 7), II(pH 10) and III(pH 12) and reduced: (type-a(pH 7) and type-n(pH 12)) forms of similar photosynthetic bacterial enzymes. The Raman spectra of type I and type-a are consistent with those of high-spin, 5-coordinate heme proteins, such as deoxyhemoglobin, while spectra of type III and type-n correspond more closely to those of low-spin, ferric- and ferrous-cytochrome c, respectively. Spectra of the CO-bound equilibrium species qualitatively resemble those of MbCO and exhibit pH dependence in the core-size sensitive mode, ν_2. Transient resonance Raman has been employed to investigate the carbon monoxide binding dynamics of type-a and type-n. Recent studies have found the CO binding dynamics in C. vinosum to be cooperative with a large, endothermic heat of ligation and a CO-linked dimer-monomer equilibrium. Our data indicate that CO photolysis is much more efficient at pH 7 than at pH 12. Moreover, the spectra of type-n species suggest that a high-spin transient species is formed immediately subsequent to ligand photolysis. The structural rearrangements at the heme active site suggested by these unusual ligand binding characteristics will be considered. Supported by the NIH (GM33330 and GM21277).

T-Pos25 **THE MOLECULAR DIMENSIONS AND MASSES OF ANNELID EXTRACELLULAR HEMOGLOBINS AND CHLOROCRUORINS.** **Oscar H. Kapp, Joseph S. Wall, Mark G. Mainwaring and Serge N. Vinogradov, Enrico Fermi Institute, University of Chicago, Chicago, IL 60637, Biology Department, Brookhaven National Laboratory, Upton, NY 11973 and Biochemistry Department, Wayne State University School of Medicine, Detroit, MI 48201.**

The molecular dimensions of negatively stained hemoglobins of the oligochaetes Lumbricus terrestris and Tubifex tubifex, the polychaetes Amphitrite ornata, Arenicola marina and Nephtys incisa and the leech Macrobdella decora and the chlorocruorins of the polychaetes Myxicola infundibulum and Eudistylia vancouverii were determined with the scanning transmission electron microscope (STEM) at the University of Chicago. The molecular masses of these molecules were determined using unstained freeze-dried specimens with dark-field STEM at the Brookhaven National Laboratory, employing tobacco mosaic virus as a molecular mass standard. The vertex-to-vertex diameters and heights of the native hexagonal bilayer structures were correlated with the elution volumes of the hemoglobins and chlorocruorins on a Superose 6 column at neutral pH using a Pharmacia FPLC system. **Supported by grants from the Department of Energy and the National Institutes of Health RR01777 (JSW) and DK 38674 (SNV).**

T-Pos26 CYANIDE ION KINETICS AND PROTON NMR STUDIES OF GLYCERA DIBRANCHIATA MONOMER HEMOGLOBINS.
J. Mintorovitch and J.D. Satterlee, Dept. of Chem., Univ. of New Mexico, Alb., NM 87131.
The monomer hemoglobin fraction from the marine annelid Glycera dibranchiata consists of at least three major fractions. Both crystal structure determination and amino acid analyses have shown that this protein possesses a three-dimensional structure similar to vertebrate hemoglobins. However, it has been shown that one, and possibly all three fractions possess the exceptional primary sequence substitution in which the distal histidine (E-7) is replaced by leucine. This substitution has shown to have significant influence on dynamics of ligand binding and spectroscopy of static ligated states. We show here that, compared to met-myoglobin, all major fractions of G. dibranchiata met hemoglobins bind cyanide at a much slower rate. Ligation studies were done at four pHs and four ratios of KCN to protein. Furthermore, k_{off} is very small compared to k_{on}, making k_{diss} ~2-3 orders of magnitude smaller than previously reported by other investigators. Also, our analysis reveals that the protein binds only CN^- at a significant rate. Separation of the bimolecular rate-constant (k_{obs}) into contributions from k_{CN} and k_{HCN} indicates that the former is at least 150 times greater. Proton NMR studies (361 MHz) of hyperfine shifted resonances in the met-cyano (low spin) form were achieved by using a combination of specifically deuterium labelled protoporphyrin IX (in collaboration with Prof. K. Smith, UC, Davis) and by ^1H-^1H nuclear Overhauser effects. These studies have determined that the two observable heme methyl resonances can be assigned to the 8-CH_3 and the 3-CH_3. The 1-CH_3 and the 5-CH_3 are both between 0-10 ppm. This observation indicates that the heme is rotated 180° about the α-γ meso axis as compared to MetMb-CN. These findings allow us to begin elucidating the elements of heme pocket structure that can discriminate ligand binding dynamics for this class of monomeric hemoglobins.

T-Pos27 A NEW SPECTROSCOPY? SPIN-TUNNELING IN HEME PROTEINS
R. H. Austin[1], B. S. Gerstman[2], P.A. Mansky[1], M.W. Roberson[1]
[1]Department of Physics, Princeton University, [2]Department of Physics, Florida International University
It is well known that iron-containing proteins undergo delicate spin changes during their reactions, the classic example being the high-low spin change in myoglobin and hemoglobin ligand binding. Although not all would agree, some workers believe that the non-adiabatic model for heme protein reactions dictates that the spin change is the kinetic throttle in reaction kinetics.
We have tested this model by an experiment which utilizes Far Infrared Radiation (FIR) from a pulsed Free Electron Laser. Basically, the idea is to observe the modulation of tunneling rates for carbon monoxide at 4.2 K by shining FIR photons of such an energy to pump between spin-tunneling and allowed crystal-field split levels. We will present data showing that there is a significant enhancement of the tunneling rate under FIR illumination. The data is time-resolved and unambiguously rules out heating artifacts.

T-Pos28 METALS, SUBUNITS AND NADPH OXIDASE ACTIVITY OF A BOVINE GRANULOCYTE CYTOCHROME b_{558} PREPARATION. Karla S. Booth and Winslow S. Caughey, Department of Biochemistry, Colorado State University, Ft. Collins, CO 80523.

An NADPH oxidase preparation containing cytochrome b_{558} was isolated from fresh bovine blood according to the procedure of Pember, et al [J. Biol. Chem. 259, 10590 (1984)]. Metal analyses by inductively coupled plasma atomic emission spectrometry showed the presence of Fe, Cu, Zn and Mg. Both non-heme and heme Fe appeared to be present. The metal atom ratios of Fe/Cu and Fe/Zn are approximately 2 and 4, respectively; Mg contents varied. CO binding to heme Fe was shown in visible/Soret spectra. SDS-urea polyacrylamide gel electrophoresis resolved two bands of 14 and 12 kDa. Gel filtration on Sephadex G-100 gave two peaks containing cyt b_{558}, one with a projected molecular weight of 43 kDa, and the other greater than 91 kDa. The preparation, isolated from unstimulated granulocytes, showed minimal NADPH oxidase activity by SOD-inhibitable cytochrome c reduction. However, HbO_2 appears to stimulate the oxidase. A novel HbO_2 autoxidation assay detected the production of superoxide and/or H_2O_2 from O_2 and NADPH, catalyzed by this cyt b_{558} preparation. Catalase stopped the reaction, while SOD decreased it by 60%. This demonstrates the direct production of H_2O_2 by NADPH oxidase without necessarily involving superoxide as an intermediate. These findings suggest that this NADPH oxidase with a critical role in the microbicidal action of phagocytes is a complex enzyme, containing several metals in addition to heme Fe, and several small subunits, which binds O_2 and CO, and catalyzes the NADPH reduction of O_2 to H_2O_2 as well as superoxide. (Supported by U.S. Public Health Service Grant No. HL-15980).

T-Pos29 HALOTHANE AND NITROUS OXIDE INHIBITION OF CYTOCHROME C OXIDASE, A POTENTIAL TARGET SITE OF GENERAL ANESTHETICS. Aichun Dong and Winslow S. Caughey, Department of Biochemistry, Colorado State University, Fort Collins, CO 80523

The basic biochemical mechanism of anesthesia remains unclear. A major problem has been an inability to determine the tissue sites that produce anesthesia when occupied by anesthetic molecules. We find that halothane and N_2O, two widely used inhalation anesthetics, inhibit the oxidase activity of purified bovine heart cytochrome c oxidase (CcO). The inhibition is dose dependent and completely reversible. At clinically relevant concentrations halothane (1.0 mM) and N_2O (80%) exhibit 31±5% and 27±5% inhibition, respectively. Furthermore the inhibitory effect of halothane is partial and saturable; a maximum inhibition of ca. 50% is achieved at 3.0 mM. Present evidence suggests that the anesthetics interfere with electron transfers from cytochrome c to the O_2 reaction site and not with the O_2 reactions per se. These findings indicate that CcO may be a critical target site of general anesthetics for producing anesthesia and possibly toxic effects as well. (Supported by U.S. Public Health Service Grant No. HL-15980).

T-Pos30 SUBPICOSECOND RESONANCE RAMAN SPECTROSCOPY OF CARBONMONOXY-HEMOGLOBIN: DYNAMICS OF HEME-PROTEIN INTERACTIONS AND VIBRATIONAL COOLING

J.W. Petrich, J.C. Lambry, C. Poyart[§] and J.L. Martin. Laboratoire d'Optique Appliquée, Ecole Polytechnique--ENSTA, INSERM U275, 91128 Palaiseau Cedex, France; [§]INSERM U299, 94275 Le Kremlin-Bicêtre, France.

Transient Raman spectroscopy is extended to the femtosecond time domain and applied to carbonmonoxy-hemoglobin. The results are interpreted in terms of a rapidly-achieved (30 ps) tight-coupling between the ligand binding site and the intersubunit interface. The spectra are also interpreted in terms of a vibrationally hot heme which cools substantially in 10 ps.

T-Pos31 CHEMICALLY MODIFIED HEMOGLOBINS, L.C. Cerny, P. Calabrese, P. Mondi, Masonic Medical Research Laboratory and Utica College, Utica, N.Y. E.L. Cerny, M. Liszczynskyj, M. Reath, Microfilm Inc., Utica, N.Y. F.J. Bruzzese, SUNY Binghamton, N.Y.

In order to alter the oxygen saturation curve for hemoglobin (Hgb), it was chemically modified by reacting it with either a diaspirin, a cyclohexanedione or a glyoxalic acid. The Hgb was obtained from several different species including human, bovine, sheep and goat. The resonance Raman spectra was used as a means of illustrating the places of attachment to the Hgb, whether peripherally or intramolecularly. This is possible by comparing the Fe spin state at 1586 cm^{-1} in the unmodified Hgb with the newly formed compounds. To increase the retention times in exchange-transfusion experiments in rats, the modified Hgb's were complexed with hydroxyethyl starch (HES) polymers which were converted to the tri and tetra aldehyde moities. The electrophoresis density patterns indicate the formation of the newly synthesized compounds. The metabolic kinetics of the exchange-transfusion experiments show that the Hgb-HES complexes are broken down step-wise. To explain this process, a mathematical kinetic analysis is presented. In conclusion, the modified Hgb molecules shift the oxygen saturation curve to the right and the HES-Hgb polymers increase the circulating retention times to make them suitable candidates for artificial blood replacement fluids. Supported in part by NIH Grant 1 R15 HL 38656-01 and Contract DAMD 17-87-C-7216.

T-Pos32 LENGTH DISTRIBUTIONS OF HEMOGLOBIN S FIBERS. ES Mann, Department of Biochemistry, Albert Einstein College of Medicine, Bronx NY 10461.

Time dependent physicochemical methods measure average properties of solution. Electron microscopy (EM), however, reveals structural detail and, through fiber lengths, polydispersity. The length distribution histogram provides a history of nucleation: If fibers are nucleated at time t' in the interval dt' then the number of fibers of length L in the increment dL is given by $F(L)dL = \dot{n}(t')dt'$. Ferrone et al (Biophys J. 32:361, 1980) proposed a double nucleation model in which reaction progress for polymer mass and number is $dCp/dt = k_1 n$ and $dn/dt = k_2 Cp + k_3$ respectively (where k_1, k_2 and k_3 are the concentration dependent pseudo rate contants for elongation and heterogeneous and homogeneous nucleation, respectively). This model predicts the nucleation rate over time so that the length distribution becomes a test of the model. The normalized distribution function, f(L), is $B\cosh(At-BL)/\sinh(At)$, where $A=\sqrt{k_1 k_2}$ and $B=\sqrt{k_2/k_1}$. For $At>5$, $f(L) \cong B\exp(-BL)$: The length distribution is a negative exponential with semilog slope -B and is time independent. Fiber length distributions by EM on hemoglobin S at 14mM heme in 0.1M potassium phosphate, pH 7.0, 20°, show (1) a negative exponential for all but short fibers, (2) time independence with $B=2/\mu$, (3) a marked deficit of short fibers and (4) a weak concentration dependence between 13 and 14mM heme. Observations (1) and (2) are consistent with the current model but (3) and (4) are not. Monomer depletion cannot explain the time independent short fiber deficit (3) and the high cooperativity of nucleation, residing in k_2, requires a large concentration dependence of B (4). Also, extensive budding of short polymers from existing longer polymers is absent. An alternative model is proposed (Mann & Briehl, these abstracts). Support: NIH grants HL-07451 & HL-28203 to RW Briehl.

T-Pos33 POLYMORPHIC BREAKAGE: A NEW, BREAKAGE-DEPENDENT, KINETIC MECHANISM FOR THE POLYMERIZATION OF HEMOGLOBIN S. ES Mann & RW Briehl. Albert Einstein College of Medicine, Bronx, NY 10461.

Hemoglobin S delay time and exponential reaction progress, their high concentration dependence and the exponential fiber length distribution (Mann, these abstracts) are explained by the double nucleation model (Ferrone et al, J Mol Biol 183:611, 1985). But the model is not consistent with the minimal dependence of the distribution on hemoglobin concentration nor with the marked short fiber deficit. A model based on breakage of newly formed segments at fiber ends (in lieu of heterogeneous nucleation) encompasses these two observations. Exponential progress arises from proportionality between number (rather than mass) of fibers and nucleation rate; a relation dependent on the rate of new segment formation and a breakage probability, k_b. If n and C_p are polymer number and mass concentrations, $dn/dt = k_b k_1 n + k_3$ and $dC_p/dt = k_1 n$ (k_1 and k_3 are concentration dependent pseudo rate constants for elongation and homogeneous nucleation). For $n(0)=0$, $n = [k_3/A'][\exp(A't)-1]$ and $C_p = [k_3/k_b A'][\exp(A't)-1-A't]$, where $A' = k_b k_1$, giving exponential progress (except at short times). f(L), the normalized length distribution, obtained by assuming fibers of length L were initiated at a previous time in accord with growth rate, is $B'\exp[A't-B'(L-L_B)]/[\exp(A't)-1]$, $\cong B'\exp[-B'(L-L_B)]$ except at short times; $B' = k_b/(1-k_b L_B)$ and L_B is the breaking length. Exponential in L at all times, f(L) depends only on concentration independent breaking processes. Cooperativity of exponential rate then must reside in k_1 which therefore represents bloc addition of monomers. The short fiber deficit results from a minimum fiber length, L_B. k_1 and k_b can be found from A', B' and L_B from kinetics and length histograms. The ratio of breaking to non-breaking polymorphic forms can be shown to be $K = B'L_B$. Supported by NIH grants HL-07451 & HL-28203.

T-Pos34 KINETIC HOLEBURNING AND CONFORMATIONAL DISORDER IN HEMEPROTEINS. Mark R. Chance, Blair F. Campbell, Joel M. Friedman, Dept. of Non-Equilibrium Physics, AT&T Bell Laboratories, Murray Hill, NJ 07974.

Analysis of spectral changes in proteins at cryogenic temperatures can be complicated by several contributing phenomena. A protocol has been designed to distinguish between structural relaxation and conformational heterogeneity as the source of the time and temperature dependent spectral changes. Using this approach, it is observed that below 70K, the spectral changes in the photoproducts of liganded myoglobins and hemoglobins are due primarily to a kinetic holeburning process. This holeburning is evidenced as lineshape and frequency changes in the 760nm photoproduct band as a function of ligand recombination, such that the slow recombining states are blue shifted compared to the faster recombining ones. The extent of the inhomogeneous broadening (and the possibility of detecting holeburning) is a function of species and solution conditions such that faster recombining systems exhibit lessened holeburning compared to slower systems. The linkage between the well known distributed kinetics and the structural disorder that engenders it remains a key question. We have attempted to directly determine the structural modes which give rise to the functionally relevant conformational heterogeneity. Our approach has included measurement of distal pocket modes (through FTIR analysis) and proximal pocket modes (the proximal histidine, using resonance Raman). Preliminary results seem to rule out the distal pocket interactions as being the primary source of 'continuous' heterogeneities, however the distal pocket does impose larger scale 'conformations' which are themselves kinetically heterogeneous. Proximal pocket influences mediated through the histidine-iron bond remains the most likely, but as yet unproven locus.

T-Pos35 EFFECTS OF SITE-SPECIFIC MUTAGENESIS ON INTRACOMPLEX ELECTRON TRANSFER KINETICS IN THE CYTOCHROME C:CYTOCHROME C PEROXIDASE COMPLEX. J.T. Hazzard[*], J.M. Mauro[§], G.L. McLendon[†] M.A. Cusanovich[*] and G. Tollin[*], [*]Dept. of Biochemistry, Univ. of Arizona, Tucson AZ 85721, [§]Dept. of Chemistry, Univ. of Calif. San Diego, LaJolla CA 92093 and [†]Dept. of Chemistry, Univ. of Rochester, Rochester NY 14627.

The effects of site-specific mutagenesis of specific residues of yeast iso-1 cytochrome c (cyt c) and yeast cytochrome c peroxidase (CcP) on the kinetics at various ionic strengths of one-electron intracomplex electron transfer within the electrostatically-stabilized or transiently-formed 1:1 complex between these proteins have been investigated using laser flash photolysis. The rate constant for intracomplex electron transfer from cyt c(II) to CcP(IV,$R^{+}\cdot$) increases from $\sim$200 s^{-1} to $\sim$1500 s^{-1} with an increase in ionic strength from 8 to 30 mM. Conversion of electrostatically charged surface residues of cyt c, believed to be important in orientation and stabilization of the electrostatic complex, to uncharged residues results in larger rate constants for intracomplex electron transfer at both low and high ionic strengths. These results suggest that the electrostatic complex formed at low ionic strengths may not be the optimal electron transfer complex, and that complementary charge-charge interactions may inhibit rapid electron transfer. Electron transfer from cyt c(II) is virtually eliminated by conversion of Trp-191 of CcP to Phe-191 at both low and high hionic strength. This residue is located near the proximal histidine and between Met-230 and Met-231, which has been suggested to be the possible site of the amino acid oxidation in the formation of Compound I. The present data will be discussed in terms of the hypothetical complex proposed by Poulos and Kraut.

T-Pos36 A NEW HYPOTHESIS FOR PROTON TRANSLOCATION IN CYTOCHROME *c* OXIDASE, Massimo Sassaroli, Yuan-chin Ching, Siddharth Dasgupta, and Denis L. Rousseau, AT&T Bell Laboratories, Murray Hill, NJ 07974

We propose a new hypothesis for proton translocation which differs radically from prior models because it has no requirement for a mechanical gate generated by a redox dependent conformational change. This model is based on new results in studies of resonance Raman scattering from cytochrome *c* oxidase in the presence of deuterated and protonated solvents. From changes in linewidths of the high frequency Raman modes, we have inferred that one or more water molecules is present in the enzyme near cytochrome *a*. Based on this finding we propose this new hypothesis for proton translocation in cytochrome *c* oxidase. In this model water has direct access to the redox site (cytochrome *a*). At the site two or more groups[1] with redox dependent pK_as are located. When cytochrome *a* is reduced these groups are fully protonated whereas when the enzyme is oxidized one is deprotonated. The released proton has an exit channel only into the intermembrane space , thereby bringing about proton translocation. In each cycle the residues which bind protons get them from the water molecules in the heme pocket. Although this hypothesis for proton translocation has no requirement for a mechanical gate, the model does not exclude such conformational changes which could augment directionality.

1. M. Wikstrom in Electron Transport and Oxygen Utilization (C. Ho, Ed.) Elsevier, North Holland, Inc., New York, 1982, p. 271-277.

T-Pos37 ALLOSTERIC ENERGY, ORGANIC PHOSPHATE, AND THE BOHR EFFECT AT THE HEMOGLOBIN BETA CHAIN C-TERMINUS STUDIED BY HYDROGEN EXCHANGE. Godfrey Louie, Thao Tran, Joan Englander, and Walter Englander. Department of Biochemistry & Biophysics, University of Pennsylvania, Philadelphia, PA 19104.

When hemoglobin switches from the deoxy (T) to the liganded (R) state, a number of its peptide group NH experience a great increase in their rate of exchange with water. Such sites can be selectively labeled with tritium (functional labeling) and located by fragment separation methods. These methods were used to identify and study 3 to 4 allosterically sensitive peptide NH at the beta chain C-terminus, located between Ala-140β and the C-terminal His-146β residue. All these NH exchange at about the same rate in deoxy Hb (halftime $\sim$5 hr at pH 7.4, 0^{o}C, with DPG). All are accelerated: a) by $\sim$3-fold (depending on salt concentration) when DPG is removed (loss of salt link from His-143 to DPG); b) by 6-fold in NES-Hb (loss of salt link from His-146β to Asp-94β); c) by 16-fold when both salt links are removed together; d) by 1200-fold when the several stabilizing interactions at this locus are lost in the T to R transition. This concerted behavior is what the local unfolding model leads one to expect and is very hard to understand on any other basis.

Local unfolding theory connects increase in HX rate with the loss in allosterically significant bond free energy. For the His-146 to Asp-94 salt link, a 1 kcal free energy loss is found, experimentally identical with the energy calculated from: a) the Bohr ΔpK shift of His-146; b) the increased subunit dissociation in NES-Hb. The two salt link energies measured separately (0.5 kcal & 1.0 kcal) equal the energy measured for the two links removed together (1.5 kcal). For the R to T transition, the data indicate that 70% to 80% of the total allosteric energy change in hemoglobin occurs at the β chain C-terminus.

In oxyhemoglobin, the His-146β salt link does not reform at low salt (cf. Russu & Ho; Perutz et al.).

T-Pos38 MAGNETIC STUDIES ON NICKEL-RECONSTITUTED HEMOGLOBIN AND MYOGLOBIN. Periannan Kuppusamy, Abraham Levy, and Joseph M. Rifkind. National Institutes of Health, National Institute on Aging, Gerontology Research Center, Baltimore, Maryland 21224.

The nature of the metal ion coordination has recently been investigated in various metal substituted hemoglobins, e.g. Cu(II) and Ni(II), which do not bind oxygen and retain a T-like protein conformation. Absorption and Resonance Raman difference spectroscopy indicate two types of metal ion environments in Ni(II) hemoglobin (NiHb), one of which is similar to that found in Ni(II) myoglobin (NiMb). Since axial interactions produce major effects on the electron distribution of d^8-Ni(II), magnetic studies are very valuable for these Ni(II) systems. Magnetic susceptibility measurements show that NiMb is paramagnetic, indicative of a strong axial coordination which destabilizes the d_{z^2} orbital. On the other hand, NiHb is only partially paramagnetic, suggesting that some fraction of the protein is in a state where the axial interactions, if any, are much weaker. EPR studies on NiMb at 5 K show a well-resolved triplet spectrum with superhyperfine splittings from porphyrin nitrogen nuclei. The EPR parameters are: g (isotropic) = 2.0185; D = 0.004 cm^{-1}; E = 0; A_N = 16.5 G. Additional splittings from an axial nitrogen (A $\sim$4 G), presumably that of the proximal histidine, is also observed. NiHb under similar conditions shows relatively less intense and poorly resolved triplet features, resulting from a mixture of diamagnetic (S = 0) and paramagnetic (S = 1) species. A comparison with model studies indicates that the detailed nature of the metal ion coordination is regulated by the globin structure. The factors which determine the various types of coordination in these proteins will be discussed.

T-Pos39 TIME-RESOLVED PHOTOACOUSTIC CALORIMETRY OF CARBOXYMYOGLOBIN: ENTHALPY AND VOLUME CHANGES Judy A. Westrick and Kevin S. Peters, Department of Chemistry and Biochemistry, University of Colorado, Boulder, Colorado 80309.

Although the association and dissociation mechanism of carbon monoxide to sperm whale myoglobin has been studied extensively, the ligand's diffusion pathway from the solvent to the heme is still unknown. Recently, time-resolved photoacoustic calorimetry has been used to investigate the dynamics of the enthalpy and volume changes produced in the photodissociation of carbon monoxide from sperm whale myoglobin. The enthalpy and volume changes of this biphasic reaction are $\Delta H = -2.2 \pm 2.8$ kcal/mole and $\Delta V = -10 \pm 1$ ml/mole for the geminate pair relative to carboxymyoglobin and $\Delta H = 14.6 \pm 3.4$ kcal/mole and $\Delta V = 5.8 \pm 1.0$ ml/mole for the dissociation of carbon monoxide relative to carboxymyoglobin. Qualitatively, the enthalpy and volume changes for the formation of the geminate pair and for the dissociation of carbon monoxide are consistent with a model proposed by Ringe et al. (Ringe, D., Petsko, G.A., Kerr, D.E.& Ortiz de Montelanno, P.R., (1984) Biochemistry, 23, 2-4.) that involves the displacement of His 64 which appears to cause a rupture of the Arg-45 proprionate salt bridge. Further studies will be presented that pertain to the role of the salt bridge as well as the possible involvement of proton release or uptake.

T-Pos40 **EVALUATION OF OXYGEN BINDING CURVES FOR HUMAN HEMOGLOBIN IN THE PRESENCE OF NON-SATURATING, FIXED QUANTITIES OF 2,3-DIPHOSPHOGLYCERATE AND INOSITOL HEXAPHOSPHATE**

Charles H. Robert and Stanley J. Gill
Department of Chemistry and Biochemistry, University of Colorado, Boulder, CO 80309

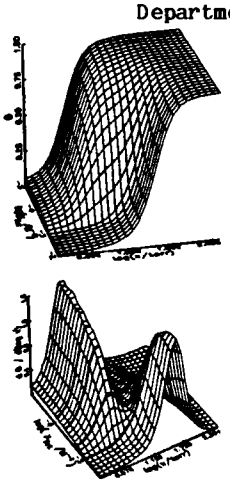

A macromolecule with two linked ligands-- a primary ligand and an effector ligand-- can exhibit biphasic binding curves when one ligand is present in nonsaturating, fixed amounts. At top left is a 3D view of the behavior of the binding curve at different fixed totals of the effector. We present a general treatment of the this behavior, which was described for the case of one-to-one stoichiometry of effector by Imai and Tyuma [Biochim. Biophys. Act. **293**, 290-294 (1973)]. The analysis is applied to oxygen binding data obtained for human hemoglobin (Hb) at high concentrations (1 mM tetramer) in the presence of a series of fixed molar ratios of effector to Hb (0,0.1,0.2,0.5,1,10) for both effectors 2,3-diphosphoglycerate (DPG) and inositol hexaphosphate (IHP). The data, taken with a thin-layer optical cell and gas-dilution valve apparatus [Dolman, D. and Gill, S.J., Anal. Biochem. **87**, 127-134 (1978)], are described essentially by the derivative curves represented at bottom left for IHP. The cuts of this surface corresponding to the present series of experiments are indicated by the thick lines in this figure and were analyzed simultaneously both in terms of the phenomenological Adair scheme and in the context of a modification of a simple allosteric model. In all analyses the triply oxygenated species was negligible. Supported by NIH grant HL 22325.

T-Pos41 FOURIER TRANSFORM INFRARED-PHOTOACOUSTIC SPECTROSCOPY AND QUANTITATIVE DETERMINATION OF SOLID-STATE MICROBIAL GROWTH

Richard V. Greene, Shelby N. Freer, and Sherald H. Gordon, USDA-ARS, Northern Regional Research Center, Peoria, IL 61604

Evaluation of biological systems which utilize particulate substrates, such as cellulose, suffers from a lack of suitable techniques which can analyze solid-state samples. A new analytical technique, photoacoustic spectroscopy (PAS), has been developed which provides information about the UV, visible and IR absorption spectra of solids, gels and other material not suited for conventional optical analyses. Growth of a filamentous fungus, Phanerochaete chrysosporium, on cellulose discs was determined by monitoring protein absorption bands in the IR region (Amide I and Amide II bands) with FTIR-PAS. Current techniques utilized to measure solid-state microbial growth are both cumbersome and unreliable, while FTIR-PAS is user simple and highly sensitive. Because numerous compounds have distinctive absorption properties in the IR region and FTIR-PAS is non-destructive to the sample, it is ideally suited for solid-state bioproduction analysis of high value compounds (i.e., drugs, hormones, biological polymers and films).

T-Pos42 MONITORING CELL GROWTH VIA FT-IR SPECTROSCOPY ON LIVING WHOLE CELLS IN SITU. Melody L. Mitchell, Timothy B. Hutson, Joseph T. Keller, Ming J.W. Chang (Intr. by Richard A. Dluhy) National Center for Biomedical FT-IR Spectroscopy, Battelle Columbus Division, 505 King Avenue, Columbus, Ohio 43201-2693.

The rapid expansion of spectroscopic research into complex biological systems has seen the recent application of FT-IR spectroscopy to whole cells (dried or suspended) for fermentation studies and bacterial speciation among others. We have developed an FT-IR technique that provides a non-invasive method of obtaining spectra of living cell cultures in situ. Chinese Hamster Ovary (CHO) cells cultured on germanium crystals in a specially designed flow cell are being studied in situ via attenuated total reflectance (ATR) FT-IR techniques. Spectra is obtained from the time when the cells are first seeded onto the crystal to when they have grown to confluence. The ATR depth of penetration is ~0.9 microns into the cells of ~2-5 micron thickness. At this depth we expect the spectra to have contributions from the cell membrane and some internal components of the cell. Plots of kinetics data (band intensity vs. time) of nearly all infrared absorbance bands in the spectra reflect growth patterns similar to those obtained when measuring cell growth via traditional methods, but with more easily obtained and cleaner results. Spectral shifts of deconvoluted bands have also been observed over time and will be discussed in light of cell synthesis and morphology.

ULTRAVIOLET RESONANCE RAMAN SPECTROSCOPY AS A PROBE OF ELECTRONIC INTERACTIONS AND HYDROGEN-BONDING IN NUCLEIC ACIDS. Thomas G. Spiro, Christine A. Grygon, and Joseph R. Perno, Department of Chemistry, Princeton University, Princeton, New Jersey 08544 - USA

Excitation profiles (EP's) for resonance Raman (RR) bands of dUMP, dAMP, and dCMP, obtained with excitation between 300 and 192 nm using a H_2-Raman shifted YAG laser, have a 2-banded appearance associated with the characteristic ∿260 nm and ∿200 nm absorption bands. The dCMP EP is flat and weak in the long wavelength region, reflecting interferences among several cytosine electronic transitions. For dUMP, dAMP, and dGMP there is evidence for 1) vibronic enhancement of specific RR modes at intermediate wavelengths and 2) enhancement via a weak π-π^* transition on the low energy side of the ∿260 nm absorption band. EP's for synthetic duplex polynucleotides show strong Raman hypochromism, associated with base-stacking. In addition, a distinct blue-shift is observed for the strong 260 nm transition of A and U in A-U duplexes. Frequency shifts attributed to hydrogen bonding at the uracil carbonyl group are complex owing to extensive coupling between ν_{C4}=O and other ring modes, but clear band assignments have been made for poly rA - poly rU. Hydrogen bonding to the base nitrogen atoms has little effect on the UVRR spectra.

T-Pos44 U.V. RESONANCE RAMAN SPECTRA AND SOLUTION STATE CONFORMATIONS OF CHOLINERGIC NEUROTRANSMITTERS.

K. J. Wilson, P. Derreumaux, G. Vergoten, & W. L. Peticolas
Dept. of Chemistry & Inst. of Molecular Biology, University of Oregon, Eugene, OR 97403.

Experimental Raman spectroscopic data and theoretical calculations show that large differences exist between the conformations of the acetylcholine cation (ACh) found in its crystalline states and in aqueous solution. Other choline esters that are strong ion channel activators (agonists) when bound to the ACh receptor protein (AChR) also show this property. This difference between crystal and solution conformation is not observed in choline esters such as acetylthiocholine that are not agonists. Utilizing observed Raman frequencies, normal coordinate analysis, coupled with CHARMM molecular mechanics calculations, the most probable solution conformations are obtained. Several minimum energy conformations are calculated using the CHARMM program. For these energy-minimized structures, the vibrational frequencies are calculated. The calculated frequencies are compared to the observed frequencies in solution, and the most probable solution state conformations are determined. It is found that ion channel activating (agonist) choline esters are flexible and bent while the non agonists are more rigid in an elongated all conformation. Methods of obtaining the UV resonance Raman spectra of agonists using 240 nm laser light presents a method for the determination of the conformations of choline esters in dilute aqueous solution and on the active site of the AChR. This should give a more coherent understanding of the structure-activity relation for ligands of cholinergic and other receptors. Supported by NSF Grant 8417199.

T-Pos45 RESONANCE RAMAN SPECTROSCOPY OF MODELS FOR BIOLOGICAL METALLOPORPHYRINS: A SYSTEMATIC STUDY OF PHENYL SUBSTITUTION AT THE *meso* POSITION. Julio C. dePaula, Robert T. Kean, Asaad Salehi, Chi K. Chang and Gerald T. Babcock, Department of Chemistry, Michigan State University, East Lansing, MI 48824-1322

We determined the effects of mono and di-phenyl substitution on the resonance Raman spectra of metallo-etioporphyrins. Using Soret band excitation, we observe that the mono-phenyl substituted metalloporphyrin exhibits a Raman spectrum that is very similar to that of the unsubstituted compound, although some modes due to phenyl vibrations are present. Phenyl substitution also affects C_bC_b vibrations because the bands ν_2 and ν_{11} both shift to lower frequency as the number of phenyl substituents increases. The totally symmetric C_aC_m stretching mode ν_3 is largely unaffected by phenyl substitution, whereas its out-of-phase counterpart ν_{10} shifts to lower frequency. Upon excitation in the vibronically allowed Q_1 band the Raman spectrum of di-phenyl substituted metalloporphyrin exhibits a number of anomalously polarized bands that are not present in the spectra of the unsubstituted metallo-etioporphyrin and metallo-tetraphenyl-porphyrin. Our results indicate that resonance Raman studies of biomimetic compounds where porphyrins are covalently attached to other groups should be based on mono-phenyl substituted porphyrins. [Supported by NIH GM 25480 (GTB) and GM 36520 (CKC)].

T-Pos46 SPECTROSCOPIC OBSERVATION OF A CHARGE TRANSFER BAND IN AN ARYL PEPTIDE. Wilson Radding, Department of Physiology, UAB, Birmingham, Alabama.

In non-polar solvent the diketopiperazine, cyclobis-N-methyl-L-phenylalanine (c-[NMe-L-Phe]$_2$), shows both circular dichroism and absorption between 305 and 395nm. There are no known vibronic bands observable in phenylalanine or its derivatives this far to the red. Therefore, the absorption and CD are probably due to charge transfer. The specific rotation of the circular dichroism centered at 350-360nm is concentration independent, indicating that the charge transfer is intramolecular. Introduction of water vapor into the solution obliterates this intensity; this part of the band therefore probably involves charge transfer between the aromatic sidechain and the carbonyl. The specific rotation of the 225nm region appears to increase with concentration. Thus there may also be an intermolecular charge transfer band in this long wavelength ultraviolet region.

T-Pos47 SPECTROSCOPIC STUDIES ON THE BINDING OF EUCARYOTIC INITIATION FACTORS 4F AND 4E TO 5' TERMINAL CAP REGION ANALOGS. M. Gulotta and D.J. Goss, Chemistry Dept., Hunter College of CUNY, New York, NY 10021.

Eucaryotic mRNA contains a unique structural feature (a "cap") at its 5'terminus consisting of 7-methylguanosine in a 5'-to-5' linkage via a triphosphate bridge to the first coded base of the mRNA. We have investigated the binding of initiation factors 4A, 4B and 4F to a cap analog (m7GpppA) to determine the effects of the initiation factors on the 5'terminal cap region conformation. Both circular dichroism and fluorescence studies of the cap analog m7GpppA indicate the two bases occur mainly in a stacked conformation at pH 7.5. Of the initiation factors tested, only the eIF-4F showed significant binding to this analog. eIF-4F caused an increased fluorescence intensity of the m7G suggesting that the cap was altered from a stacked to an unstacked conformation. This change in conformation may be a significant function of the eIF-4F in modulating polypeptide initiation. When eIF-4F was fractionated into separated peptide components, the conformational transition in the cap structure was induced by the 28,000 MW component (eIF-4E). We are currently pursuing more detailed studies of the "cap" conformation using vibrational circular dichroism.

Grant Support: AHA NYC Affil., NSF 86007070, and PSC-CUNY Research Award

T-Pos48 SOLVENT POLARIZABILITY EFFECTS ON CIRCULAR DICHROISM SPECTROSCOPY OF MEMBRANE PROTEINS. M. Cascio[1,2] and B. A. Wallace[1], [1]Department of Chemistry, Rensselaer Polytechnic Institute, Troy, NY 12180, [2]Department of Biochemistry, Columbia University, New York, NY 10032.

Net secondary structures of soluble proteins may be determined empirically from their circular dichroism (CD) spectra in the near-UV region, utilizing a data base derived from the spectra of water-soluble proteins of known structure. The CD spectrum of this region is a linear combination of three peptide transitions: $n \rightarrow \pi^*$, $\pi \rightarrow \pi^*_{\parallel}$ and $\pi \rightarrow \pi^*_{\perp}$. As in any absorptive phenomenon, the wavelengths of these transitions are influenced by the local environment: the interaction of a peptide transition dipole with its microenvironment may cause an increase or decrease in energy, thus leading to red- or blue-shifting of the absorption bands, relative to those in water. The hydrophobic lipid bilayer in which membrane proteins are embedded has a very different dipole moment and polarizability than does water, and thus may produce such shifts.

In this study, the component absorption bands of the reference data spectra were deconvoluted and shifted independently to maximize the correspondence of experimental and calculated curves for several proteins of known structure solubilized in a variety of non-denaturing solvents with different dipole moments. The $n \rightarrow \pi^*$ and $\pi \rightarrow \pi^*$ transitions were found to be shifted differentially with solvent, and the shifts appear to correspond with solvent polarizabilities. The convergence of maximal fit with accuracy in the secondary structure determination indicates that this method of analysis may be appropriate for proteins in a non-aqueous environment, and may therefore be of particular use in determining membrane protein secondary structures. (Supported by NIH Grants GM27292 and AM31089).

T-Pos49 ELASTIC LIGHT SCATTERING AND HIGHER ORDER CHROMATIN STRUCTURE. W. Chen*, D. Forster#, S. Zietz@ and F.M. Kendall*. #Department of Physics and *Department of Physiology, Temple University, Philadelphia, PA 19140. @Department of Mathematics and Computer Science and BMES Institute, Drexel University, Philadelphia, PA 19104

The scattering model consists of an array of dipoles distributed along a helix. Each scatterer is an oblate ellipsoid (composed of an isotropic dielectric with an anisotropic polarizability tensor) whose short axis has a specified angle β with respect to a tangent to the helix. The scatterer is not optically active. Starting with the magnitude matrix and first Born approximation we derived explicit angle-dependent parametric functions for each of 10 independent elements of the Mueller matrix when the intensity of scattered polarized light is averaged for all orientations of the scattering array. Two of these functions are sensitive to helical handedness and three are zero as expected. These zero functions can become non-zero in models which also include internal elastic scattering and they can thus supply 3 additional independent observables which are necessary to estimate the parameters of the scatterer from experimental data.

T-Pos50 THERMAL HYSTERESIS IN MICROVISCOSITY OF VERY DILUTED AGAROSE SOLUTION PROBED BY QELS.
F.Madonia,P.L.San Biagio and M.U.Palma Univ.,Phys.Dept.,and CNR-IAIF Palermo (Italy)*.

Quasielastic light scattering (QELS) of polystyrene latex spheres was used to measure the zero-shear viscosity of a very diluted solution of Agarose (Seakem HGT(p)) in water[1]. Results at 0.005% w/w (1/50 the minimum concentration for macroscopic gelation) show the existence of a thermal hysteresis in the viscosity. Specific viscosity stays constant when the temperature is decreased from 80 to 30 °C. Below this temperature specific viscosity increases, with kinetics of hours (depending on temperature). At about 70°C it goes back to its initial value. This behavior, which parallels the gelation of Agarose at higher concentrations[2], agrees with the existence of a spinodal decomposition which we observed in more concentrated Agarose sample[3]. The spinodal transition results in a spatially modulated polymer concentrations. Under these conditions gelation in small domains without macroscopic percolation is facilitated affecting the viscosity, according to the Einstein relation $n = n (1 + k\Phi)$ where Φ is the fractional volume. It is worth noting that QELS is most suitable to study this effect without introducing perturbing shears[1]. Further, preliminary data show a dependence of this behavior from concentration and solvent substitution as it is expected in a spinodal transition.

* Supported in part from CRRN-SM and MPI local fundings.

1. Madonia, F. et al. Nature 412, 302, 1983.
2. Indovina, P.L. et al. J.Chem.Phys. 2841, 70, 1979.
3. San Biagio,P.L. et al. Biopolymers 2255, 24, 1986.

T-Pos51 PHOTOPHYSICS AND ENZYME INHIBITION BY ROSE BENGAL: DEPENDENCE ON INTENSITY AND WAVELENGTH. Eric N. Fluhler, John K. Hurley and Irene E. Kochevar. Wellman Laboratories, Massachusetts General Hospital and Harvard Medical School. Boston, MA 02114.

Irradiation of dyes with peak power lasers often results in multiphoton resonant or non-resonant absorption, thereby populating excited states which are not reached using low irradiance sources. Reactions from these higher-lying states may, in turn, alter the photochemistry or phototoxicity of the dyes. We have studied the wavelength and intensity dependence of rose bengal (RB) mediated photoinhibition of red blood cell (RBC) acetylcholinesterase. Irradiation of RBC ghost suspensions containing RB with increasing intensities (Nd:YAG @ 532 nm, 30 psec pulses) resulted in a decrease in enzyme inhibition. Coincident with this decrease was an increase in transmitted light intensity and a decrease in the fluorescence intensity. These results can be explained by ground state depletion at the higher intensities. Irradiation of ghost suspensions in the presence of sodium azide or after argon purging greatly decreased enzyme inhibition, suggesting the participation of singlet oxygen in the inhibition mechanism. Finally, irradiation of RB solutions with high intensities of 1064 nm radiation (Nd:YAG, 30 psec pulses), a region where RB is transparent, resulted in observable emission, demonstrating that effects due to non-resonant absorption may be of importance at high irradiances.

T-Pos52 FLUORESCENCE STUDIES OF PHOSPHORIBULOKINASE, A LIGHT-REGULATED, CHLOROPLASTIC ENZYME. Camillo A. Ghiron[1], Maurice R. Eftink[2], Michael A. Porter[3], and Fred C. Hartman[3], [1]Department of Biochemistry, University of Missouri, USA, [2]Department of Chemistry, University of Mississippi, USA, and [3]Biology Division, Oak Ridge National Laboratory, USA.

Recent characterization of spinach phosphoribulokinase has revealed that the homodimeric molecule contains only two tryptophans per 44 kDa subunit. We have performed steady state and frequency domain studies of the intrinsic fluorescence of this protein. The fluorescence properties reflect contributions from both types of tryptophan residues. One of these appears a) to be relatively exposed to solvent and the quencher, acrylamide, b) to fluoresce with a λ_{max} of 345 nm, c) to decay with a fluorescence lifetime of 6.3 nsec, d) to have a relatively red-shifted absorption spectrum, and e) to have a certain degree of independent motional freedom, with respect to the protein. The other tryptophan residue appears a) to be more buried. It b) fluoresces with a λ_{max} of 325 nm, c) has a lifetime of 1.7 nsec, d) has a relatively blue-shifted absorption spectrum, and e) does not appear to enjoy independent motional freedom. On comparison of phase resolved spectral data and solute quenching data, we suggest that resonance energy transfer between the blue and red tryptophan residues may occur.

We also describe the strategy of simultaneously fitting Stern-Volmer quenching data collected at two emission wavelengths. This research was supported by the National Science Foundation (DMB 85-11569), by the US Dept. of Agriculture (84-CRCR-1-1520), and by the US Dept. of Energy (DE-AC05-840R21400).

T-Pos53 PRESSURE DEPENDENCE OF THE ACRYLAMIDE QUENCHING OF THE FLUORESCENCE OF TRYPTOPHAN RESIDUES IN PROTEINS. Maurice R. Eftink, Department of Chemistry, University of Mississippi, University, MS 38677.

The effect of hydrostatic pressure (0-2.6 kbar) on the acrylamide quenching of several single trp proteins has been studied using phase fluorescence lifetime measurements at 25°C. For the model system, indole in water, we find essentially no dependence of the quenching rate constant, k_q, on pressure. Changes in the aqueous volume and viscosity are small (<8%) in this pressure range; thus the activation volume, $\Delta V^{\#}$, for the diffusional quenching of indole fluorescence by acrylamide in water is ~0 ml/mole. For the internal trp residues in ribonuclease T_1 and cod parvalbumin, we also find essentially no pressure dependence ($\Delta V^{\#}$ ~0 ml/mole). Previous studies indicate that some sort of conformational fluctuations are required for collision of acrylamide with the trp residues. The low $\Delta V^{\#}$ values characterize these fluctuations as being very low in amplitude and not involving a significant unfolding of the globular proteins. A pressure dependence for k_q has been demonstrated for the peptide melittin, which was poised at its monomer tetramer equilibrium. In 0.5 M KCl at pH 7.5, melittin is approximately 50% associated in its tetrameric form. An increase in pressure shifts the equilibrium toward the monomeric form (Thompson and Lakowicz, Biochemistry 23, 3411 (1984)) and we observe a concomitant increase in the acrylamide k_q (the single trp being more exposed in the monomeric form). This melittin system is poised to show a pressure dependence, but it lends credence to our above reports of an absence of a pressure dependence. (This research was supported by NSF grant DMB 85-11569).

T-Pos54 OXYGEN FLUORESCENCE QUENCHING STUDIES WITH SEVERAL SINGLE TRYPTOPHAN CONTAINING PROTEINS. Maurice R. Eftink[1] and Camillo A. Ghiron[2], [1]Department of Chemistry, University of Mississippi, USA, [2]Department of Biochemistry, University of Missouri, USA. Sponsored by Mumtaz Dinno, Department of Physics, University of Mississippi, USA.

The work of Lakowicz and Weber (Biochemistry 12, 4161 (1973)) demonstrated that molecular oxygen is a powerful quencher of trp fluorescence in proteins. Here we will report some recent studies of the oxygen quenching of several proteins which have single, internal trp residues. Among these are apoazurin (Pseudomonas aeruginosa), aspariginase (E. coli), ribonuclease T_1, and cod parvalbumin. Both fluorescence intensity and phase lifetime quenching data will be reported. By comparison of these we find that there is a significant degree of apparent static quenching in these proteins. The dynamic quenching rate constants that we find are low compared to those for trp residues in other proteins. For example, for apoazurin we find an apparent k_q of 0.8×10^9 M^{-1} s^{-1} at 25°C. This value is the lowest that has been reported for the oxygen quenching of trp fluorescence.

The key to these measurements has been the development of a more rapid means of equilibrating the oxygen gas with the pressurized aqueous sample. This we have done with an arrangement in which the oxygen gas is forced to bubble through the solution in the cell. This allows for equilibrium to be reached, at any O_2 pressure, in 5-10 minutes. This research was supported by NSF grant DMB-85-11569.

T-Pos55 MAGNETICALLY INDUCED BIREFRINGENCE OF MUSCLE THICK AND THIN FILAMENTS AND THEIR MAJOR CONSTITUENTS.* T. William Houk, Thomas R. Branham, and Sondra F. Karipides, Department of Physics, Miami University, Oxford, Ohio 45056.

Macroscopic sections of muscle tissue have been shown to possess sufficient magnetic susceptibility to experience orientational effects in strong magnetic fields. We present data from experiments on magnetically induced birefringence performed on each of the major protein constituents of the thick and thin filaments and on synthetic thick filaments and reconstituted thin filaments. Experiments were performed using an automatic compensating Pockels cell system at the Francis Bitter National Magnet Laboratory. The monomeric forms of myosin and actin showed little or no significant Δn at fields up to 10 T. Tropomyosin showed a small positive birefringence while troponin gave a slightly negative birefringence. Synthetic thick filaments showed a positive birefringence with a slight hysteresis in the change in birefringence as the magnetic field was cycled. F-Actin filaments showed virtually no induced birefringence in and of themselves, but when reconstituted with tropomyosin and troponin a dramatically increased birefringence resulted. This birefringence also showed a very large hysteresis with cycling of the magnetic field. This hysteresis is most likely due to the delay in orientation of the reconstituted thin filaments due to their large rotational diffusion constants. A value for the decay time of the induced birefringence which should be related to relaxation by rotational diffusion was calculated.
*Supported by NIH Grant #NIH 1R15AR37822-01A1, part of this work was performed while the author was a Guest Scientist at the Francis Bitter National Magnet Laboratory, M.I.T., which is supported by the N.S.F.

T-Pos56 ON THE DISTANCE DEPENDENCE OF THE TRYPTOPHAN-DISULFIDE INTERACTION IN GLOBULAR PROTEINS FROM TIME-DEPENDENT PHOSPHORESCENCE MEASUREMENTS ON A MODEL SYSTEM. by Z. Li, W.E. Lee and W.C. Galley. Department of Chemistry, McGill University, Montreal, Quebec H3A 2K6.

Earlier studies by Longworth et al., and our observations of ligand-induced changes, have suggested that it would be useful to establish the distance dependence of tryptophan-disulfide interactions in globular proteins. Observations were made on mixtures of isobutyl disulfide and 2-(3-indolyl) ethyl phenyl ketone (IEPK) in rigid glass at 77K. The IEPK molecule excited with a 296 nm laser pulse gave constant initial phosphorescence intensities at various disulfide concentrations, suggesting the singlet quenching is essentially eliminated due to the highly efficient intersystem crossing to the triplet level of the indole moiety. Non-exponential decays arising from a distribution of fixed indole-disulfide separations were analyzed assuming a Dexter-type exponential dependence of the quenching rate constant k with separation x, or $k=K\ Exp(-2x/L)$, in which K is the quenching constant at van der Waals' contact and L is the average effective Bohr radius of the the interacting partners. Reasonable fits of the decays are found with L values in the range of 1.41-1.69 A and values of K of 18-40 sec^{-1}. The fits of the model to the experimental decays are considerably improved with smaller values of L at close to van der Waals' contact, reflecting the expected increase in effective nuclear charge as the electron approaches the nuclei. The parameters found for the distance dependence of the perturbation predict that tryptophan triplet lifetimes should decrease by 3.3-4 fold for each Angstrom separation out to a detectable distance of 4 A between partners. The distance dependence is seen to account for the anomalous triplet lifetimes of some disulfide-containing proteins of known structure.

T-Pos57 THE HETEROGENEOUS FLUORESCENCE OF YEAST OTCase: DIFFERENTIAL RESPONSE TO ACTIVE SITE OCCUPANCY. Preston Hensley* and Jay R. Knutson, *Dept. of Biochemistry, Georgetown University, Medical Center, Washington, DC 20007 and Laboratory of Technical Development, NIH-NHLBI, Bethesda, MD 20892

Active-site ligand-binding promoted conformational changes have been proposed as controlling events in the association of OTCase with arginase to form a regulatory multienzyme complex. We have examined the intrinsic fluorescence of OTCase (single tryptophan) as a probe for these conformational changes. Time-resolved emission profiles were obtained with a mode locked laser source, and three distinct decay times were extracted via global analyses. The corresponding decay-associated spectra (DAS) were found to respond differently to active site occupation. The shortest decay component was indifferent to binding, while the intermediate and long components were sensitive in different ways. The middle DAS decreased in response to any liganding, without discrimination, while the long-lived component exhibited a differential response: occupation of both the ornithine and carbamoyl phosphate sites caused a significant decrease in this DAS, while single occupation provided an increase (compared to the unoccupied enzyme). Steady-state quenching with iodide also exhibited a single-vs.-dual occupation sensitivity; again, the data were analyzed globally to provide quenching DAS (=QDAS) ranked according to accessibility. We will discuss the microheterogeneous origins of these signals and reassert the importance of multiwavelength overdetermination, especially for discerning discrete vs. continuous lifetime models. (Supported in part by NIH GM28731 to P.H.)

T-Pos58 NANOSECOND TIME-RESOLVED FLUORESCENT ANISOTROPY: ANOTHER TOOL FOR KINETIC STUDIES.
Dana G. Walbridge, Myun K. Han, Jay R. Knutson, and Ludwig Brand, Department of Biology, The Johns Hopkins Univ., Baltimore, MD 21218 and The Laboratory of Technical Development, NHLBI, NIH, Bethesda, MD 20892

It has been shown previously that a single photon counting fluorescence lifetime spectrophotometer can be adapted to study rapid reactions of proteins (Walbridge et al., Anal. Biochem. 161, 467, 1987; Han et al., Anal. Biochem. 161, 479, 1987). We now show that the same technique can be extended to obtain anisotropy parameters during changes in protein conformation and subunit interactions. Polarization data can be obtained by employing one of two revisions to the original technique. One (L format) requires alternation between parallel and perpendicular polarizer orientation. The other exploits a T format (with parallel and perpendicular polarizers on opposing ends of the sample compartment) which allows simultaneous polarization measurements. The following examples are examined. During the acid denaturation of HLADH, zinc is released from the protein resulting in subunit dissociation prior to unfolding. Previous studies have shown that the decay times of 4 and 7 ns change to 2 and 5 ns during the denturation (Walbridge et al. Biophys. J. 51, 283a, 1987). The examination of this process with kinetic anisotropy measurements will be presented. Enzyme I of the PTS exhibits a temperature-dependent monomer/dimer equilibrium. We have examined the subunit interactions following rapid temperature changes. This enzyme also shows pH dependent activity and we will describe concomitant subunit dissociation. Supported by NIH grant GM11632.

T-Pos59 A REVERSIBLE THERMAL TRANSITION OF DODECAMERIC GLUTAMINE SYNTHETASE FROM *E. coli*.
A. Shrake, P. J. McFarland, M. T. Fisher, & A. Ginsburg, NHLBI, NIH, Bethesda, MD 20892

Glutamine synthetase (GS), M_r 622,000, contains 12 active sites formed at heterologous interfaces between subunits. Temperature-induced UV difference spectra from 5-68°C were reversible with the Mn^{2+}- or Mg^{2+}-enzyme at pH 7.3 (30°C) in 100 mM KCl. The thermal transition involves the exposure of 1 of the 2 Trp residues/subunit ($\Delta\varepsilon_{\sim 294-\sim 289nm}$ = 1100 $M^{-1}cm^{-1}$) and 2 of the 17 Tyr residues/subunit (by second derivative analysis). The data conform to a 2-state model of unfolding. In 1 mM $MnCl_2$ and 10 mM $MgCl_2$, midpoints of the transition (T_m) were 324 and 327 K, respectively, with corresponding ΔH_{vH} values of 91 and 105 kcal/mol (where the cooperative unit is most likely the dodecamer). No dissociation or aggregation of dodecamer occurred at high temperatures. Moreover, there was no change in Trp or Tyr exposure on heating the inactive apoenzyme. Increasing [$MnCl_2$] from 1 to 10 mM decreased T_m, indicating preferential interaction between Mn^{2+} and the partially unfolded enzyme. Conversely, the addition of substrate Gln, ADP, Gln + ADP, or L-Met-sulfoximine increased the T_m value to a varying extent by preferential binding to the folded form. The transition state complex GS•(Mn_2•ADP•L-Met-S-sulfoximine-phosphate)$_{12}$ was stable in the folded form at least to 72°C. An Arrhenius plot of V_{max} in γ-glutamyl transfer was linear from 3-72°C with E_A = 17.4 kcal/mol. However, a plot of ln K_m for Gln vs 1/T was biphasic with a crossing point at $K_m \simeq 1.5$ mM at ~38°C; ΔH_{vH} = -3.3 and -14.5 kcal(mol subunit)$^{-1}$ for the low and high temperature segments corresponding to high- and low-affinity forms. Thus, the thermally induced transition of dodecameric GS involves the melting of active site structures that affect the K_m for Gln but not k_{cat}.

T-Pos60 DIFFERENTIAL SCANNING CALORIMETRIC STUDIES OF E. COLI THIOREDOXIN, M. Santoro and W. Bolen, Department of Chemistry and Biochemistry, Southern Illinois University, Carbondale, IL 62901.

Differential scanning calorimetry (DSC) of E. coli thioredoxin (TRX) was determined as a function of pH in order to assess the thermal characteristics and reversibility of thermal unfolding. pH values of 2.7 and 7.0 were found to be optimal conditions in that, at these pH values, the system appears to exhibit two state behavior with $\Delta H_{cal}/\Delta H_{vantHoff}$ ratios very close to unity. Rescans of thermal unfolding at these pH values yielded DSC peaks with areas of from 90 to 100% of the original scan, indicating a high degree of reversibility. By contrast, in the acid range near the pI (4.5) of the protein, thermal unfolding was found to be much less reversible with a $\Delta H_{cal}/\Delta H_{vantHoff}$ ratio significantly less than unity. Calorimetric ΔH values of 69 and 105 kcal/mol and T_m values of 64.3°C and 86.3°C were determined at pH 2.7 and 7.0 respectively.

The dependence of ΔH_{cal} on T_m has often been used to calculate ΔC_p and a value of 1.3 kcal/mole*deg was estimated from the pH 2.7 and 7.0 data. However, the observed ΔC_p values derived from the actual thermal unfolding plots at these pH values were found to be near zero. The origin of the discrepancies in ΔC_p quantities determined by the two methods is not clear.

In order to explore further the meaning of these experimental results, work involving chemically modified and mutated TRX is now in progress.

T-Pos61 THE INFLUENCE OF DODECYL SULFATE ON THE AMIDE EXCHANGE KINETICS OF MICELLE-SOLUBILIZED, HYDROPHOBIC PEPTIDES. J.D.J. O'Neil and B.D. Sykes, Department of Biochemistry, Univ. of Alberta, Edmonton, Alberta, Canada, T6G 2H7.

Backbone amide hydrogen exchange measurements provide information about the internal dynamics of proteins. However, before such measurements can be unambiguously interpreted, contributions to hydrogen exchange rates from the chemical and physical environment of the amides must be accounted for. Membrane proteins are often solubilized in detergents, yet there have not been any systematic investigations of the possible effects of detergents on amide hydrogen exchange. We have measured individual backbone amide exchange rates for the amphipathic tripeptide leu-val-ile-amide dissolved in water and dodecyl sulfate (SDS) micelles using ^{1}H NMR spectroscopy. The broadening effects of micelle-incorporated spin labelled fatty acid (12-doxyl-stearate) on the ^{1}H NMR spectra of both the detergent and the peptide resonances were used to demonstrate that the tripeptide is in intimate association with the micelle either as a co-micellar complex or at the micellar surface. The detergent did not retard the exchange rates which suggests that the micelle cannot restrict access of charged catalysts to the peptide backbone. However, the minimum pD for amide exchange of the peptide in detergent was increased by 1.3 to 1.7 units compared to exchange in water. This is because the negatively charged surface of the micelle effectively condenses protons lowering the pH at its surface. The pH_{min} of exchange also increased for the side-chain exchangeable amides of trp and gln in hydrophobic peptides solubilized by SDS. These results have enabled us to separate the contribution to amide exchange by the structure of the protein from the effect due to detergent in the interpretation of the backbone and side-chain amide exchange rates of M13 coat protein solubilized with SDS.

T-Pos62 QUANTITATIVE DETECTION OF RAPID MOTIONS IN SPECTRIN BY NMR Leslie W.M. Fung[1], Hwei-Zu Lu[1], Rex P. Hjelm, Jr.[2] and Michael E. Johnson[3], [1]Department of Chemistry, Loyola University of Chicago, Chicago, IL 60626; [2]LANSCE, Mail Stop H805, Los Alamos National Laboratory, Los Alamos, NM 87545; [3]Department of Medicinal Chemistry and Pharmacognosy, University of Illinois at Chicago, PO Box 6998, Chicago IL 60680.

Our previous high resolution proton NMR data on human erythrocyte spectrin molecules indicate the existence of regions exhibiting rapid internal motions within the intact molecules *[Fung, L. W.-M., Lu, H.-Z., Hjelm,jr, R. P., Johnson, M. E. (1986) FEBS Lett., 197, 234-238].* We have extended the studies by developing quantitative NMR methods to determine the fraction of the spectrin protons exhibiting rapid internal motions, in both the isolated molecule and within the spectrin-actin network. Using both one-pulse and spin echo pulse sequences, we find that the fraction of the protons in rapid motion is about 15 % of the total protons in the spectrin molecule at 37 °C in phosphate buffer with 150 mM NaCl at pH 7.4. The value decreases to about 11 % when NaCl is removed. We believe that quantitative information on these rapid motions will be important in understanding the mechanical and functional properties of spectrin molecules. (Supported in part by grants from NIH and DOE.)

T-Pos63 THE COMBINED USE OF FRET AND CROSSLINKING TO ESTIMATE DISTANCES BETWEEN MOBILE SITES Peter D. Chantler, Susanne M. Bower, Terence Tao & Walter F. Stafford. Med. Coll. PA., Phila. PA. 19129 & Bos. Biomed. Res. Inst., Boston, MA. 02114.

The techniques of fluorescence resonance energy transfer (FRET) and crosslinking can provide complementary approaches concerning the relative separation of a pair of sites. In the static case they represent independent methods of measuring a fixed distance. In the dynamic case, where motion is possible between the two sites, the complementarity of the two approaches is not necessarily intuitive. We have taken advantage of hybrid myosins in order to understand the relationship between distances obtained for the same pair of translationally equivalent sites, one on each myosin head, using both FRET (steady-state (SS) and time-decay (TD)) and crosslinking. 4-4'-dimaleimidyl-stilbene-2-2'-disulfonic acid (DMSDS), a rigid crosslinker, can efficiently crosslink the two myosin regulatory light-chains, each at Cys-50 (Chantler,P.D. & Bower,S.M. (1987). Biophys.J. 51. 322a), indicating that these sites can come within 18A of each other. In addition, we show 5-5' dithiobis (2-nitrobenzoic acid) promotes disulfide formation between these same two sites indicating that they can also approach within 2.0A of each other. Alternatively, SS & TD-FRET measurements using donor/acceptor pairs located at these same sites, indicate transfer efficiencies of $<20\%$ (Chantler,P.D. & Tao,T. (1986). J.Mol.Biol. 192. 87-99). The SS results suggest a mean separation of >50A between sites. Although crosslinking indicated a close approach of ≤ 18A, the TD results gave no indication of a population of molecules possessing very short lifetimes, suggesting a relatively small subpopulation of such molecules at any one time. Using simple 'worst-case' models we explain how efficient crosslinking can be readily achieved in dynamic systems even though the necessary subpopulation of proximate molecules at any instant may be below the detection limits of TD-FRET.

T-Pos64 THE EFFECT OF PARTICLE SIZE AND TEMPERATURE ON THE SECONDARY STRUCTURE OF BOUND APOE
Martha P. Mims, Maurizio R. Soma, & Joel D. Morrisett. Baylor College of Medicine Houston, Tx.
ApoE mediates binding of CER-VLDL and HDL_c (from cholesterol fed animals) and $VLDL_1$ (from hypertriglyceridemic subjects) to the LDL receptor of fibroblasts. ApoE/DMPC bilayer disks also bind to the receptor; apoE alone does not. It has been proposed that the conformation of apoE on the surface of a lipoprotein determines its capacity to bind to the receptor. We have examined this proposal using large (LME) and small (SME) microemulsion models of cholesteryl ester rich lipoproteins containing DMPC and CO; these are in the VLDL (~750 Å) and LDL (220 Å) size ranges. LME and SME have DSC transitions at 25°-30°C due to the surface DMPC, and at ~42°C due to the CO core. ApoE binds to both populations to form model lipoproteins. The CD spectra of apoE bound to LME (apoE/LME) and SME (apoE/SME), and to DMPC vesicles (apoE/DMPC disks) were examined to determine if particle size, or the order/disorder of the surface or core domains affected the conformation of bound apoE. At 4°C, apoE bound to disks displayed the greatest α helicity followed in order by SME and LME. For apoE/DMPC and apoE/SME, the α helicity decreased monotonically over the range 4°-50°C. ApoE bound to LME showed a large drop in α helicity between 18° and 25°C (near the surface transition) which remained constant up to 50°C. In competition studies with ^{125}I LDL for binding to the LDL receptor of fibroblasts, apoE/SME and apoE/DMPC competed more effectively than LDL for binding, uptake, and degradation by the receptor; apoE/LME was much less effective. In direct binding studies, apoE/SME and apoE/DMPC were bound to a greater extent than apoE/LME. The data suggest a relationship between lipoprotein size, apoE secondary structure, and binding to the LDL receptor. (Supported by HL-27341, HL-07341, Welch Q-837)

T-Pos65 RESOLUTION OF A DISTRIBUTION OF DISTANCES BY STEADY STATE MEASUREMENTS OF ENERGY TRANSFER AND QUENCHING-INDUCED VARIATION IN THE FORSTER DISTANCE. Ignacy Gryczynski, Wieslaw Wiczk, Michael L. Johnson, Nanda Joshi, and Joseph Lakowicz, University of Maryland, Department of Biological Chemistry, Baltimore, Maryland 21201, and Herbert C. Cheung, University of Alabama, Department of Biochemistry, Birmingham, Alabama 35294.

We describe a new method to recover the distribution of donor-to-acceptor (D-A) distances in flexible molecules using steady state measurements of the efficiency of fluorescence energy transfer. The method depends upon changes in the Forster distance (R_o) which are induced by collisional quenching of the donor emission. The R_o-dependent transfer efficiencies are analyzed using non-linear least squares to recover the mean D-A distance and the width of the distribution. We recovered the distance distributions of three D-A pairs separated by flexible alkyl chains of varying lengths. Two different D-A pairs were examined with each of the same three flexible spacers. Both D-A pairs yielded the same distribution of D-A distances. Additionally, we examined the distribution of distances from the single tryptophan residue (158) in troponinI (TNI) to IEADANS-labeled cysteine 133. A relatively narrow distribution with a 12 A^o half-width was found for the native state, and the width increased dramatically to 47 A^o upon denaturation by guanidine hydrochloride. In all cases the distance distributions recovered from the steady state transfer efficiencies were in excellent agreement with the distributions recovered using the more sophisticated frequency-domain method. These measurements are now being extended to donor and acceptor-labeled peptides.

T-Pos66 EXCITED STATE IONIZATION OF TYROSINES IN CALMODULIN. Lynn M. Richard and Gautam Sanyal, Department of Chemistry, Hamilton College, Clinton, N.Y. 13323

The single tyrosine residue (tyr-138) of wheat-germ calmodulin (WG-CaM) and the two tyrosine residues (tyr-99 and tyr-138) of bovine testes and bovine brain calmodulin (BT-CaM and BB-CaM) exhibited tyrosinate (ionized tyrosine) fluorescence in the 330-360 nm wavelength range, in addition to tyrosine (unionized) fluorescence. The tyrosine and tyrosinate emission intensities of CaM from all three sources were independent of pH in the pH 5-9 range. The excitation spectra in this pH range showed a pH-independent maximum at 278 nm, irrespective of whether emission was monitored at 305 nm (tyrosine) or at 345 nm (tyrosinate). These data strongly suggest that tyrosinate fluorescence of both tyr-99 and tyr-138 arise from ionization of tyrosine in the excited state with a pK_a below 5.0. Both vertebrate and plant CaMs showed progressive decrease of 305 nm fluorescence with increasing pH above 9.5. Concomitantly, the excitation maximum gradually shifted towards longer wavelengths. These data are consistent with ground-state ionizations of tyr-99 and tyr-138 with pK_a's $\geq$10. Parallel UV absorbance measurements supported these conclusions. We do not have any evidence for ground-state ionization of tyr-99 with an unusually acidic pK_a, as it was reported earlier (S. Pundak & R.S. Roche, Biochemistry 23, 1549, 1984). Excited-state tyrosinate fluorescence occurs in the same wavelength range as tryptophan (trp) and thus may have a small (because of low quantum yield of tyrosinate) effect on fluorescence studies of interactions of trp-containing peptides with CaM. A quantitative measure of the tyrosinate effect will be provided in terms of relative quantum yields.

Supported by NIH Grant # GM 37471 (GS).

T-Pos67 CONSERVED CYSTEINE AND HISTIDINE RESIDUES IN AVIAN MYELOBLASTOSIS VIRUS NUCLEOCAPSID PROTEIN pp12 ARE NOT ZINC BINDING LIGANDS. Lisa M. Smith and Joyce E. Jentoft, Department of Biochemistry, Case Western Reserve University, Cleveland, OH 44106.

Small retroviral nucleocapid proteins contain regions of homologous peptide sequence, namely, C-X-X-C-X-X-X-G-H-X-X-X-X-C. pp12, the primary nucleocapsid protein of avian myeloblastosis virus (AMV), contains two of these regions. It has been proposed (Berg, J.M. (1986) Science 232, 485-487) that the cysteine and histidine residues in these regions bind zinc ions as part of the structural organization of these small proteins (5-12 kDa). AMV pp12 isolated either in the absence of detergents and chelating agents, or in the absence of organic solvents and chelating agents, showed no stoichiometrically bound metal ions when studied by plasma emission spectroscopy. pp12 incubated with a five-fold molar excess of zinc will bind three zinc ions per pp12 molecule, but with low affinity. The interaction of pp12 and 3 Zn-pp12 with poly(ethenoadenylic acid), a fluorescent polynucleotide, has also been studied. The K_d values for both pp12 and 3 Zn-pp12 are in the micromolar range. The results from these investigations indicate that zinc binding is nonessential to nucleic acid binding, and that it is not a structural component of AMV pp12.

T-Pos68 ^{13}C NMR STUDIES OF REDUCTIVELY ^{13}C-METHYLATED BOVINE INSULIN. Josephine Secnik and Joyce E. Jentoft. Department of Biochemistry, Case Western Reserve University, Cleveland, OH 44106.

^{13}C chemical shifts, signal intensities and T_1 relaxation times of the three ^{13}C-methylated amino groups of bovine insulin (Gly 1 of the A chain, Phe 1 and Lys 29 of the B chain) were studied as a function of pH and ionic strength. The dimethylated N-termini titrated with a very small change in chemical shift. Dimethylated lysine B29, in contrast, displayed a normal titration curve with a pKa value of 10.31 ± 0.02 at low ionic strength. The pKa value decreased to 9.87 ± 0.05 in 0.1M KCl, suggesting that Lys B29 may be involved in an ion pair interaction in solution. No further ionic strength effects were observed at higher concentrations of KCl. The widths at half-height of the dimethylated Gly-A1 and Phe -B1 resonances increase two-fold over the pH range 6 to 8, suggesting that either their mobility or their exchange rate changes with pH. T_1 values, however, changed in a different manner, changing in accord with the known pH dependence of insulin aggregation. Below pH 3.5, where the insulin is predominantly in the monomer form, the T_1 value was higher than at 7, 8, or 9, where the dimer form is dominant. The lysine B29 resonance had a higher T_1 value than either of the N-termini. This may reflect both the greater intrinsic mobility of the lysine dimethylamino group and the greater immobilization of the dimethylated N-termini on the surface of the protein and at the dimer interface. These changes in line widths and T_1 values may also be affected by the exchange rates of association and dissociation of insulin aggregates under varying conditions of pH and ionic strength.

T-Pos69 Do D_2O-mediated changes in protein/peptide fluorescence predict W accessibility. H.V. Jakubowski, S. Sedarous, and F.G. Prendergast, Mayo Foundation, Rochester, MN. D_2O effects on fluorescence lifetimes (τ) and quantum yields (I) of tryptophan (W) in δ-sleep inducing peptide (SIP), WAGGDASGE, cholecystokinin tetrapeptide (CCK), WMDF, lutinizing hormone releasing hormone (LHRH), $EHWSYGLRPGNH_2$, and an analog, $D\text{-}F^2,D\text{-}A^6$-LHRH were investigated. τ's were determined as a function of pH and temp.(T) by multi-frequency phase fluorometry using a synch-pumped, mode-locked and cavity-dumped Nd:YAG laser. I and τ values for SIP and CCK decreased with decreasing pH, consistent with increased collisional quenching of W fluorescence by the charged N-terminus. However, isotope effects, calculated as ratios of I (K_{DI}) or τ (K_{DT}) for both peptides were bell-shaped, with a minimum at pH 7.7. In addition, τ vs T curves (pH 7.4) in D_2O and H_2O were linear, and intersected, with $K_{DT} < 1$ at $T < 23^oC$. In contrast, the I and τ profiles for LHRH were bell-shaped with a maximum at pH 7.5-8, consistent with quenching by H. K_{DI} and K_{DT}, however, varied minimally from pH 5-9.4. T dependencies of τ's for either LHRH or the H(-) analog in D_2O and H_2O gave nearly parallel ln $1/\tau$ vs T plots, consistent with expectations for a single, T-dependent quenching process. K_{DT} increased slightly with T. D_2O effects for several proteins will be presented. Clearly, D_2O effects on fluorescence of solvently accessible W residues in these peptides are complex and are influenced markedly by nearest neighbor effects. Supported by GM34847.

T-Pos70 ENZYMATIC ACTIVITY AND THERMODYNAMIC STABILITY OF YEAST CYTOCHROME C OXIDASE. D. Diggs and E. Freire, Department of Biology, The Johns Hopkins University, Baltimore, MD 21218

Yeast cytochrome c oxidase has been purified and reconstituted into dimyristoyl phosphatidylcholine (DMPC) bilayer vesicles using a detergent dialysis technique. The thermodynamic stability of the reconstituted enzyme has been measured using high sensitivity differential scanning calorimetry. As in the case of the beef heart enzyme, the thermal unfolding of the yeast enzyme is characterized by the existence of two well defined peaks in the calorimetric profile. The low temperature peak is centered at 45°C and the high temperature at 54°C. Under similar conditions, the beef heart cytochrome c oxidase peaks are centered at 52°C and 63°C, respectively. For the beef heart enzyme, we have previously determined (Rigell, C. and Freire, E. (1987) Biochemistry 26, 4366) that subunit III is the main component in the low temperature peak and that subunits I, II and IV are the main contributors to the high temperature peak. Even though the yeast oxidase peaks have not been structurally resolved, it is important to note that the temperature dependence of the electron transfer activity shows a large inflection centered at 45°C but that residual activity can be observed up to 60°C. (Supported by NIH grant GM-37911.)

T-Pos71 FLUORESCENCE STUDIES OF TRYPTOPHAN-47 IN VARIANT-3 SCORPION NEUROTOXIN. J. Hedstrom, S. Sedarous and F.G. Prendergast, Dept. of Biochemistry and Molecular Biology, Mayo Foundation, Rochester, MN 55905. The fluorescence properties of scorpion neurotoxin variant 3 (SN3) were studied under conditions of varied temperature and quencher concentration. Steady state anisotropy (r_{ss}) values were insensitive to temperature between 10-50°C. The high r_{ss} of ~ 0.23 supports molecular dynamic calculations which have shown that W-47 rotational motion is restricted by local packing of amino acid residues. Values of r_{ss} for varied quencher concentrations at 25°C and differential polarized phase fluorometry data indicate that the rotational correlation time for W-47 is comparable to the fluorescence lifetime. Differential polarization and fluorescence lifetimes were measured using a laser based multi-frequency phase and modulation fluorometer. Both exponential and distribution analyses were performed on the fluorescence lifetime data and both sets of analyses support the existence of distinct conformational substates, each with markedly different fluorescence lifetime. The emission maximum of W-47 is blue-shifted from free W in water, implying that W-47 is at least partially shielded from the solvent, an inference supported by molecular graphics depictions employing Connolly surfaces. We are attempting to correlate the photophysical properties of the protein with the results of the molecular dynamics simulations. Supported by GM 34847.

T-Pos72 TIME-RESOLVED FLUORESCENCE DURING ACID DENATURATION OF STAPHYLOCOCCAL NUCLEASE. J. Wages, M. Han, J. Feitelson*, E.A. James, C.J. Baldick, J .R. Knutson**, and L. Brand, Dept. of Biology, The Johns Hopkins Univ., Baltimore, MD; *The Hebrew Univ., Jerusalem, Israel; and **Laboratory of Technical Development, National Institutes of Health, Bethesda, MD.

The nuclease from Staphylococcus aureus contains a single tryptophan residue. This makes it an ideal candidate for intrinsic fluorescence studies, especially with respect to conformational heterogeneity. Recently, Shortle (Shortle, D. and Lin, B. Genetics 110: 539 (1985)) introduced site-specific mutagenesis of nuclease, with a plasmid-based means for expression in E. coli. Availability of these mutants allows us to examine the complex decay of tryptophan fluorescence by changing residues proximate to tryptophan, as well as by introducing cysteine residues for labeling with specific fluorescence probes. The fluorescence of the single tryptophan in nuclease exhibits multiexponential decay kinetics. These complex decays have been examined with decay-associated spectra (DAS) under various conditions. At pH 6, biexponential decay is observed, with a dominant 5.7 ns component and a shorter component; the DAS of the 5.7 ns component is red-shifted with respect to the DAS of the shorter component. At pH 3, where the protein is completely unfolded as indicated by the tryptophan fluorescence, at least three exponential decay components are evident. Interestingly, each decay component has a unique spectrum. At pH greater than 9, addition of 10 mM Ca^{2+} results in shortened lifetimes and in a decrease in the steady-state emission intensity of about 10%. DAS obtained under these conditions will also be presented. Implications of the time-resolved data, including DAS,to protein conformation and the microheterogeneity of the tryptophan environment will be discussed. Supported by NIH GM11632.

T-Pos73 ^{1}H-NMR STUDIES ON THE STRUCTURE OF CALMODULIN AND CALMODULIN-PEPTIDE COMPLEXES. Steven H. Seeholzer and A. Joshua Wand. Institute for Cancer Research, Philadelphia, PA 19111.

Calmodulin, a ubiquitous Ca^{2+}-binding protein, regulates a wide range of cellular processes in response to changes in intracellular Ca^{2+} concentration. Regulation occurs by the Ca^{2+}-dependent action of calmodulin on specific target enzymes within the cell. We are using 2D ^{1}H-NMR techniques to study the structural basis for the tight binding interaction between $(Ca^{2+})_4$-calmodulin (CaM) and peptides derived from the calmodulin binding domains of smooth and skeletal muscle myosin light chain kinase. Obtaining comprehensive structural information from this approach requires an extensive set of ^{1}H-NMR spectral assignments of both free CaM and the CaM-peptide complexes. We are applying the recently introduced main chain directed assignment algorithm to these problems. In parallel studies, we are collecting information on the structure of bound peptide by examining the considerably simplified spectra obtained from complexes of peptide with perdeuterated CaM. These and other studies have allowed us to determine the orientation and structure of bound peptide and to probe the structural perturbations brought about by CaM-peptide complex formation. Results of these studies will be presented.

T-Pos74 **LINKED FUNCTIONS FOR SITE-SPECIFIC THERMODYNAMIC TRANSITIONS 0F MACROMOLECULES.** Gary K. Ackers, Department of Biology, The Johns Hopkins University, Baltimore, MD 21218.

A growing number of experimental techniques permit the measurement of local-site binding isotherms and conformational transitions at local sites in macromolecular systems (i.e. spectroscopic methods involving NMR or fluorescence, DNase footprint titration). All the interesting cases are those in which the process monitored at a local site is coupled to other events (binding, melting) at structurally separate sites within the same macromolecule; such intramolecular coupling is fundamental to biological function and lies at the heart of many regulatory mechanisms.

The theory of free energy coupling in local-site binding systems, presented in 1983 (1), is extended here. Linked functions for local-site transitions are compared with those applicable to "classical" systems as treated by Wyman (2), Schellman (3), and Hermans and Scheraga (4). Major differences exist between local-site thermodynamics and these "classical" theories due to the fact that the local sites cannot have separable partition functions; hence they do not conform to the standard methods of generating thermodynamic properties from the partition function. Recent developments in our understanding of this problem are providing a foundation for meaningful application of local-site experimental techniques. 1. Ackers, G.K., Shea, M.A. and Smith, F.R. (1983) J. Mol. Biol. 170, 223-242. 2. Wyman, J. (1964) Adv. Prot. Chem. 18, 223-286. 3. Schellman, J.A. (1975) Biopolymers 14, 999-1018. 4. Hermans, J. and Scheraga, H.A. (1961) J. Am. Chem. Soc. 83, 3283-3292, Appendix II.

T-Pos75 ACCOMMODATION OF INTERNAL MOTION IN THE GENERATION OF SOLUTION STRUCTURES OF PROTEINS BY ^{1}H NMR. M.J. Dellwo and A.J. Wand, Institute for Cancer Research, Fox Chase Cancer Center, Philadelphia, PA 19111

A major emphasis of modern nuclear magnetic resonance studies of proteins is the generation of three dimensional models of their structure in solution. While current methods emphasize a static interpretation of the geometric information available from the experimentally determined nuclear Overhauser effect (NOE), they do not include the effects of internal motion on this observable. In order to accommodate the distortion of the magnitude of the ^{1}H-^{1}H NOE, due to the presence of internal motion, we have extended the model independent theory of Lipari and Szabo to the multiple dipole-dipole interactions characteristic of proton relaxation networks. In principle, this treatment can provide information on the degree of internal disorder via the magnitude of the generalized order parameter of each proton-proton vector. The ultimate aim is to generate a sufficient, model independent, basis upon which distances, derived from the observed NOEs, may be weighted in the refinement of structures. Several methods of weighting are being explored and their application to the structural analysis of the cyclic peptide cyclosporin A examined. The potential uses of this approach in the structural analysis of large proteins will also be discussed.

T-Pos76 CONTINUOUS LIFETIME DISTRIBUTIONS USED IN INTERPRETATION OF THIOREDOXIN FLUORESCENCE. Martin J. vandeVen, Laboratory for Fluorescence Dynamics, Department of Physics, University of Illinois at Urbana-Champaign, Urbana, IL 61801.

The tryptophan excited state in a protein is sensitive to its surrounding environment, i.e., the large number of conformational substates. The resulting, often complex, decay of the fluorescence can be analyzed by a sum of exponentials or, alternatively, by using continuous distributions of lifetimes. Following the latter approach, fluorescence data obtained for both the oxidized and reduced form of thioredoxin from E.coli have been analyzed. This protein is of interest since it contains two tryptophan residues, trp28 and trp31, close to two cysteine residues, cys32 and cys35, which form a disulfide bridge. The influence of the presence or absence of this disulfide bond on continuous distributions of lifetimes has been investigated using unimodal and multimodal probability density functions. The results are compared with a sum of exponentials analysis giving a best-fit with a triple exponential decay to the fluorescence data of both oxidized and reduced thioredoxin. Supported by NIH grant RR03155.

T-Pos77 HYDRATION AND PROTEIN DYNAMICS: A FLUORESCENCE LIFETIME APPROACH. Sergio T. Ferreira, Biochemistry, Univ.Fed.Rio de Janeiro, Brazil 21910; Enrico Gratton, LFD, Physics, Univ. of Illinois at Urbana, 61801; and Frank G. Prendergast, Biochemistry, Mayo Found., Rochester, 55905.

In order to perform their functions, proteins must be relatively flexible and it is reasonable to expect that solvent interactions will play an important role in modulating this flexibility. We have explored the role of hydration in protein dynamics through the measurement of tryptophan fluorescence under various hydration conditions, using reverse micelles of aerosol OT in n-hexane, which enabled us to control hydration levels over a large range. Multifrequency phase modulation lifetime data for tryptophan in AOT reverse micelles at low hydration levels could be best described in terms of a continuous lifetime distribution, instead of the usual biexponential decay verified in solution. As hydration levels were increased, both the mean lifetime and the width of the distribution decreased markedly. The same results were obtained with NATA, suggesting that solvation, rather than different rotameric forms in tryptophan, determines the number of the different substates and the interconversion rate between substates. Lifetime distribution analysis of Lysozyme and Troponin C give the same qualitative results: as hydration increases, lifetime distributions get progressively narrower and the mean lifetimes decrease, going towards their fully hydrated solution values. Our results indicate an increased mobility of tryptophan residues as hydration increases, evidenced by increasing interconversion rates between substates pointing at the crucial role of water in determining the amount of structural flexibility in the protein matrix and the ability to perform its biological function. Supported by CAPES (STF), NIH grants RR03155 (EG) and GM24847 (FGP).

T-Pos78 STRUCTURE AND DYNAMICS OF A MODEL MEMBRANE PROTEIN; INDIVIDUAL AMIDE EXCHANGE RATES IN M13 COAT PROTEIN MEASURED BY ^{15}N NMR SPECTROSCOPY. Gillian D. Henry and Brian D. Sykes, Department of Biochemistry, Univeristy of Alberta, Edmonton, Alberta, T6G 2H7, Canada.

The 50-residue coat protein of the filamentous coliphage M13 is inserted as an integral protein in the inner membrane of the *E. coli* host during virus reproduction. Amide hydrogen exchange kinetics have proved to be a useful probe of structure and dynamics of micelle-bound coat protein. Multiple exponential fits to the decay of the broad amide proton envelope observed by ^{1}H NMR spectroscopy suggested the existence of a number of kinetic sets which correlate approximately with the hydrophobic and hydrophilic domains. ^{13}C NMR isotope shift experiments located many of the more rapidly exchanging amides in the hydrophilic terminal regions, suggesting that the most retarded set of amides reside in the hydrophobic core. The exchange rates of several individual, assigned, slowly-exchanging amides of the hydrophobic core have been determined as a function of pH in SDS-solubilized coat protein using ^{15}N NMR spectroscopy of biosynthetically labelled protein. Polarization transfer experiments, such as INEPT, transfer magnetization from the amide proton to the directly bonded ^{15}N nucleus; when protonated protein is dissolved in D_2O in a classic 'exchange out' experiment, the INEPT signal disappears with time. H-exchange is catalysed by both H^+ and OH^-, the greater efficiency of OH^- resulting in a minimum rate at pH 3 for model peptides. A significant basic shift of the pH minimum was observed for residues of the hydrophobic domain (eg. all valines) whereas leucine-14 in the N-terminal hydrophilic domain showed a minimum at pH 3. This is interpreted in terms of electrostatic effects at the surface of the charged micelle (see abstract by O'Neil and Sykes). Retardation of exchange rates and rate minima have been used in conjunction with ^{13}C relaxation and other data to derive a model of micelle-bound coat protein.

T-Pos79 AN ANALYSIS OF CONFORMATIONAL PERTURBATION IN TRYPSIN AS MONITORED BY FT-IR SPECTROSCOPY AND X-RAY CRYSTALLOGRAPHY. Steven J. Prestrelski,(1) Alan H. Lipkus,(3) and Michael N. Liebman,(1,2). Departments of (1) Physiology and Biophysics and of (2) Pharmacology, Mt. Sinai School of Medicine of the City University of New York, and (3) Batelle (Columbus) Laboratory, National Center for Biomedical Infrared Spectroscopy.

Resolution-enhanced FT-IR spectroscopy has been used to study the serine protease trypsin and examine the conformational effects induced by various inhibitors that interact with a "macromolecular recognition surface", previously identified by computational analysis, in terms of conformation sensitive IR bands (Amide I,II and III regions). Information contained in high-resolution x-ray structures has been used to interpret changes in the FT-IR spectra in terms of conformational changes which occur upon binding of polypeptide (e.g. BPTI) and non-protein (e.g. diisopropyl fluorophosphate) inhibitors as well as activation of zymogen to active enzyme. Tools of macrostructural analysis, including linear distance plot analysis, distance matrix analysis and structural superposition, developed at this laboratory (1,2) provide a description of protein structure at secondary, tertiary and quaternary levels. Use of such macrostructural analysis of x-ray structures in conjunction with resolution-enhanced FT-IR spectroscopy provides a powerful method for producing spectral/structural correlations necessary for complete assignment of conformation-sensitive protein infrared bands.

This research is funded in part by grants from ImClone Systems, Inc. (MNL) and NIH #RR01367 (AHL).

T-Pos80 **Evolution of Fibril Forming Collagens.** Joanne Kelly, Shizuko Tanaka, Thomas Hardt, Eric F. Eikenberry, and Barbara Brodsky. Departments of Biochemistry and Pathology, UMDNJ-Robert Wood Johnson Medical School, Piscataway, N.J. 08854.

In mammals and birds, there are five genetically distinct collagens which form fibrils with a D = 67 nm periodicity in their axial structure: types I, II, III, V and XI. These collagens all have triple-helical domains 300 nm in length, with uninterrupted Gly-X-Y amino acid sequences, and have similar gene exon structures and regularities in their primary structures. Fibril forming collagens evolved early in the development of multicellular animals, but it is not known when the various genetic types diverged. We characterized the D-periodic fibrillar collagens present in the lamprey, a member of the most primitive vertebrate class, and found five types with triple helical domains 300 nm in length. The notochord, a cartilagenous tissue, contained a major and minor collagen identifiable, respectively, as type II and XI on the basis of chain composition, amino acid composition, solubility characteristics and susceptibility to vertebrate collagenase. By the same criteria, a minor collagen of the body wall was identifiable as type V. The chains of the dermis collagen and the major collagen of the body wall had some features of type I and type III, but did not correspond to either molecule. The molecular packing, the fibril diameters and the interfibrillar architecture in three lamprey tissues containing different genetic types were characterized by x-ray diffraction and electron microscopy. The notochord, with its well conserved type II and type XI, showed a striking conservation of molecular and fibrillar organization. In contrast, the dermis and body wall fibrils contained a molecular packing similar to that in higher vertebrates, but showed a significantly different distribution of diameters. These findings indicate that the structure of cartilagenous tissues was fixed very early in evolution, whereas the architecture of skin has evolved considerably since the separation of mammals and fish.

T-Pos81 AN ELECTRON MICROSCOPE STUDY OF THE SHAPE OF APOLIPOPROTEIN B UPON ORGANIC SOLVENT EXTRACTION OF LOW DENSITY LIPOPROTEINS BEFORE AND AFTER GLUTARALDEHYDE FIXATION. Martin L. Phillips and Verne N. Schumaker, Department of Chemistry and Biochemistry and the Molecular Biology Institute, University of California, Los Angeles CA 90024.

We have examined the shape of apolipoprotein B (apo B) from low density lipoporteins (LDL) using a new method to prepare the electron microscope grids. After absorption of the lipoproteins to a carbon-coated copper grid, lipids were extracted with 4:1 ethanol:ether; an aqueous negative stain was then applied. When the LDL residue were examined after this treatment, apo B, together with residual lipid, appeared as an elongated, flexible structure about 60-70 nm in length consisting of multiple domains of variable width from 2-7 nm. Occasionally, the elongated apo B formed an irregular, ring-shaped structure, but most of the rings were open. When LDL were pretreated with glutaraldehyde, then absorbed, extracted and strained, most of the images were closed rings with an average contour length of 70 nm, again consisting of multiple domains of variable sizes. These results imply that apo B is composed of multiple domains arranged in a belt-like structure on the surface of the LDL, and that distant domains possess a mutual affinity which favors crosslinkage.

T-Pos82 PROTEIN CRYSTAL GROWTH MECHANISMS: VISUALIZATION BY ELECTRON MICROSCOPY;* S. D. Durbin and G. Feher, U.C.S.D., La Jolla, CA 92093

To understand the basic processes of crystallization, convenient assays for the progress of nucleation and growth need to be developed. Here we report on the use of freeze-etch electron microscopy techniques to examine the growing surface of tetragonal lysozyme crystals at molecular resolution. Both (101) and (110) faces exhibit islands and steps of unit cell height (see Fig.). The density of islands and steps increased with increasing protein concentration. From these data and measured growth rates, kinetic parameters such as step velocity and two-dimensional nucleation rate may be deduced. Crystals grown at low concentration exhibited lattice defects which acted as sources of parallel steps. These observations support the hypothesis of a crossover from a defect-mediated to a two-dimensional nucleation growth mechanism as supersaturation increases (1). We have also observed the distribution of aggregates during the pre-nucleation stage in a crystallizing solution of tomato bushy stunt virus.

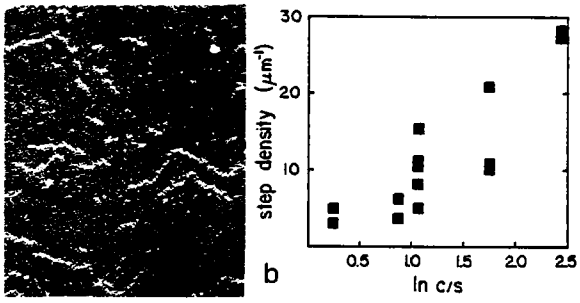

(a) Micrograph of lysozyme crystal grown at lysozyme concentration c=1% w/v. (b) Step densities observed on (101) surfaces of lysozyme crystals grown at different supersaturations c/s (s=solubility).

(1) S.D. Durbin and G. Feher, J. Crystal Growth 76, (1986), 583. *Work supported by the NIH.

T-Pos83 IN VIVO THIOPHOSPHORYLATION IS NOT EQUIVALENT TO PHOSPHORYLATION: A HIGH RESOLUTION TWO-DIMENSIONAL GEL ELECTROPHORESIS STUDY. Authors: Daniel C. F. Chan and T. T. Puck. Eleanor Roosevelt Institute for Cancer Research, 1899 Gaylord Street, Denver, CO 80206

We have used high resolution two-dimensional gel electrophoresis to study the in vivo phosphorylation patterns of several established cell lines in culture, using sodium (^{35}S) thiophosphoric acid (a generous gift from N.E.N.) and orthophosphoric acid (^{32}P) as the primary substrates. The results obtained by using these two compounds turned out to be very different, even though they share a similar chemical structure. Cells were labeled in vivo under similar conditions, and less than 5% of the radioactivity of (^{35}S) thiophosphate was incorporated into the cells when compared to a normalized 100% incorporation of orthophosphate (^{32}P). Several labeling conditions including electroporation have been tried and no significant enhancement of the (^{35}S) thiophosphate incorporation was obtained. In addition, the phosphorylation pattern is completely different between these two compounds, as demonstrated by 2-D gel autoradiographs. Proteins normally phosphorylated with orthophosphate (^{32}P) are not thiophosphorylated (^{35}P), while quite a few proteins normally not detected with orthophosphate (^{32}P) are strongly thiophosphorylated (^{35}S). Adenosine 5'-(γ,^{35}S) triphosphate was introduced into the cells by electroporation and similar thiophosphorylation patterns were obtained as those labeled with (^{35}S) thiophosphoric acid. Our data suggest that while these two systems are not equivalent, thiophosphorylation can be a complement to the study of phosphorylation.

T-Pos84 SOLVENT SCATTERING DENSITY IN NEUTRON PROTEIN CRYSTALLOGRAPHY

Xiao D. Cheng & Benno P. Schoenborn, Department of Biology,
Center for Structural Biology, Brookhaven National Laboratory, Upton, NY 11973

In protein crystallography, it has been customary to omit the contribution of bulk solvent to the low angle data in refinement procedures. These data contain, however, important information about the gross features of the unit cell contents and particularly about the solvent structure. In order to use the low angle reflections, a solvent-evaluation procedure has been developed which describes the reflections as a combination of solvent and protein terms. The solvent volume is divided into shells with shell thickness varying from 0.1 to 1.0 angstrom extending outward from the protein surface. The best scattering length density and "liquidity" B factor is assigned to individual shells, which allows a better evaluation of the protein surface structure, improved placement of "bound" solvent molecules, and determination of regions of solvent with different fluidities. When this procedure is applied to a high resolution neutron data from a crystal of metmyoglobin, we observe very low scattering length density for the innermost shell. This suggests that the surface stability might be less than that inferred from the B factors of the surface protein hydrogen atoms. Advantages of our technique are: 1) The overall fit to the observed data is improved, and hence the R factor is lowered. This implies that we have improved the accuracy of the atomic coordinates. 2) We understand better the solvation of the protein. 3) We can analyze the amount of salt present in the solvent volumes coupled with the measurement of the crystal density of protein.

This work was supported by the Office of Health and Environmental Research of the U.S.D.O.E.

T-Pos85 5 K EXAFS AND 40 K 10-SECOND RESOLVED EXAFS STUDIES OF PHOTOLYZED CARBOXYMYOGLOBIN*--Huey W. Huang, T. Y. Teng@, and Glenn A. Olah, Physics Department, Rice University, Houston, TX 77251

A previous extended x-ray absorption fine structures (EXAFS) study of photolyzed carboxymyoglobin (MbCO) [Chance, B., Fishchetti, R., & Powers, L. (1983) Biochemistry **22**, 3820- 3829; Powers, L., Sessler, J. L., Woolery, G. L., & Chance, B. (1984) Biochemistry **23**, 5519-5523] has provoked much discussion on the heme structure of the photoproduct (Mb*CO). The EXAFS interpretation that the Fe-CO distance increases by no more than 0.05 Å following photodissociation has been regarded as inconsistent with optical, infrared, and magnetic susceptibility studies [Fiamingo, F. G., & Alben, J. O. (1985) Biochemistry **24**, 7694-7970; Sassaroli, M., & Rousseau, D. L. (1986) J. Biol. Chem. **261**, 16292-16294]. The present experiment was performed with well characterized dry film samples in which MbCO molecules were embedded in a poly(vinyl alcohol) matrix [Teng, T. Y., & Huang, H. W. (1986) Biochim. Biophys. Acta **874**, 13-18]. The sample had a high protein concentration (12 mM) to yield adequate EXAFS signals but was very thin (40 μm) so that complete photolysis could be easily achieved by a single flash from a Xenon lamp. Although the electronic state of Mb*CO resembles deoxymyoglobin (deoxy-Mb), direct comparison of EXAFS spectra indicates that structurally Mb*CO is much closer to MbCO than to deoxy-Mb. Our EXAFS analysis shows that photolysis of MbCO at 5 K leads to a stable intermediate state in which CO has moved away form iron by a distance of 0.27 Å to 0.45 Å, but the 5-coordinate heme structure is strained in a form similar to MbCO; the resolution of the CO position depends on the structure parameters of MbCO which we use as a reference for the analysis of Mb*CO. At 40 K, from 1 s to 10 s after photolysis, 42% of the photoproduct has relaxed to the ground state, and the EXAFS spectrum of the remaining photoproduct is indistinguishable from that of the 5 K photoproduct.

*Supported in part by NIH, ONR and Welch Foundation.; @Now at Cornell.

T-Pos86 THE CRYSTAL AND MOLECULAR STRUCTURE OF B-PHYCOERYTHRIN Robert M. Sweet, Biology Department, Brookhaven National Laboratory, Upton, NY 11973 and Francis C. K. Tsui, Jules Stein Eye Institute, University of California, Los Angeles, CA 90024

The phycobiliproteins harvest light for photosynthesis in cyanobacteria and red algae. There are several different color classes of these proteins, which carry bilins as colored prosthetic groups. Together they span much of the visible spectrum. They are organized in the cell into phycobilisomes, which provide the proper structural organization for the the proteins so that energy can easily be transfered among them by Forster coupling. Phycoerythrin is the shortest-wavelength absorbing species, with a λ_{max} of 550 nm.

The 3-dimensional structure of B-phycoerythrin is being investigated by crystallographic means. Diffraction data have been measured with a multi-wire proportional counter area detector in the laboratory of Xuong and Hamlin and by rotation photographic methods at the National Synchrotron Light Source at Brookhaven National Laboratory. An electron density map was determined by isomorphous replacement phasing and density modification methods. This map was interpreted by use of the model of phycocyanin provided by Schirmer, Bode and Huber and the sequence of P. cruentum B-phycoerythrin provided by Glazer and Zuber.

The refinement to high resolution which is in progress should provide information about the disposition of the additional chromophores that phycoerythrin carries relative to phycocyanin and about the role of a single copy peptide located at a non-symmetric position at the center of the D_3-symmetric molecule. Supported by the U.S. Dept. of Energy, Office of Health and Environ. Res.